MULTI-MODULAR NUCLEAR REACTOR PLANT SIMULATION AND CONTROL

by

MATHER KNIGHT WALTRIP

Bachelor of Science in Mechanical Engineering,
The University of Texas at Austin (1982)

Submitted to the Department of Nuclear Engineering
in Partial Fulfillment of the Requirements for the Degrees of:

Master of Science in Nuclear Engineering
and
Master of Science in Mechanical Engineering

at the

MASSACHUSETTS INSTITUTE OF TECHNOLOGY
May 1989

MULTI-MODULAR NUCLEAR REACTOR PLANT
SIMULATION AND CONTROL

by

MATHER KNIGHT WALTRIP

ABSTRACT

A new generation of nuclear power plants now being considered will likely incorporate a multi-modular design strategy, in which separate nuclear steam supply modules provide steam to an aggregate turbine-generator. Smaller reactor cores in each module allow for the implementation of advanced safety features with relative ease and economy. Use of one relatively large turbine-generator set should help the multi-modular nuclear power plant to capture economies of scale by sharing the balance of plant components between several steam supply modules. Operating nuclear steam supplies in parallel while supplying the common turbine through a shared steam header requires load sharing between modules, a requirement which dominates considerations for the overall plant control principle.

Control principles for operation of a multi-modular array of liquid metal cooled reactors (LMRs) under a variable power demand are discussed, and one proposed principle is analyzed and evaluated. The proposed control system requires that both steam flow and steam pressure be specified to each module in the form of a demand signal. The module controller responds to the demand signal by referring to a control program which estimates the equilibrium values of plant temperatures and flows necessary to meet the demanded steam flow and pressure. Analysis of the multi-modular control problem is performed by modeling the components of the nuclear steam supply module. The non-linear physical model is used to obtain the plant control program and to perform dynamic simulations of plant transients. A special purpose simulation language, the Dynamic Simulator for Nuclear Power Plants (DSNP), is used to implement the plant model on a personal computer.

A non-linear constraint-based temperature controller monitors operating conditions in the reactor and, using estimates of reactivity and delayed neutron precursor activity, takes appropriate supervisory action as necessary during transients. The supervisory check of control actions is performed as part of a fault-tolerant approach to reactor control designed to

automatically avoid overshoot of plant power and temperature limits. Simulated transients which study the response of the plant under the proposed control system provide evidence that the controller will not challenge the reactor plant safety system.

Thesis Supervisor: David D. Lanning
Title: Professor of Nuclear Engineering

3

Acknowledgements

The author would like to take this opportunity to thank some of the individuals who have helped make this thesis and my education at M.I.T. possible.

First, my thanks go to my thesis supervisor, Prof. David Lanning and co-supervisor, Dr. John Bernard, Jr., for their support, patience and encouragement over the lengthy process of researching and preparing this document. Their experience in solving problems and obtaining results has been of great value. Prof. John Meyer has also helped me in my research by asking probing questions. I would also like to thank Prof. Derek Rowell for his assistance in the review of this report. All of these men have challenged me to dig deeper for answers and to provide more complete explanations in this report.

Many thanks also go to Dr. John T. Madell, of System Simulation & Analyses, Inc., for providing technical support with the DSNP software. His personal service, interest and commitment are greatly appreciated.

Mr. Brian Aviles, a fellow graduate student and close associate, also deserves recognition for consistently supplying encouragement and good humor at times when they were needed. His understanding of nuclear technology and reactor plant simulation is exceeded only by his considerable dedication to Pink Floyd and their music. Mr. Kwan Kwok deserves acknowledgement for technical support provided with the computation facilities used to produce much of this report. Mr. Greg Broadbent also deserves thanks for technical assistance with the Codeview debugger. Mr. Peter J. Coxon provided technical support as well with the Lotus Manuscript software and the Project Athena Postscript printer used to produce this great looking document.
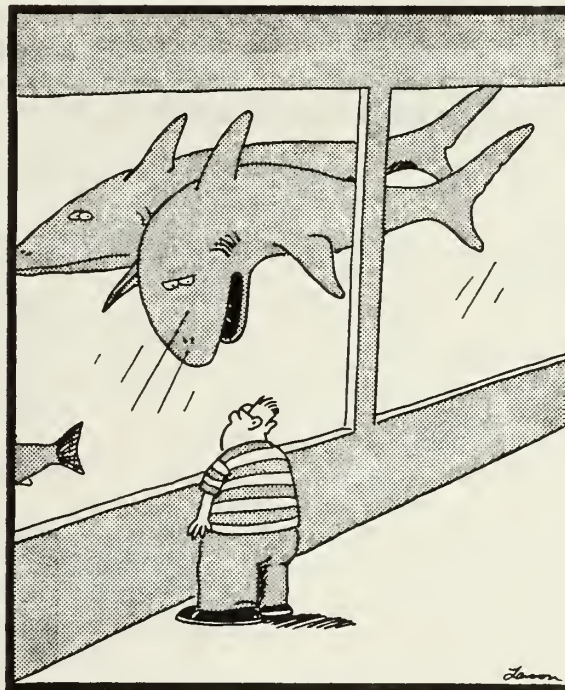
Clare Egan, the Nuclear Engineering Department graduate student administrator, has always been one of the most pleasant and helpful people at the Institute and deserves recognition. Thanks, Clare, I hope you get that raise you so richly deserve!

Much love and gratitude goes to my wonderful parents for their enduring confidence in me and my ability. I can never repay them for the affection and love they have given me yet, as parents, they never seem to mind.

Last, but not least, I would like to acknowledge the U.S. Navy for their financial support M.I.T., and also for the many challenging opportunities to excel as a professional engineer and naval officer. These facts imply that I will soon be repaying the Navy for their financial support. Anchors aweigh!

This page is dedicated to Gary Larson for the humor he has provided in *The Far Side* comic strip, which has helped me to keep my sanity while preparing this report.

"So close and yet so far."

Table of Contents

Table of Figures

Table of Tables

Nomenclature

$\vec{A}$	coefficient matrix (dimensionless)
A	area (m^2)
α	vapor volume fraction (dimensionless)
β	liquid volume fraction (dimensionless)
$\bar{\beta}$	delayed neutron precursor effective fraction (dimensionless)
$\bar{\beta}_i$	ith delayed neutron precursor effective fraction (dimensionless)
C	specific heat capacity (J/kg°C)
C_i	ith delayed neutron precursor group concentration (dimensionless)
C_p	specific heat capacity (J/kg°C)
D_e	hydraulic diameter (m)
E	total energy (J)
h	specific enthalpy (J/kg)
h_d	downcomer fluid specific enthalpy (J/kg)
h_{fdw}	feedwater specific enthalpy (J/kg)
h_r	riser fluid specific enthalpy (J/kg)
H_{mgb}	overall heat transfer coefficient, metal-to-water in steam generator boiling region (W/°C)
H_{mgn}	overall heat transfer coefficient, metal-to-water in steam generator non-boiling region (W/°C)
H_{mxs}	overall heat transfer coefficient, metal-to-secondary fluid in intermediate heat exchanger (W/°C)
H_{pmg}	overall heat transfer coefficient, primary fluid-to-metal in steam generator (W/°C)
H_{pmx}	overall heat transfer coefficient, primary fluid-to-metal in intermediate heat exchanger (W/°C)
K	thermal conductivity (W/m°C)
K_d	Doppler reactivity coefficient in plant model (dk/k)
K_e	core expansion reactivity coefficient im plant model (dk/k/°C)
K_{fbk}	feedback reactivity coefficient in plant controller (dk/k/°C)
K_s	sodium expansion reactivity coefficient in plant model (dk/k/°C)
Λ	prompt neutron lifetime (sec)
λ_e	standard effective delayed neutron precursor parameter (sec^{-1})

λ_i	i^{th} delayed neutron precursor group decay constant (sec $^{-1}$)
M	mass (kg)
μ	fluid viscosity (kg/m sec)
M_{pgi}	mass of primary fluid in i^{th} node of steam generator (kg)
M_{pxi}	mass of primary fluid in i^{th} node of intermediate heat exchanger (kg)
M_{sxk}	mass of secondary fluid in k^{th} node of intermediate heat exchanger (kg)
MC	total heat capacity (J/°C)
$(MC)_{pgi}$	total heat capacity of primary fluid in i^{th} node of steam generator (J/°C)
$(MC)_{pxi}$	total heat capacity of primary fluid in i^{th} node of intermediate heat exchanger (J/°C)
$(MC)sxk$	total heat capacity of secondary fluid in k^{th} node of intermediate heat exchanger (J/°C)
N	total neutron population (dimensionless)
Nu	Nusselt number (dimensionless)
P	wetted perimeter (m)
P_{sat}	saturation pressure (Pa)
Pe	Peclet number (dimensionless)
Pr	Prandtl number (dimensionless)
$\dot{Q}$	thermal power (W)
$\dot{Q}_{core}$	core thermal power (W)
$\dot{Q}_{load}$	load demand thermal power (W)
ρ	reactivity (dk/k)
ρ	density (kg/m³)
ρ_c	control reactivity (dk/k)
ρ_f	feedback reactivity (dk/k)
ρ_{rod}	control rod reactivity (dk/k)
Re	Reynolds number (dimensionless)
T	temperature (°C)
τ	reactor period (sec)
τ_A	available time to complete transient (sec)
τ_R	required time to establish feasibility of control (sec)
Tc	clad temperature (°C)

T_{core}	core coolant temperature (°C)
T_f	fuel temperature (°C)
T_m	metal temperature (°C)
T_{mgi}	temperature of metal in ith node of steam generator (°C)
T_{mxj}	temperature of metal in jth node of intermediate heat exchanger (°C)
T_{pgi}	temperature of primary fluid in ith node of steam generator (°C)
T_{pxi}	temperature of primary fluid in ith node of intermediate heat exchanger (°C)
T_r	temperature of subcooled water in riser of steam generator (°C)
T_s	sodium coolant temperature (°C)
T_{sxi}	temperature of secondary fluid in ith node of intermediate heat exchanger (°C)
T_{sat}	saturation temperature of steam in steam generator (°C)
u	specific internal energy (J/kg)
U	heat transfer coefficient (W/°Cm^2)
(UA)	overall heat transfer coefficient (W/°C)
V	velocity (m/sec)
V	volume (m^3)
W	mass flow rate (kg/sec)
W_{fdw}	feedwater mass flow rate (kg/sec)
W_p	primary coolant mass flow rate (kg/sec)
W_r	riser fluid mass flow rate (kg/sec)
W_s	secondary coolant mass flow rate (kg/sec)
X	steam quality (dimensionless)

Chapter 1 - Introduction

1.1 Objectives of this Report

This report investigates the requirements for closed-loop, digital control of a multi-modular sodium cooled nuclear power plant. Detailed analysis of a single module is performed by developing non-linear plant model. The model will be used to synthesize and evaluate a plant controller. Design emphasis is placed on the coordinated control of the reactor neutronic power, module thermal power, coolant temperatures, and steam pressure. The application of the reactivity constraint methodology as a supervisory control element has proven successful in the control of neutronic power in research reactors [1] and primary coolant temperature in pressurized water reactor (PWR) simulators [2]. It is anticipated that a similar approach can be successfully applied to the non-linear control problem of the liquid metal reactor (LMR) in a multi-modular array. The multi-modular design concept and the control problems posed are discussed in detail below.

Simulation of the plant for control system synthesis is an important part of this study because of the complex, non-linear behavior of the plant. The large number of differential equations which describe the plant precludes the use of transfer function analysis and frequency response design techniques. Although linearization does help the engineer to visualize behaviour of the plant, simulation is perhaps the best analytical tool for use in transient response studies.

Oak Ridge National Laboratory (ORNL) has been conducting work in the area of advanced automatic controls for nuclear power plants, and has requested M.I.T. to examine the multi-modular control problem and provide some innovative solutions. Although both General Electric and ORNL have developed simulators for the particular type of plant design studied, this report provides independent simulation results for a single nuclear steam supply module. Although a complete simulation of multiple nuclear steam supply modules, with the

13

aggregate steam turbine and balance of plant, is beyond the scope of this report, the findings contained in the proceeding chapters can be extended with further research into the multi-modular nuclear reactor plant control problem.

1.2 Multi-Modular Design Philosophy

The next generation of nuclear power plants must prove to the general public that nuclear power is safe and cost effective. Even though the nuclear industry has established high safety standards by making evolutionary improvements in design and in operational practices, a new reactor may be needed and this design must be revolutionary in its standards of safety and performance in order to be accepted. Such a plant would need to withstand worst case design accidents without fuel melting. In addition, the next generation of reactor plants must be economically viable, costing no more to operate than the present generation of light water reactors (LWRs).

Proposed multi-modular reactor plants, with power blocks of modules supplying steam to a common turbine generator set, may be the key to the problem of supplying safe and cost effective electricity to the public. See Figure (1) for a schematic diagram of the multi-modular plant arrangement. Electric utilities understand that smaller reactors are generally easier to operate than large LWRs. Also, removing a large generating unit from service for refueling or a maintenance outage, requires that a significant fraction of electrical demand must normally be supplied by using more expensive fuels. The high nuclear plant capital costs can only be justified by a high capacity factor. Multi-modular reactor plants, with multiple sources of thermal energy, have the potential to provide high capacity factors; one reactor can be shut-down for refueling while the others supply steam to the turbine-generator set. Advanced safety features, including passive means of decay heat removal, may simplify the plants and reduce the number of required active safety systems. These concepts are more easily

implemented in a smaller sized reactor core. Proponents cite other advantages of the multi-modular design philosophy as well, e.g. factory fabrication and learning curve economies [3]. Thus, the multi-modular approach may be cost effective while enhancing safety.

One of the multi-modular plant designs, developed by General Electric, is the Power Reactor Inherently Safe Module (PRISM) [4]. The PRISM design concept utilizes advanced safety characteristics and modularity to improve licensablity, reduce owner's risk, and reduce costs. The relatively small size of each reactor module facilitates the use of passive, inherent self-shutdown and shutdown heat removal features, which allow simplification and reduction of safety-related systems. PRISM consists of a compact sodium cooled reactor module producing about 138 MW_e (425 MW_t). Together with its steam generating system, it can be installed in groups to form power blocks of varying size. Each module in the power block supplies steam to a common steam header and turbine-generator, and shares a common feedwater system. More information about the nuclear steam supply module can be found in Chapter 2.
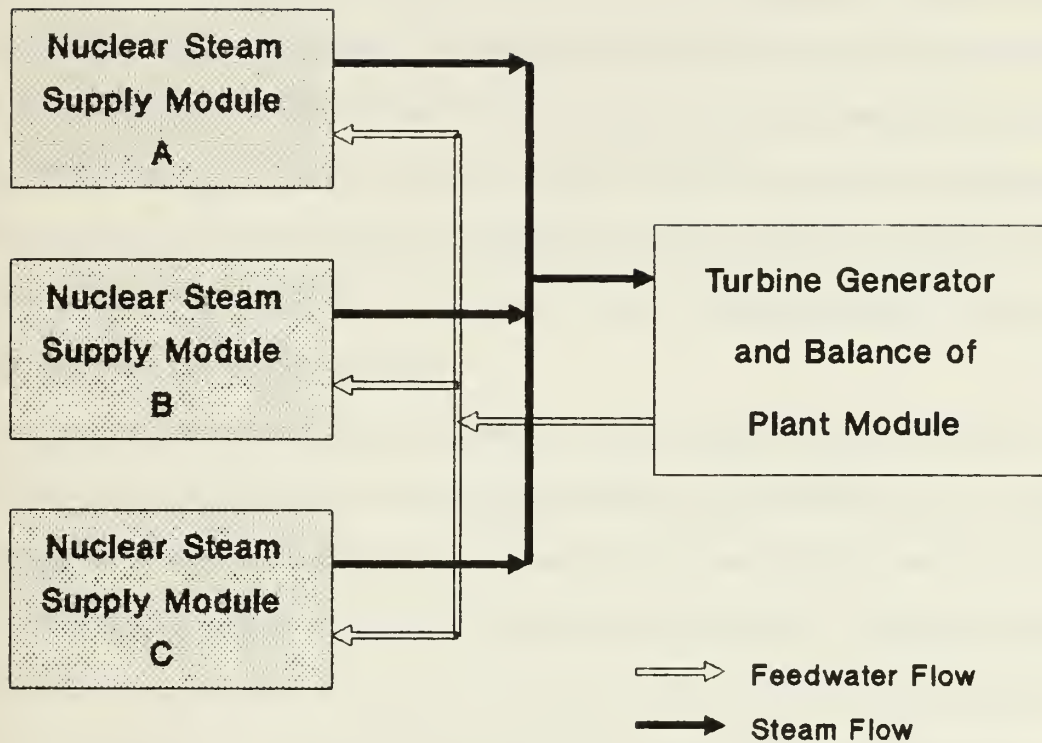
Figure (1) Multi-Modular Power Plant Arrangement Schematic

1.3 Using Automatic Controls in Multi-Modular Reactor Plants

To take full advantage of the modular concept, one central control room should be able to control all the individual modules of the power blocks during all modes of operation. Automation, if properly conceived and implemented, may allow the same number of operating personnel who operate one large reactor plant today to operate two or three proposed reactors of modular design. Reducing the number of personnel represents not just a reduction in salaries required for operators; it also represents a substantial reduction in the costs of operator training.

Automatic control of modules would aid fuel management by allowing parallel operation at different power levels. Fuel burnup rate could be carefully monitored and adjusted to prevent more than one module at a time from being shutdown for refueling. Such an operational strategy would result in a high capacity factor for the power block as a whole, and reduce the need for expensive replacement electricity.

The passive protection features planned for multi-modular reactors, and their more forgiving operational characteristics should make automatic control strategies more acceptable by licensing authorities. Current doctrine requires that a licensed human operator always be placed within the control loop for reactivity adjustments on the reactor. The current position may yield if a new generation of reactor technology can be proven to have a significantly higher level of safety than current LWR technology. Nuclear regulatory authorities would license the software and hardware used in the supervisory element of the reactor plant control system. Reactors with built-in passive safety systems may have the ability to withstand a complete control system failure without the need for operator action. More discussion of the licensing aspects of automatic reactor controls is found in Ref. [5].

17

1.4 Scope of Control Problem

Having each module operate at a different fuel burnup rate leads to a complex problem since each reactor is supplying steam to a common header and turbine. That is, the pressure of the steam generated must be controlled to allow each module to supply a desired fraction of the total plant load, independent of the load carried by other modules. Given the total load to be carried, the power block controller must divide the load appropriately between modules. With the load demand as input from the power block controller, the module controller must then decide how to best supply the steam demand. Maintaining a suitable steam pressure and flow for the given thermal power demand places constraints on other reactor module operating parameters. Given these restrictions, choosing the best method for controlling the process of steam production poses a complex problem. Investigation into steady state and transient strategies for control is found in Chapter 3.

1.5 Organization of this Report

This report contains five chapters. Chapter 1 introduces the reader to multi-modular reactor design as a candidate for the next generation of nuclear power plants. Some of the salient features of the proposed multi-modular plant design are discussed, and the importance of automatic controls and their possible uses in the future are presented.

Chapter 2 investigates specific design features of PRISM reactor plant technology. Models of liquid metal cooled reactor plant components and their state equations are developed. State equations are obtained from the component models using the physical laws of mass and energy conservation. Simplifying assumptions made in the plant model are listed, keeping in mind the purpose of the model for conducting control system synthesis.

Chapter 3 describes the steady state and dynamic considerations for reactor plant control. The possible steady state operational strategies for nuclear power plants are discussed, and

an overview of control strategies used on designs similar to PRISM is presented. A suitable control program is chosen for the multi-modular reactor plant and equilibrium values for plant flows and temperatures, given steam flow and steam pressure demands is evaluated. A reactor plant supervisory algorithm, using the "reactivity constraint approach" is developed to ensure safe plant response during automatic control of transients. Information from a plant model is used by the supervisory control element to guarantee that constraints which insure safe operation are not violated during the transient. Implementation of the proposed controller logic with respect to the plant simulator is detailed.

In Chapter 4, the proposed controller is evaluated during a series of transients. Time domain dynamic response of the plant is used to illustrate the necessity for and the effectiveness of power and temperature constraints. A very simple control law is deliberately chosen in the reactor plant controller to demonstrate the effectiveness of the supervisory constraints.

Chapter 5 summarizes the report and concludes with recommendations for further research.

Chapter 2 - PRISM Technology & Modeling

2.1 PRISM Concept

The Power Reactor Inherently Safe Module (PRISM) is a concept currently under development by General Electric as part of the innovative liquid metal reactor program sponsored by the U.S. Department of Energy. The purpose of the project is to develop a design for an inherently safe, reliable and marketable liquid metal fast reactor power plant. PRISM represents a typical multi-modular nuclear reactor plant design, and will be used as a basis for multi-modular control strategies in this report.

PRISM is a compact sodium cooled reactor module producing approximately 138 MW_e (425 MW_t). Together with its steam generating system, it can be installed in groups to form power blocks of varying size. A typical power block is composed of three modules, in a plant composed of one or more power blocks. The reactor module is factory fabricated and shipped as a unit to the site. Among other design goals, PRISM is intended to have a high availability and be easy to operate. Automatic control of power blocks, modules, and module systems should enhance the ease of operation.

2.2 Heat Transport System

Liquid metal cooled reactors (LMRs) typically use sodium as the liquid metal coolant, and are designed with three heat transport loops. The primary loop circulates sodium coolant through the core of the reactor to remove heat generated by the fission process. Unfortunately, sodium becomes activated by the neutron flux in the core. The radioactivity emitted by the activated sodium represents a hazard to personnel due to the high energy (2.754 MeV) gamma photons emitted and a significant half-life (~ 15 hr.). To isolate the radioactive coolant, primary coolant is pumped through an intermediate heat exchanger. A secondary sodium coolant loop transports the thermal energy from the intermediate heat exchanger (IHX) to a

steam generator. This secondary loop affects the response time of an LMR to load variations by introducing an additional transport delay between heat production in the core and steam generation in the boiler. Refer to Figure (2) below for a diagram of the heat transport system.
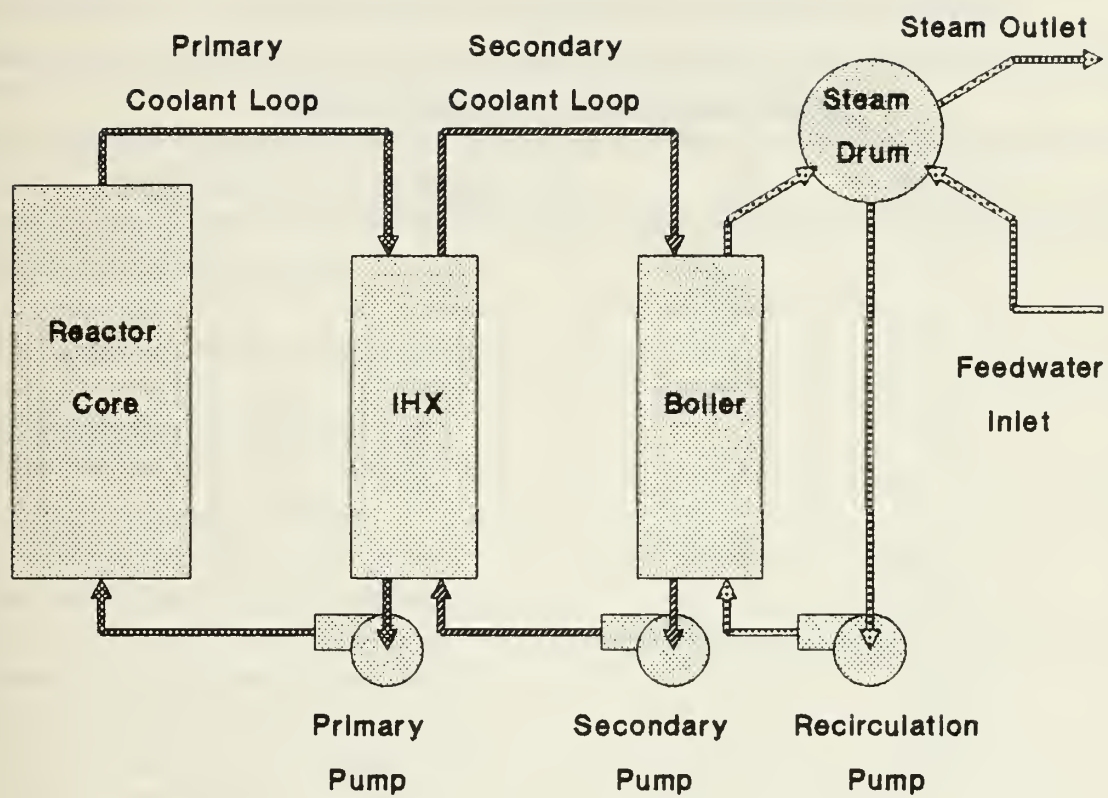
Figure (2) PRISM Heat Transport System Schematic Diagram

2.2.1 PRISM Plant Parameters

Some of the important PRISM plant parameters are included in Table (1) shown below as taken from Ref. [6]. The simulator developed for this report operates at values close to these parameters, but has reduced complexity. Lumping the two IHXs into one unit allows for simplification of the model and the resulting system of differential equations.

Table (1)PRISM PLANT PARAMETERS	
POWER BLOCK PARAMETER	**VALUE**
Number of PRISM modules	3
Rated turbine-generator output (MW$_e$)	415
Net thermodynamic efficiency (%)	32.5
Rated thermal output (MW$_t$)	1275
Rated steam flow to turbine (kg/sec)	622.4
Turbine throttle steam pressure (MPa)	6.653
Turbine throttle steam temperature ($^\circ$C)	282
Feedwater temperature at steam drum ($^\circ$C)	216
MODULE PARAMETER	**VALUE**
Number of primary pumps (EM type)	4
Number of intermediate heat exchangers	2
Number of steam generators	1

Rated thermal output (MW$_t$)	425
Primary sodium hot leg temperature (°C)	468
Primary sodium cold leg temperature (°C)	352
Primary flow rate through core (kg/sec)	2912
Average linear power (KW/m)	18.4
Peak linear power (KW/m)	31.2
Core height (m)	1.2
Rated steam flow (kg/sec)	205.5

2.2.2 Steam Generator System

The steam generator consists of a double-wall, straight tube and shell evaporator section, and a steam drum containing a mixture of saturated liquid and vapor. Double-wall construction (similar to Experimental Breeder Reactor-II design) maximizes system reliability by reducing the likelihood of a sodium-water reaction. Secondary sodium flows on the shell side of the evaporator, causing the sub-cooled water on the tube side of the heat exchanger to boil. Boiling length varies according to operating conditions, with the steam-water mixture collecting in a steam drum located above the evaporator. The feedwater system introduces subcooled condensate to the steam drum, improving recirculation flow by quenching the saturated vapor entrained by flow through the downcomer tubes. A recirculation pump forces downcomer flow to recirculate through the evaporator. Before leaving the steam drum, steam flow passes through a separator to reduce the moisture content of the steam. The PRISM power block

uses a simple saturated steam cycle, and the steam produced in the forced recirculation boiler of each module is carried through a shared steam header to an aggregate turbine-generator without passing through a superheater.

2.2.3 Reactor Module

The entire PRISM primary system is contained within the reactor module, along with other plant components. The reactor module is a compact pool-type reactor. The pool-type design possesses several advantages over the so-called loop-type design [7]. Leakage in the primary system components and piping will not result in leakage from the primary system and a primary system pipe rupture may be less likely. The mass of sodium in the primary system is on the order of three times that of a loop system, thus providing greater heat capacity. This large capacity results in a lower plant temperature rise during off-normal transients or a longer time to reach boiling if heat sinks are isolated. The large thermal capacity of the primary sodium pool, or upper plenum, also tends to dampen transient effects in other parts of the system. Control system design and plant load following capability will be influenced by the relatively large mass of sodium in the hot leg of the primary system.

Refer to Figure (3) for the flow path diagram. Primary sodium, at relatively low pressure under normal conditions, is circulated through the core to the shell side of the two IHXs by four electromagnetic pumps. Heat from the primary sodium coolant is transferred to the non-radioactive, secondary sodium coolant flowing on the tube side of the IHXs. Secondary sodium is then circulated through dual loops to a single steam generator.
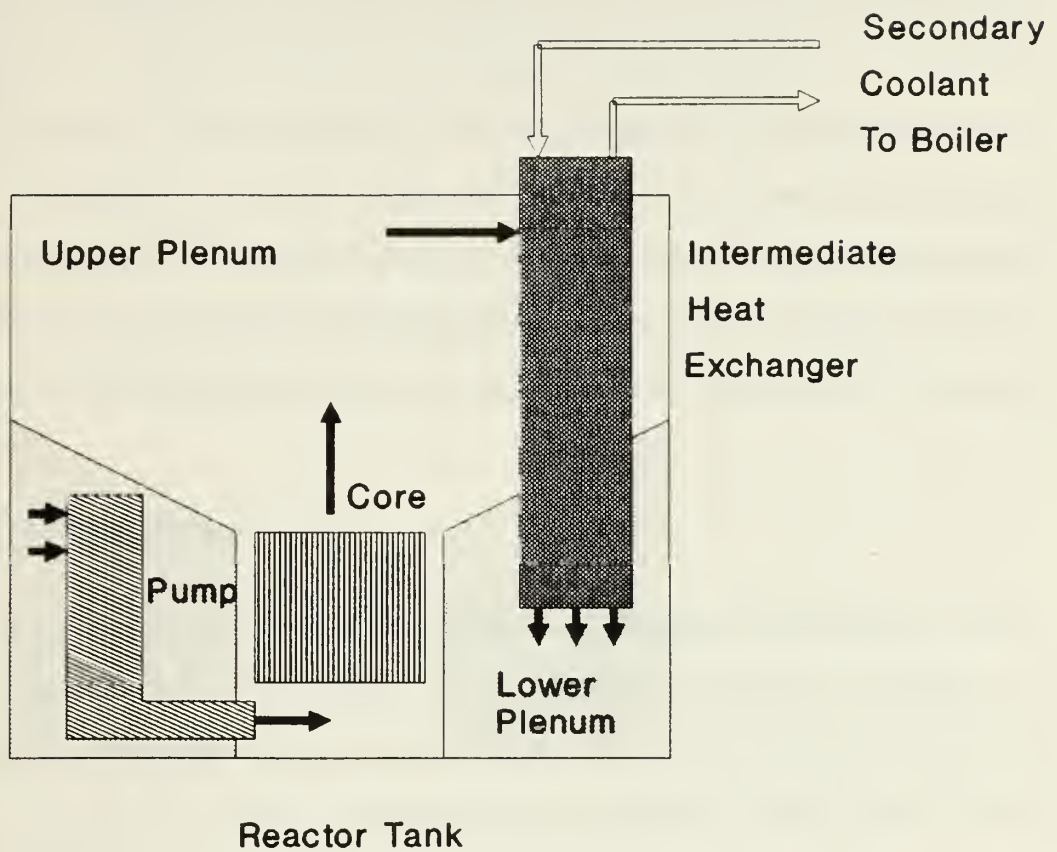
Figure (3) Pool Type LMR Design

2.3 Reactor Core

PRISM is designed to accept either oxide fuel or metal fuel assemblies. This report will consider the characteristics of the metal fuel core only. The U-Pu-Zr metal alloy proposed for the fuel cycle promises to make the concept of an integral fast reactor fuel cycle possible, but feasibility of the new fuel is strongly dependent on proof of adequate performance [8]. Recent results have achieved extremely long burnups of 180 GWD/MT in tests at EBR-II[1]. The metal core operates at low temperatures due to its low nominal peak specific power (<46 kW/m) and a conservative core outlet temperature (468 °C) used in conjunction with a simple saturated steam cycle. The total integral reactivity worth of the most active rod is also relatively low (only $0.22). These and other advanced safety features provide for excellent response to loss of flow, unprotected transient overpower (rod withdrawal) and loss of normal heat sink transients [9].

2.3.1 Reactivity Control

Reactivity for normal operations of startup, load following, and shutdown is accomplished by a system of six control rods. The six control rod assemblies are identical. A stepping motor, controlled by the plant control system, actuates a lead screw attached to the control rod assembly to insert and withdraw the neutron absorber. The plant control system actuates only one control rod at a time.

The absorber is connected to the driveline by a mechanical latch held in place by an electromagnet. For a rapid emergency shutdown (SCRAM), the reactor protection system causes the electromagnets on all six control rod assemblies to de-energize at once, and the absorbers are released, dropping into the core under the force of gravity and a mechanical spring. As a diverse backup, a powerful separate fast insertion motor within each drive

---

1 According to results presented by Y.I. Chang at M.I.T. seminar, March 1989.

mechanism rapidly inserts each control rod assembly in the unlikely event that the absorber rod sticks or fails to unlatch. All six fast insertion motors are actuated at once by the reactor protection system; they are not reversible. The absorbers have sufficient worth that any one of the six rods can shut down the reactor to a cold subcritical condition, providing six-fold redundancy.

At the normal full power position, movement of all six control rods at the maximum rate corresponds to a reactivity insertion rate of ± 2 ¢/sec.

2.4 Plant Modeling

The plant model used in this report is developed from state equations based upon the conservation of energy, and implemented using the DSNP simulation language. DSNP is described in more detail in Ref. [10] and Appendix A. This report focuses on the development of a fault-tolerant module controller, so simulation of a single module is emphasized. By writing the state equations which describe the dynamic interaction of various plant processes, insight into the operation of the plant is gained. By making some simplifying assumptions, the complexity of the model can be reduced while still maintaining sufficient fidelity.

Each module is represented for the sake of simplicity as having one primary loop (instead of four), and one secondary loop (instead of two). Asymmetric transients cannot be simulated, but this shortcoming does not impede the investigation of this report.

The following assumptions are made in the model developed:

     1) distributed parameters are lumped into nodes

     2) heat flow occurs in one dimension only across nodes

     3) thermodynamic equilibrium exists between phases

     4) all water in the boiler exists at a uniform pressure

     5) the steam drum contains a perfect mixture

     6) steam separation allows only dry steam to leave drum

7) prompt jump approximation used in kinetics equations

2.4.1 Power Generation Dynamics

The power generated in the reactor core is represented by the set of non-linear point kinetics equations. The kinetics equations are obtained from the integro-differential equations describing the neutron population for a given system by assuming that the spatial distribution of neutrons remains constant with time. This makes the magnitude of the neutron flux a function of time only. For a detailed derivation, see Ref. [11]. In small reactor cores with transients in which the instantaneous reactor period is large compared to the neutron lifetime, this assumption holds very well.

Neutrons produced from fission can be grouped into two categories: prompt and delayed. Prompt neutron population is proportional to reactor power level. Delayed neutrons, which are produced after a brief time delay by their precursors, depend upon the power history of the reactor. During normal power range operation, the reactor operates about the critical condition, changing power level by going slightly super- or sub-critical. In steady state and transient conditions, the fission process in the reactor depends upon the contribution of delayed neutrons. From the analysis performed in Ref. [12] we know that a reactor would be unstable without delayed neutrons. Six delayed neutron groups are used in the point kinetics equations to account for the decay of delayed neutron precursors with widely ranging decay constants. We shall see later on how a controller can use information about the behavior of delayed neutron precursors to anticipate control actions. The prompt jump approximation is also used in this analysis. Excess reactivity is taken to be small enough that the transient behavior is primarily due to the delayed neutrons after a small reactivity induced jump in the prompt neutron population. Thus, for all transients studied, the time derivative of the neutron population is assumed to be zero in Eq. (2-1) below. Such a simplification provides an important savings in computer execution time, and is justified since the instantaneous reactor periods

in the transients being studied are so much greater than the prompt neutron lifetime. The point kinetics equations take the form below in Eqs. (2-1), (2-2), and (2-3). The neutron source term has been neglected since this term is negligible in a real reactor operating within the power range. N represents the total neutron population, C_i is the ith delayed neutron precursor group concentration, λ_i is the ith delayed neutron precursor group decay constant, ρ represents net reactivity, $\overline{\beta}_i$ is the ith delayed neutron group effective fraction, and Λ is the prompt neutron lifetime.

$$\frac{dN}{dt} = \frac{\rho - \overline{\beta}}{\Lambda}N + \sum_{i=1}^{6} \lambda_i C_i \qquad (2-1)$$

$$\frac{dC_i}{dt} = \frac{\overline{\beta}_i}{\Lambda}N - \lambda_i C_i \qquad (i=1,6) \qquad (2-2)$$

$$\overline{\beta} = \sum_{i=1}^{6} \overline{\beta}_i \qquad (2-3)$$

For the prompt jump approximation, $\quad \Lambda\dfrac{dN}{dt} \ll (\rho - \overline{\beta})N + \Lambda\sum_{i=1}^{6}\lambda_i C_i$

Power generated in the core is obtained by multiplying the total neutron population present by a proportionality constant ($Q_{core} = K_p N$). Any heat generated due to decay of fission products is neglected since it is a small percentage of the overall heat generated during power operation. Recall that this simulator is not intended for study of abnormal transients where decay heat generation becomes significant. Heat input due to pumps is also neglected since this only accounts for about 1% of the rated core power.

One of the coefficients in the point kinetics equation, reactivity (ρ), varies significantly with time depending upon conditions in the core. Reactivity determines whether the reactor is critical, subcritical, or supercritical and is directly related to the multiplication ratio of the reactor. In a critical reactor, the multiplication ratio equals unity, meaning that the rate at which neutrons are consumed in the core exactly equals the rate at which they are produced.

If the ratio is less than unity, as in a subcritical reactor, then neutrons are consumed faster than they are produced. In a supercritical core, the multiplication ratio exceeds unity. Reactivity is defined as the fractional departure of the multiplication ratio from unity. If reactivity (ρ) is positive, then the core neutron population is increasing; if ρ is negative, then the population is decreasing. If a controller could directly control the amount of reactivity in the core, power control would be simplified. Unfortunately, reactivity is a state which cannot be observed directly, and many factors contribute to the total reactivity in the core. We can only measure reactivity indirectly.

Reactivity is fed back to the reactor core through various physical processes. Important contributors to total reactivity include fuel Doppler reactivity, core expansion reactivity, and sodium coolant expansion reactivity. These contributions to core reactivity are not subject to direct control, in contrast with control rod reactivity. From our knowledge of linear system behavior, positive feedback generally makes a system unstable. The same is true in this case. A reactor is said to be stable in the power range if, for any small disturbance, such as a change in coolant flow or a control rod movement, the reactor response will tend to hold power at a constant value that differs from the initial value by only a small amount. A power excursion or an oscillation of increasing amplitude could result in core damage if not terminated quickly by the control system. Therefore, every reactor should be designed to be stable. The sum of the various temperature feedback reactivities should cause an overall negative effect as core temperature increases to prevent autocataclytic or oscillating instabilities.

In the implementation of reactivity effects in the simulation, the algorithm initially assumes zero reactivity in the core (the core is exactly critical) at the beginning of the transient. Changes in reactivity due to control rod movement, fuel temperature changes, etc. are then calculated with Eq. (2-4) and inserted into the point kinetics equations. ρ_{rod} represents control

rod reactivity, K_d is the Doppler reactivity coefficient, K_e is the core expansion reactivity coefficient, and K_s is the sodium expansion reactivity coefficient. Values of these parameters used in the simulation may be found in Appendix C.

$$\rho - \rho_0 \;=\; (\rho - \rho_0)_{rod} \;+\; K_d \ln\!\left(\frac{T_f}{T_{f0}}\right) \;+\; K_e(T_f - T_{f0}) \;+\; K_s(T_c - T_{c0}) \quad (2-4)$$

The transient behavior of a reactor is very sensitive to small changes in reactivity, but fairly insensitive to small changes in the other parameters, $\overline{\beta}_i, \overline{\beta}, \lambda_i, \Lambda$, etc. Hence the latter parameters can be considered as constants although they do vary with reactivity.

The core neutronic characteristics are simulated by using the DSNP modules NEUTP1 and FDBEK1.

2.4.2 Core Thermal Hydraulics

As in all other plant components, the core model represents a simple lumped parameter approximation of the core thermodynamics. Distributed parameters for power plant components are lumped into a single node. Mass and energy balances are written for the node as appropriate. In the core, the fuel, cladding, and coolant are each represented as a node. A uniform temperature exists throughout each node, allowing the nodal stored energy to be represented by a single variable. The rate of change of fuel temperature is determined in Eq. (2-5) from an energy balance. Power is generated within the fuel and transferred to the cladding. T_f represents fuel average temperature, T_c is clad average temperature, $\dot{Q}_{core}$ core thermal power, $(UA)_{fc}$ is the overall heat transfer coefficient fuel-to-clad (W/°C), and $(MC)_f$ is the heat capacity of the fuel (J/°C).

$$\frac{dT_f}{dt} \;=\; \frac{\dot{Q}_{core} - (UA)_{fc}(T_f - T_c)}{(MC)_f} \quad (2-5)$$

Performing an analogous energy balance on the cladding node, we obtain an equation describing the dynamic temperature of the clad, shown in Eq. (2-6). Power is transferred in from the fuel and carried out by the coolant. T_s represents sodium coolant average temperature, $(UA)_{cs}$ is the overall heat transfer coefficient clad-to-sodium (W/°C), and $(MC)_c$ is the heat capacity of the clad (J/°C).

$$\frac{dT_c}{dt} = \frac{(UA)_{fc}(T_f - T_c) - (UA)_{cs}(T_c - T_s)}{(MC)_c} \tag{2-6}$$

The heat transfer coefficient for a sodium-cooled fuel element is computed by the empirical relationship for the Nusselt number in Eq. (2-7), the Peclet dimensionless parameter in Eq. (2-8), and from the definition of the Nusselt number in Eq. (2-9). See Ref. [13] for more information. Nu represents the dimensionless Nusselt number, Pe is the dimensionless Peclet number, V is fluid velocity across heat transfer surface, P/D is the pitch to diameter ratio, C is the sodium specific heat (J/kg°C), K is the sodium thermal conductivity (W/m°C), and ρ is the sodium density. All geometrical effects are accounted for in calculation of the heat transfer coefficients. Once the heat transfer coefficient for a single fuel pin is known, the overall coefficient is obtained by multiplying by the total area of fuel pins.

$$Nu = 4 + 0.33(P/D)^{3.8}(Pe/100)^{0.86} + 0.16(P/D)^{5.0} \tag{2-7}$$

$$Pe = \frac{\rho VDC}{K} \tag{2-8}$$

$$U_{cs} = \frac{KNu}{D} \tag{2-9}$$

The coolant temperature is described by another differential equation derived from an energy balance in Eq. (2-10). $(MC)_s$ represents the total heat capacity of the sodium coolant, M_c is the mass of sodium in the core, and W_p is the primary coolant mass flow rate. Note that

33

for all the core energy balances, all heat is produced exclusively within the fuel node. Heat generated in the cladding, coolant, or core structure is not modeled. For the transient conditions studied in this report, this simplification does not introduce significant error.

$$\frac{dT_s}{dt} = \frac{(UA)_{cs}(T_c - T_s)}{(MC)_s} + \frac{W_p(T_s^{in} - T_s^{out})}{M_s} \qquad (2-10)$$

The core thermohydraulic model is implemented using the DSNP modules CORTP1(LMFBR) and TPOWR1.

Next we will examine the components through which the heat generated within the fuel passes on its way to the turbine-generator. As mentioned earlier, all modeling uses the lumped parameter approach with mass and energy balance equations used to describe the thermodynamic behavior.

2.4.3 Reactor Coolant Plenums

Since PRISM is a pool-type design, the upper and lower plenums represent significant energy storage reservoirs. By performing energy balances on two nodes, one containing all the metal of the plenum, the other holding all the sodium coolant, we can describe the temperatures in the plenum with Eq. (2-11) and (2-12). T_s represents the sodium average temperature in the plenum, T_m is the plenum metal average temperature, $(MC)_s$ is the total heat capacity of the sodium in the plenum (J/oC), $(MC)_m$ is the total heat capacity of the plenum metal structure (J/oC), and $(UA)_{ms}$ is the overall heat transfer coefficient metal-to-sodium (W/oC).

$$\frac{dT_s}{dt} = \frac{(UA)_{ms}(T_m - T_s)}{(MC)_s} + \frac{W_p(T_s^{in} - T_s)}{M_s} \qquad (2-11)$$

$$\frac{dT_m}{dt} = \frac{(UA)_{ms}(T_s - T_m)}{(MC)_m} \qquad (2-12)$$

34

A schematic diagram of the plenum lumped parameter model is shown in Figure (4). The differential equations for both the upper and lower plenums are similar. Plenum thermal dynamic behavior is implemented in the simulation using the DSNP modules LPLEN1 and UPLEN1.
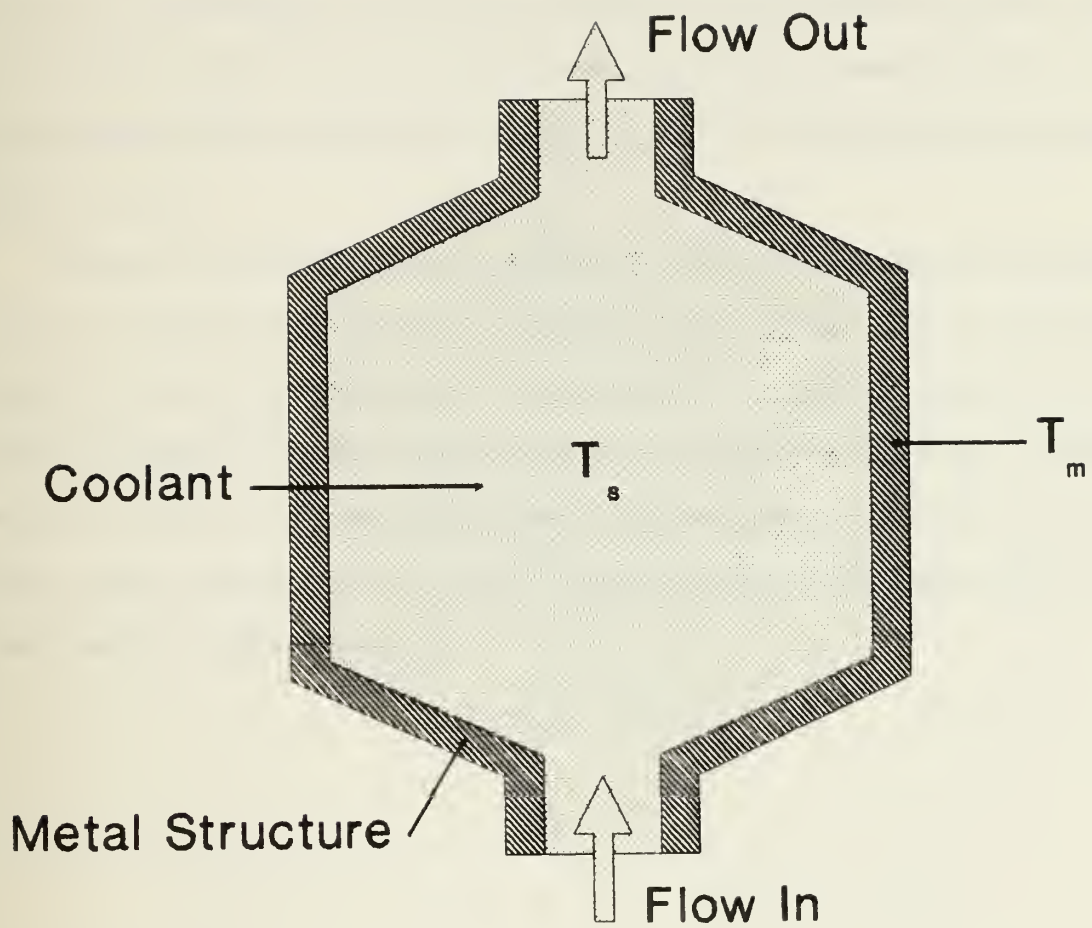
Figure (4) Core Plenum Lumped Parameter Model Schematic

2.4.4 Intermediate Heat Exchanger

The dual, counter-flow, intermediate heat exchangers (IHX) of the PRISM reactor module are collapsed into a single unit for modeling purposes. All individual IHX tubes are modeled by a single equivalent tube partitioned into several axial nodes. Any number of axial nodes can be determined by the user when setting up the DSNP problem, but three are used in this simulation. Each axial node contains three radial nodes representing primary coolant, tube wall material, and secondary coolant. See Figure (5) below for a schematic representation of the IHX model.

Because of the lumped parameter approach, the energy of each node can be expressed in terms of temperature, obtained by performing an energy balance. Eq. (2-13) shows the results for a primary side fluid node. T_{pxi} represents the ith primary side node coolant temperature, T_i^{in} is the primary side upstream node coolant temperature, T_{mxj} is the jth metal node temperature, $(UA)_{pmx}$ is the overall heat transfer coefficient fluid-to-metal (W/°C), W_p is the primary coolant mass flow rate, M_{pxi} is the ith primary side node coolant mass, and C_{pxi} is the primary coolant specific heat (J/kg°C).
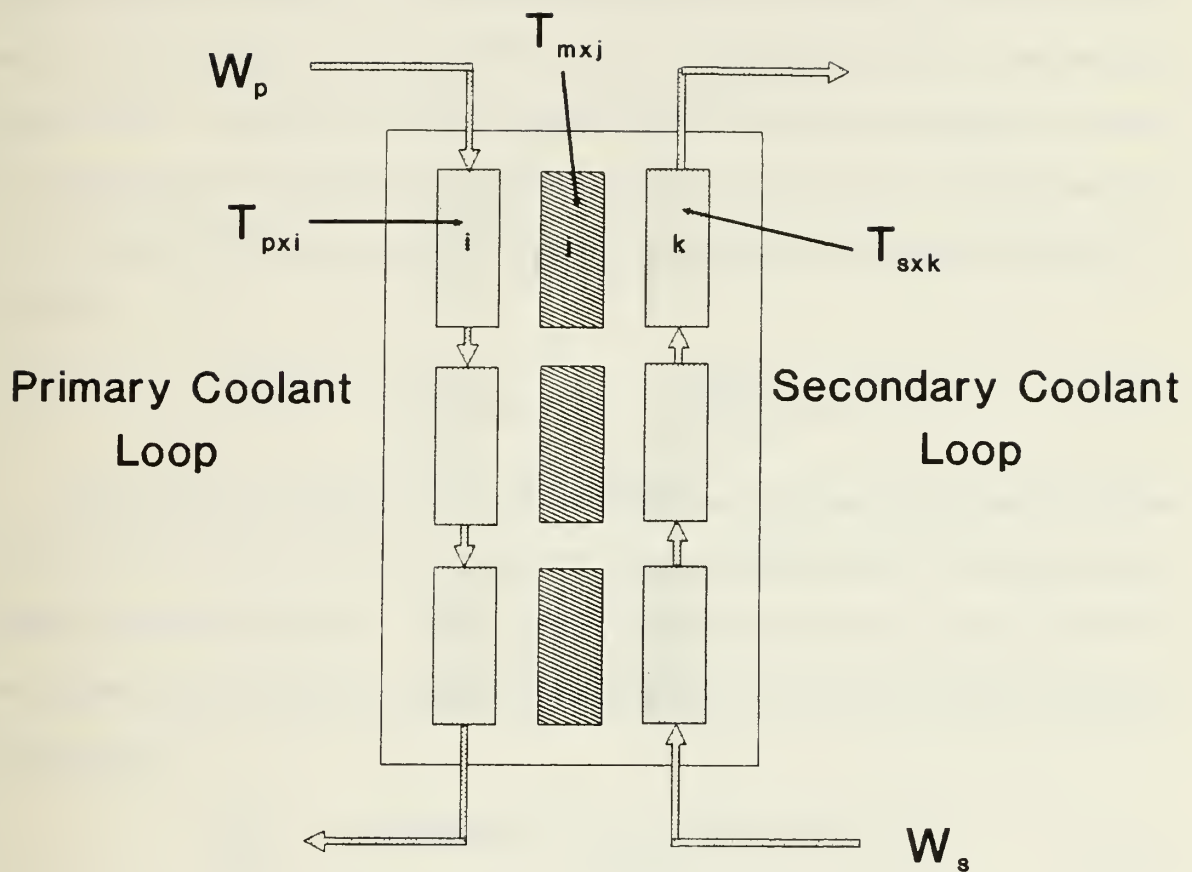
Figure (5) Intermediate Heat Exchanger Lumped Parameter Schematic

(See Eqs. (2-13) through (2-15) for explanation of symbols used)

$$\frac{dT_{pxi}}{dt} = \frac{W_p}{M_{pxi}}(T_i^{in} - T_{pxi}) - \frac{(UA)_{pmx}}{(MC)_{pxi}}(T_{pxi} - T_{mxj}) \qquad (2-13)$$

The secondary side fluid node temperature is described by an analogous expression in Eq. (2-14). T_{sxk} is the kth secondary side node coolant coolant temperature, $T_{s(k-1)}$ is the $(k-1)^{th}$ secondary side upstream node coolant temperature, $(UA)_{mxs}$ is the overall heat transfer coefficient metal-to-fluid (W/°C), W_s is secondary coolant mass flow rate, M_{sxk} is the kth secondary side node coolant temperature, and $(MC)_{sxk}$ is the kth secondary side node coolant total heat capacity (J/°C). Temperature changes along the length of the node are assumed to be linear. By using this linear relationship, the outlet temperature of the node can be determined. This is the same approximation used for the evaporator section primary side nodes. See Eq. (2-18) and 2-20).

$$\frac{dT_{sxk}}{dt} = \frac{W_s}{M_{sxk}}(T_{sxk}^{in} - T_{sxk}) - \frac{(UA)_{mxs}}{(MC)_{sxk}}(T_{sxk} - T_{mxj}) \qquad (2-14)$$

The metal node temperature of the tube wall between the primary and secondary coolant is obtained in the same manner as the primary and secondary fluid nodes, by writing an energy balance as shown in Eq. (2-15). $(MC)_{mxj}$ is the jth metal node total heat capacity (J/°C). The overall heat transfer coefficients for the heat exchanger are calculated in the manner described in Appendix B.

$$\frac{dT_{mxj}}{dt} = \frac{(UA)_{pmx}(T_{pxi} - T_{mxj}) - (UA)_{mxs}(T_{mxj} - T_{sxk})}{(MC)_{mxj}} \qquad (2-15)$$

In this section, we have taken a complex component and modeled it in a straightforward and yet realistic manner, using the physical laws of energy conservation. The process of writing a thermodynamic energy balance on a small lump of a heat exchanger yields important relationships, which can be solved together with the other state equations to completely determine the state of the component.

The IHX is simulated by use of the DSNP module IHXMA1.

2.4.5 Pipes

The thermal energy transport delays which take place inside pipes connecting major plant components are approximated by first order time delays. Once again, the energy conservation equation is used to derive this relationship, shown in Eq. (2-16). T_{out} is the pipe outlet temperature, T_{in} is the pipe inlet temperature, W_c is pipe coolant mass flow rate, and M_c is the pipe coolant mass.

$$\frac{dT_{out}}{dt} = \frac{W_c(T_{in} - T_{out})}{M_c} \qquad (2-16)$$

Two pipes are needed for the PRISM model. One connects the IHX to the boiler primary inlet, and one runs from the boiler primary outlet back to the IHX. These elements, in addition to the inlet and outlet plenums should realistically model the time delays in thermal transport. Changes in state of the boiler are reflected back to the reactor through coolant temperatures. Likewise, changes in the core power output are transported to the boiler through the coolant.

The pipe time delay element is simulated using the DSNP module PIPE01.

2.4.6 Steam Generator

The steam generator consists of two separate elements, a boiler and a steam drum. In the evaporator section, subcooled water is heated to saturation temperature and then converted into steam in the riser section. The wet steam is collected in a steam drum which contains a mixture of saturated liquid and vapor. Feedwater is injected into the steam drum just above the downcomer tubes to collapse any vapor bubbles present in the liquid. The subcooled liquid is then drawn into the downcomer by a recirculation pump and forced back into the evaporator section. A boiling pot model for conditions in the steam drum has been developed, but its use was not needed to demonstrate the final results of this report. The steam drum model is presented in Appendix D.

The evaporator uses a two axial node, three radial node, lumped parameter, counter-flow heat exchanger model with a variable boundary location between the two axial regions. The lower, non-boiling region represents the preheater section in which water is heated up to saturated conditions by the sodium coolant on the primary side of the boiler. In the upper region, boiling takes place under saturated conditions with no superheating, and a mixture of saturated liquid and vapor leaves the evaporator. The boundary between the two regions is not fixed but is a time dependent variable obtained from heat balance equations. A total of six nodes represent the heat transport process in the boiler:

1) primary sodium in boiling region

2) primary sodium in non-boiling region

3) metal wall in boiling region

4) metal wall in non-boiling region

5) secondary subcooled water

6) secondary water-steam mixture

The division of the boiler into nodes is illustrated in Figure (6) below.

Dynamic equations describing the behavior of this model are obtained by writing energy balances on the component. For the primary sodium coolant nodes and metal wall nodes, the state equations take forms similar to those in the IHX. The coefficients in the equation, however, are not fixed and can change with time. Both the heat transfer area and mass contained in each node change according to the boiling length (L_b) determined by the secondary nodal equations.

For the primary coolant in the boiling region, the energy balance provides a dynamic equation for temperature shown in Eq. (2-17). T_{pgb} represents primary side sodium coolant temperature in the boiling region, T_{mgb} is boiling region metal node temperature, $(UA)_{pmgb}$ is

41
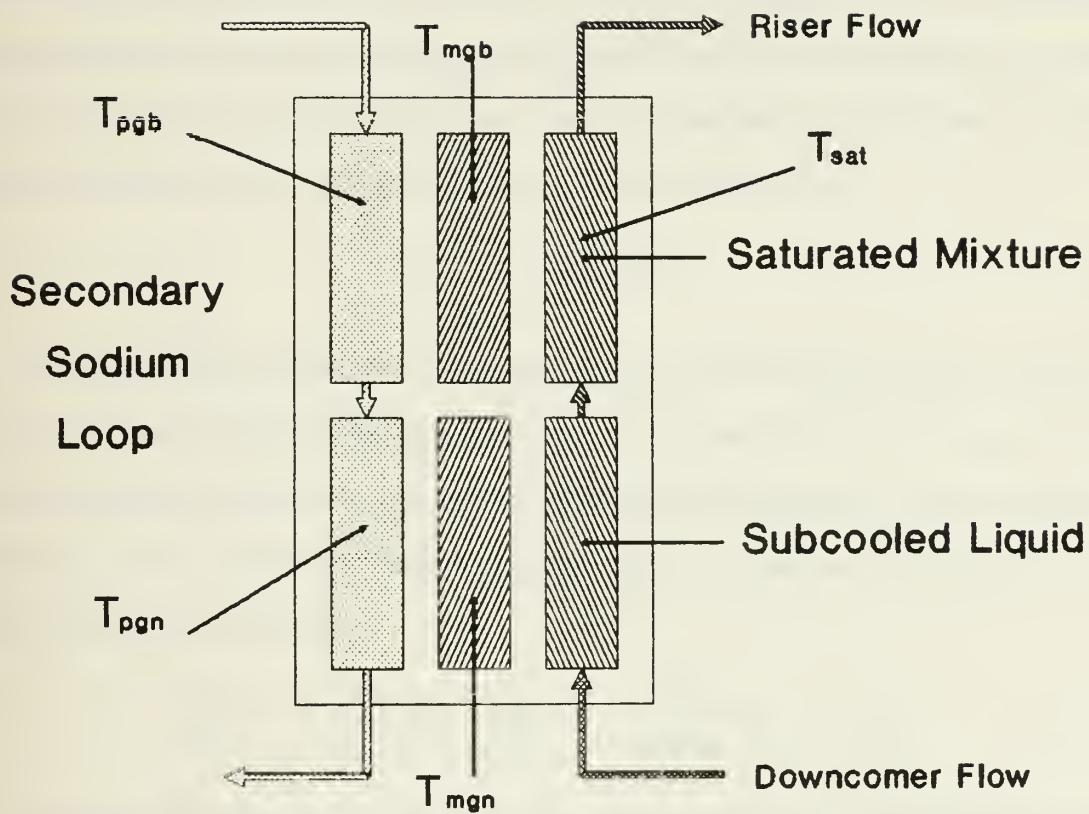
Figure (6) Boiler Lumped Parameter Schematic Diagram

the boiling region overall heat transfer coefficient primary sodium-to-metal (W/°C), M_{pgb} is the primary side boiling region node fluid mass (kg), and C_{pgb} is the primary side fluid specific heat (J/kg°C).

$$\frac{dT_{pgb}}{dt} = \frac{W_s}{M_{pgb}}(T_{pgb}^{in} - T_{pgb}^{out}) - \frac{(UA)_{pmgb}}{(MC)_{pgb}}(T_{pgb} - T_{mgb}) \qquad (2-17)$$

The average primary coolant temperature in the steam generator boiling region can be determined by substituting Eq. (2-18) into (2-17). The relationship in (2-18) is obtained by assuming a linear temperature change along the length of the node. Rearranging (2-18) allows one to solve for the node outlet temperature. This outlet temperature will be used as the inlet temperature for the primary coolant non-boiling region nodal equation.

$$T_{pgb} = \frac{T_{pgb}^{in} + T_{pgb}^{out}}{2} \qquad (2-18)$$

In the non-boiling region of the steam generator, a nodal equation similar to that in the boiling region can be derived from the energy balance, as shown in Eq. (2-19). T_{pgn} represents the sodium coolant temperature in the primary side non-boiling region, T_{mgn} is the metal node temperature in the non-boiling region, M_{pgn} is the metal node mass, and $(MC)_{pgn}$ is the metal node total heat capacity (J/°C).

$$\frac{dT_{pgn}}{dt} = \frac{W_s}{M_{pgn}}(T_{pgn}^{in} - T_{pgn}^{out}) - \frac{(UA)_{pmgn}}{(MC)_{pgn}}(T_{pgn} - T_{mgn}) \qquad (2-19)$$

As in the boiling region, a linear change in primary side sodium coolant temperature is assumed. This relation ship, shown in Eq. (2-20), is substituted into (2-19) to solve for the nodal temperature. (2-20) is then used to solve for the steam generator primary outlet temperature (T_{pgn}^{out}). The temperature at the outlet is then linked to the IHX secondary inlet by the pipe element discussed earlier.

$$T_{pgn} = \frac{T_{pgn}^{in} + T_{pgn}^{out}}{2} \qquad (2-20)$$

43

The boiling region metal wall nodal temperature is described by an energy balance as shown in Eq. (2-21). $(UA)_{pmgb}$ represents the overall heat transfer coefficient primary for sodium-to-metal wall (W/°C), $(UA)_{mgrb}$ is the overall heat transfer coefficient metal-to-riser fluid, and $(MC)_{mgb}$ is the boiling region metal node heat capacity (J/°C).

$$\frac{dT_{mgb}}{dt} = \frac{(UA)_{pmgb}(T_{pgb} - T_{mgb}) - (UA)_{mgrb}(T_{mgb} - T_{sat})}{(MC)_{mgb}} \qquad (2-21)$$

In the non-boiling region of the steam generator, the metal node is described by Eq. (2-22), which is obtained from an energy balance. T_r is the riser fluid temperature, $(UA)_{pmgn}$ is the overall heat transfer coefficient for primary sodium-to-metal, $(UA)_{mgrn}$ is the overall heat transfer coefficient for metal-to-riser fluid, and $(MC)_{mgn}$ is the non-boiling region metal node heat capacity (J/°C).

$$\frac{dT_{mgn}}{dt} = \frac{(UA)_{pmgn}(T_{pgn} - T_{mgn}) - (UA)_{mgrn}(T_{mgn} - T_r)}{(MC)_{mgn}} \qquad (2-22)$$

Since the two nodes on the secondary, or riser, side of the steam generator involve water in either subcooled or saturated mixture states, the energy balance will take on a modified form. In this model, we choose subcooled region (non-boiling) length and steam exit quality as the steam generator evaporator section states. The energy balance equations are derived in terms of these two states. The subcooled region length determines the size of the two axial regions in the steam generator, and the steam exit quality will help determine the amount of energy removed from the secondary side of the evaporator.

The subcooled region length time derivative is given by a dynamic energy balance on a control volume in the riser which has a moveable boundary. The position of this boundary determines the subcooled region length and is found by integrating Eq. (2-23). L_n represents the non-boiling length, $(UA)_{mgrn}$ is the overall heat transfer coefficient for metal-to-riser fluid, W_r is riser fluid mass flow rate, h_f is saturated liquid specific enthalpy, h_{in} is downcomer fluid

44

specific enthalpy, ρ_r is riser fluid density, C_{rn} is riser subcooled fluid specific heat capacity, and V_r is the volume per unit length of the riser channel. The boiling length is obtained by subtracting the non-boiling length from the overall channel length.

$$\frac{dL_n}{dt} \;=\; \frac{(UA)_{mgrn}\,(T_{mgn}-T_r)\;-\;W_r(h_f-h_{in})}{T_r\rho_r C_{rn} V_r} \qquad (2-23)$$

By analyzing the boiling region of the steam generator and writing another energy balance, we can use Eq. (2-24) to describe the dynamic behavior of the saturated mixture specific enthalpy. h_{out} represents saturated mixture specific enthalpy at the outlet of the evaporator (J/kg), $(UA)_{mgrb}$ is the overall heat transfer coefficient for metal-to-riser fluid, M_{rb} is the boiling region riser fluid mass, and T_{sat} is the riser fluid saturation temperature.

$$\frac{dh_{out}}{dt} \;=\; \frac{(UA)_{mgrb}\,(T_{mgb}-T_{sat})\;-\;W_r(h_{out}-h_f)}{M_{rb}} \qquad (2-24)$$

Exit steam quality is found from the relationship in Eq. (2-25). X is the steam quality, and h_{fg} is the latent heat of vaporization (J/kg).

$$X \;=\; \frac{h_{out}-h_f}{h_{fg}} \qquad (2-25)$$

The boiler is simulated using the DSNP module BOILG1.

2.5 Chapter Summary

In this chapter, we presented the state equations which determine the dynamic behavior of one module of a PRISM type steam supply system. All the equations are derived from physical models, using the conservation of mass and energy as underlying principals. By linking the state variables together in the proper manner, and using a suitable integration scheme for solving the time derivatives, it is now possible to simulate the dynamic characteristics of a power plant on a digital computer (see Chapter 4). Or, the state equations can be used to analyze the steady state characteristics of the power plant thermal energy transport

system (see Appendix B). Although many details have been lumped together into reasonably simple relationships, the physical characteristics of the power plant system have been preserved without resulting to linear approximations. The resulting plant model will serve the purpose for which it has been developed, namely, for use in the synthesis of a digital control system which will be discussed in Chapter 3.

Chapter 3 - Control System Synthesis

3.1 Introduction to the Multi-Modular Control Problem

This chapter provides an overview of the control problem in the multi-modular reactor plant, balancing requirements of the nuclear heat generation process against the requirements of the steam generation process and results in the selection of a plant control principle. In addition, a concept for a fault-tolerant supervisory controller utilizing a non-linear, reactivity constraint-based control methodology is presented.

In a nuclear power plant, the purpose of the control system is to maintain the power output of the reactor at a level which matches the load placed upon it. Nuclear power plants differ from other processes by having to operate with an independent safety system which will shut down (SCRAM[2]) the plant if an unsafe condition exists. Any automatic control of the reactor should never pose a challenge to the safety system. SCRAMs, while protecting the plant from potential damage, place undesirable cyclic thermal stresses on plant components and penalize plant availability factors. Therefore, a well designed fault-tolerant reactor plant controller will be designed to ensure that the plant parameters never reach values which would cause the safety system to activate.

Electric power demand follows a daily cycle, with the largest demand occuring during daylight hours, and the lowest demand during late night and early morning hours. Generating stations connected to the grid must be able to meet these changing demands to prevent cutbacks in service. Large nuclear plants have been used mostly for base-load operation in the past due to their low fuel cost, allowing the power level of the reactor to determine the output of

---

2 <u>S</u>afety <u>C</u>ontrol <u>R</u>od <u>A</u>xe <u>M</u>an, from the original critical pile (CP-1) experiments at the University of Chicago in 1942. In case the fission chain reaction were to go out of control, a safety observer would cut the rope which suspended a neutron absorbing control rod above the pile with an axe.

the electric generating plant. Fossil fueled plants, with their higher fuel costs, are generally operated in load-follow mode. As the amount of installed nuclear generating capacity increases, however, the ability for nuclear plants to operate in load-follow mode will become increasingly important. So, a properly configured controller should be flexible enough to operate the plant in either a load-follow or a reactor-follow mode.

A multi-modular reactor plant with a digital control system can be made to operate in a number of ways. In the proposed multi-modular power block controller, the plant control computer would receive a signal from the load dispatcher, specifying a load demand to be carried by the turbo-electric generator. This load demand signal would then be divided up amongst the on-line modules and a fraction of the total load signal would be sent to each module controller. At the same time, another signal would be sent to the turbine controller to adjust the throttle valve. For reactor-follow operation, the load demand signal would be initiated by the plant operator at the control console. Demands from the load dispatcher would be ignored by the power-block controller. Analysis of the control problem in this report focuses on the action of the module controller and assumes that the power level to be maintained by the nuclear steam supply module is an input supplied by the load dispatcher (load-follow) or plant operator (reactor-follow). Required measurements include reactor neutronic power and coolant temperatures. Other quantities needed for proper control will have to be estimated from mathematical models.

3.2 Control Strategies

Requirements for operation of the steam plant dominate control system considerations. Unfortunately, the best method of operating the steam plant conflicts with the simplest method of operating the reactor plant. Much of the discussion to follow on control strategy considerations and specific control system designs for fast reactor plants is taken from Ref. [14]. Generally speaking the strategies available are [15]:

48

1) sliding steam pressure

2) constant steam pressure

3) combination of the above

Since the module steam generators will generally be in parallel operation at different thermal power levels, the delivered steam pressure must be carefully controlled. If the steam pressure varies as little as possible over the range of power operation, parallel operation is simplified. Such a strategy minimizes the chance of instability and reverse flow which could occur with sliding steam pressure operation. If steam supply pressure varies widely between modules, the module supplying steam at the highest pressure would carry most of the thermal load, and the module at the lowest pressure would carry little thermal load, and possibly experience undesirable reverse flow instability. Before choosing a strategy, however, let us consider the alternatives in more detail.

3.2.1 Sliding Steam Pressure Program

Operating a reactor with sliding steam pressure is the simplest principle of control. Average reactor coolant temperature is maintained at a constant value, regardless of load. Though frequently referred to as "power control", the temperature is actually the controlled variable [16]. Reactor power automatically adjusts to changes in load through the negative temperature coefficient of reactivity. This control program is illustrated graphically in Figure (7) below. Since virtually all reactors are designed with negative temperature coefficients for stability and safety, operating at a constant average coolant temperature in the sliding steam pressure mode is the natural choice and requires the least amount of external control equipment.

Consider plant operation using the sliding steam pressure program. Assume the plant is at some steady power level and possesses a negative temperature coefficient of reactivity. Now suppose the load demand increases. For a short period, the additional energy needed to supply the load may be drawn from the stored energy in the coolant. However, this loss of

49

Temperature

Avg. Primary Temp.

Avg. Secondary Temp.

Saturation Temp.

Power
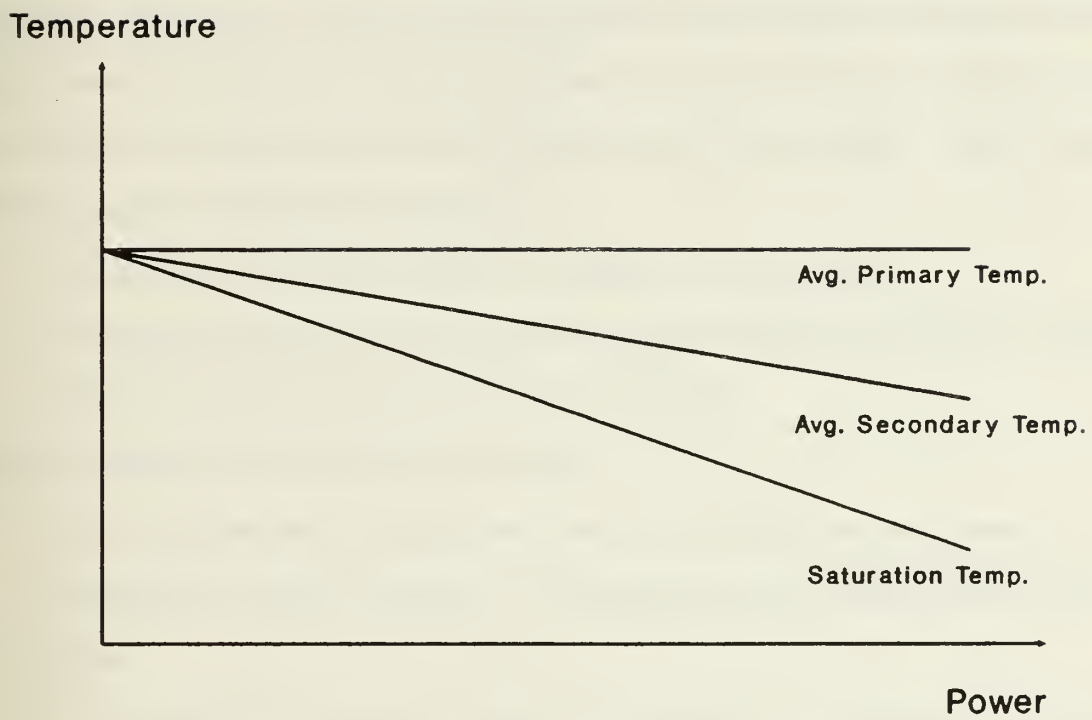
Figure (7) Sliding Steam Pressure

Control Program

50

energy will soon lower the temperature of the coolant entering the reactor. The lower inlet temperature will tend to lower the temperature of the fuel, which provides the major contribution to the negative temperature coefficient, and insert positive reactivity. Initially critical, the reactor will become temporarily supercritical and increase power. The additional power will restore the plant to its initial temperature and the negative temperature coefficient will level power back at its initial value. All this has occurred without the need for any control mechanism whatsoever. In other words, if the plant operational strategy is properly conceived and implemented with a constant average coolant temperature in mind, no control rod motion or other external means of reactivity control is necessary to handle changes in power demand. The advantages to this method of control are:

1) No external reactor control action is required for a load change.

2) The system is stable (for heat transfer time constants found in typical reactor designs).

3) Stored energy is used to meet increases in demand.

The disadvantages to this method of control are:

1) Secondary pressure and temperature must vary widely as the load changes, causing steam specific volume to fluctuate. Turbine size cannot be optimized and efficiency suffers.

2) To achieve the necessary variation in secondary side conditions, an automatic throttling valve may be necessary.

3) The boiler feed pressure variation is large, complicating feed pump design.

4) A sufficiently high and negative value for the temperature coefficient of reactivity is necessary to adjust the reactor power level with a reasonable response time. A low temperature coefficient will not change reactor power quickly enough to avoid thermal margins. Alternatively, a large temperature coefficient may result in unacceptable reactor power oscillations.

51

Generally speaking, constant average coolant temperature control works very well for operating the reactor plant, but not as well for operating the steam plant. In its most basic form, no instrumentation or active control is required on the reactor plant side. However, relying on negative temperature coefficient effects alone rarely enables the reactor to respond to load changes quickly. Control rod motion is frequently used to compensate for heat transport delays.

3.2.2 Constant Steam Pressure Program

Another strategy for plant control maintains steam pressure constant over all operating loads. In this type of program, active control actions are necessary to maintain constant saturation pressure conditions. Actually, in order to maintain a constant pressure at some reference point in the steam plant (e.g. steam header or turbine inlet), pressure would need to rise slightly with load to make up for additional head losses at increased steam flow rates. See Figure (8) for a graphical representation of a constant steam generator pressure operational strategy.

Consider a plant transient with the constant steam pressure control strategy. The load on the turbine generator increases, causing the turbine governor valve to open, admitting more steam. This increased steam flow rate is supplied by stored energy from the steam generator. When steam is removed faster than it is generated, pressure drops. This change in steam pressure is sensed by the pressure controller, and an error signal demands higher power from the reactor. Higher power is corresponds to a higher average coolant temperature. The reactor controller withdraws control rods from the core, allowing the neutron population and fission rate to increase. As core temperature increases, the negative temperature coefficient of reactivity will tend to turn back the increase in power by inserting negative reactivity. Control

52

Temperature

Avg. Primary Temp.

Avg. Secondary Temp.

Saturation Temp.

Power
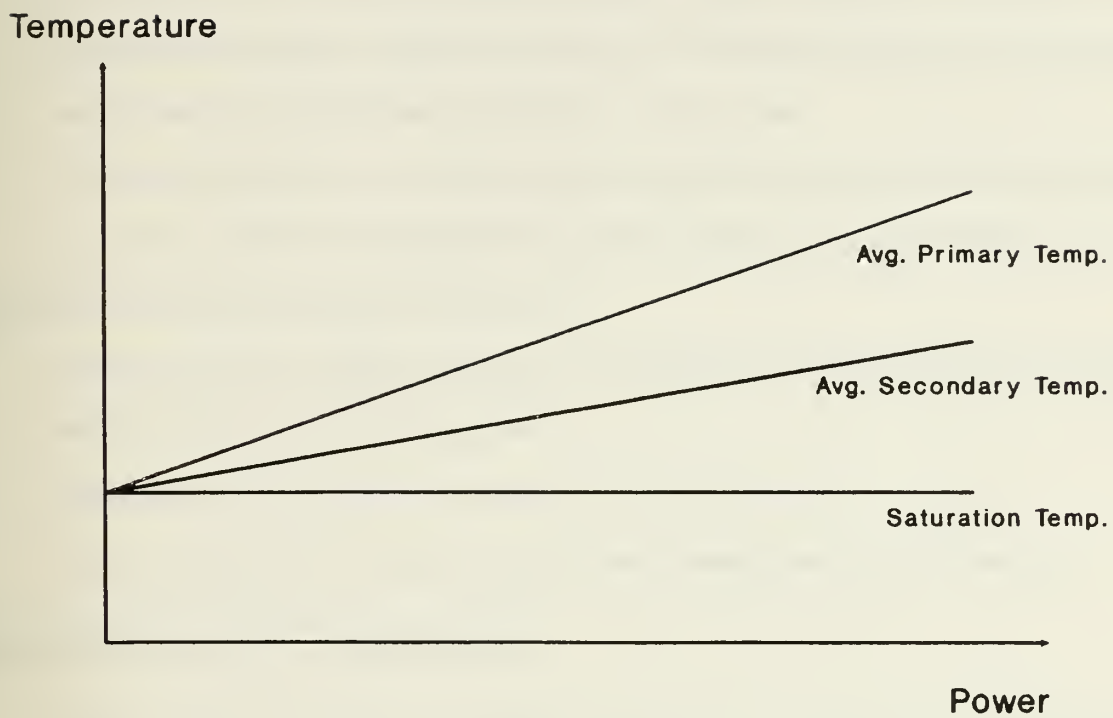
Figure (8) Constant Steam Pressure Control Program

53

rod motion must compensate for the reactivity inserted by the increasing primary temperature. The reactivity "worth" of the control rods must be great enough to overcome the effect of increasing average temperature over the operating range.

The advantages to the constant pressure method of control are:

1) The total steam volumetric flow rate through the turbine at high loads is not excessive, allowing for a more optimal turbine design. This is especially significant for the multi-modular design in which the turbine may be operating at partial load with just one module on-line, or at full load with three modules on line.

2) The secondary plant as a whole may be designed for optimum operation with fewer automatic controls (i.e. throttling valves, boiler feedwater pressure controls, etc.).

The disadvantages to this type of control are:

1) The effects of the negative temperature coefficient must be overcome when changing between steady state operating points.

2) Stability problems may arise during certain load transients.

3) The reactor plant must quickly replace stored energy used during transients.

3.2.3 Flow Control Considerations

Reactor plant coolant flow conditions must also be considered when choosing the multi-modular reactor plant control principle. The possible choices include constant coolant flow, variable coolant flow, or some combination thereof. The relationship between coolant flow and temperature change across the reactor core and heat exchangers is expressed by the simple relationship in Eq. (3-1). $\dot{Q}$ represents the thermal energy transfer rate, W is the mass flow rate, C_p is the fluid specific heat capacity (J/kg°C), and T_h and T_c represent the coolant hot and cold temperatures, respectively.

$$\dot{Q} = WC_p(T_h - T_c) \qquad (3-1)$$

The advantages of the variable coolant flow program are:

54

1) Thermal shocks to structural components are minimized upon scrams from full power operation.

2) Increased efficiency for the plant at low power is provided because of the reduction in pumping power.

3) Loop transport delay times are minimized, thus providing a faster response time.

The disadvantages of the variable coolant flow program are:

1) Nuclear stability is more difficult to analyze, due to the variable time constant in loop thermal transport delays.

2) Thermal shocks to plant components can be greater upon scrams from low power.

The advantages of the constant coolant flow program are:

1) Control system complexity is reduced.

The disadvantages of the constant coolant flow program are:

1) Plant control and operational flexibility is reduced; e.g. one pump could not provide service for two coolant loops by operating at an increased capacity.

2) Loop transport delay times are increased at lower flow rates, reducing the ability of the plant to respond to load changes.

The average temperature increase of liquid metal coolant as it flows through the reactor core is five to six times greater than the temperature increase in a water cooled reactor. Because of sodium's high thermal conductivity, coolant temperature transients occur relatively quickly in a liquid metal cooled reactor (LMR). Conceivably, the bulk primary coolant average temperature could be used to effectively regulate the neutron power level since it lags closely behind the power level. Outlet temperature could be adjusted using primary flow control. Using variable flow allows for greater flexibility in operation of the plant and, if a constant steam pressure control principle is chosen, reduces thermal stresses in the plant upon load

changes. The rapid response of sodium temperature also requires that some means be provided to prevent over-cooling of the plant upon a reactor scram. This might be accomplished by the safety system through a controlled flow reduction upon a large power decrease.

3.3 Overview of Control Strategies Used on LMR Plants

From the preceding discussion, we can see the LMR plant lends itself to a number of alternate control strategies and offers the control system engineer a wide range of options. Further evidence of the diversity of control options can be found by examining the methods employed on earlier LMR designs. All of the plants considered below share common characteristics with a PRISM module of having a reactor, one or more primary loops, intermediate heat exchangers, secondary loops, and steam generators. They differ from the PRISM power block by utilizing only one reactor plant per turbine generator set (as opposed to being multi-modular designs), and also by using superheated steam cycles (PRISM is currently designed to supply saturated steam only).

3.3.1 Enrico Fermi Atomic Power Plant

The design of the Enrico Fermi control system [17] [18] is based upon three basic conditions:

1) Power changes are initiated at the reactor.

2) Sodium flows in the primary and secondary loops will be constant from startup to 100% power level.

3) The normal rate of change of power will be preset in the control system.

The system controls the reactor outlet temperature specified by a temperature set point and maintains a programmed reactor outlet temperature, regardless of the action of other variables, including reactor power and sodium flows. With constant sodium flows and a

56

scheduled reactor inlet temperature, reactor power is a function of the reactor outlet temperature. The reactor outlet temperature signal is used to position the regulating rod. A plant control program, for the Fermi reactor is shown in Figure (9)

The major components of the reactor control system are shown in Figure (10). The system consists of three channels:

1) Temperature error rate of change of power channel

2) Neutron flux or actual rate of change channel

3) Regulating rod velocity demand channel

A given power level setting is represented by the temperature demand signal, which is compared with the actual reactor outlet temperature signal. The difference between the temperature demand signal and the actual temperature signal is converted to a rate of change of power demand. A limiter provides positive protection against excessive loading rates. The lag unit prevents a sudden change in the rod velocity demand signal if a step change is made in the rate of change of power demand channel.
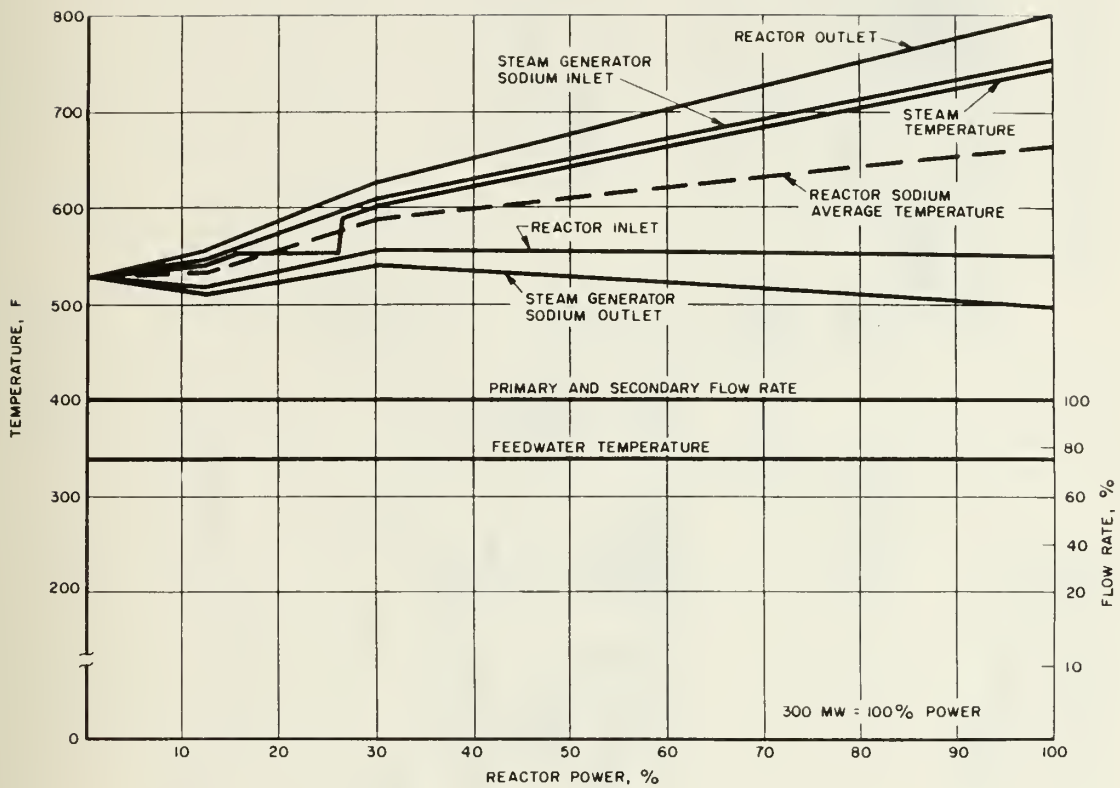
Figure (9) Fermi Atomic Power Plant

Control Program [19]

58
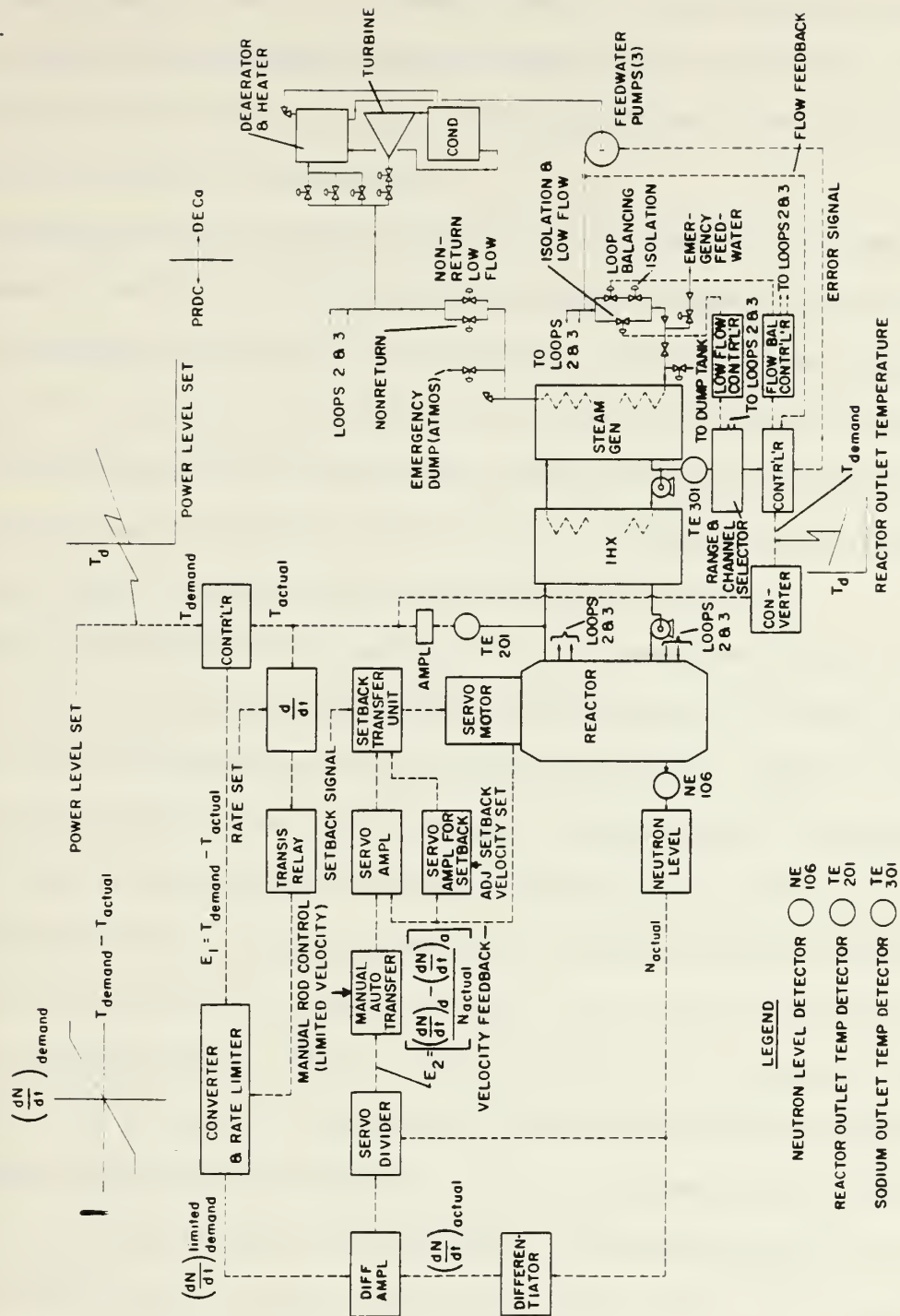
Figure (10) Fermi Atomic Power Plant

Control System [20]

The neutron flux, or actual rate of change channel is driven by the larger of two auctioneered signals from uncompensated ionization chambers. After amplification to a level compatible with the control system, the signal is differentiated in the rate unit. The output of the rate unit is the actual rate of change signal.

The regulating rod velocity demand channel compares the neutron rate of change with the temperature demand signal, and its output is the error signal. Because of the non-linearity of power level changes, the error signal is divided by the neutron flux signal in the servo divider to provide a constant control loop gain at all power levels. The output of the servo divider is the regulating rod velocity demand signal, which is one input to the control servo. The second input is actual rod velocity. The two inputs are combined, and the resulting error signal is used to supply a variable voltage to the regulating rod drive motor.

In order to block feedback to the reactor plant from the steam plant, feedwater flow is scheduled to maintain the steam generator sodium outlet temperature at a constant value, in accordance with the programmed temperature versus power schedule. Signals to schedule feedwater flow are from the reactor outlet temperature and steam generator sodium outlet temperature. Reactor outlet temperature, the reader will recall, is a load index which determines the operating point on the control program since with constant sodium flow and constant temperature of the sodium leaving the steam generator, it is a measurement of the thermal input to the steam generators. In addition, a signal proportional to steam generator sodium outlet temperature is compared with a temperature demand set point to establish a feedwater flow correction signal if the flow scheduled from reactor outlet temperature does not provide the correct steam generator sodium outlet temperature. The correction signal is fed to the scheduled feedwater flow relay, where it is compared with the reactor outlet temperature signal. The modified signal is the final feedwater flow demand. Feedwater flow to each steam generator is measured by pressure drop across an orifice. A signal proportional to actual flow

is compared with the feedwater flow demand signal. If a difference between the two signals exists, the feedwater regulating valve is opened or closed until the measured flow equals demand.

Pressure in the steam generator is controlled during startup by dumping steam through dump lines or bypass lines. The set point is adjusted according to the mode of operation (startup or power operation).

The Enrico Fermi control design provides insight into a scheme for operating a plant in the reactor follow mode. Especially important is the method of using feedwater flow to control the secondary cold leg temperature, thus preventing feedback to the reactor from the steam plant.

3.3.2 Experimental Breeder Reactor-II

Experimental Breeder Reactor-II (EBR-II) bears many similarities to the PRISM design. Its primary loop is contained within a tank of sodium, much like PRISM. Also, EBR-II uses recirculating steam generators with steam drums. Much of its operational strategy could be applied to multi-modular reactors, although only the simplest controls are designed for automatic operation [3]. See Figure (11) for a diagram of the EBR-II primary and secondary control systems.

The basic control philosophy [21] consists of:

1) Provide a balance between the rates of heat removal in each of the major thermal systems, from cooling tower to reactor.

2) Provide essentially complete isolation of the reactor from the effects of turbine generator load variation.

---

3 EBR-II is currently being back-fitted with automatic controls.

Balance of heat flow between the thermal systems consists principally of balancing the heat removal rate of the secondary heat transport with the heat generation rate in the reactor. Any unbalance in these two rates produces a continuous change in the primary tank bulk sodium temperature. The EBR-II temperature and flow program is shown in Figure (12). Proper balance is maintained by regulating the primary system flow rate to provide a predetermined reactor coolant outlet temperature. The temperature variation between low and full power is used to maintain a constant steam pressure at all power levels. The secondary heat transport system flow rate is regulated so that the primary tank bulk sodium temperature remains constant. Regardless of power level, the temperature of the secondary system cold leg remains within a fixed range, and the temperature of the hot leg remains relatively constant, varying within a small range from very low power to full power. In this way, the rates of heat removal from both the primary and secondary heat transport systems are approximately proportional to the secondary sodium coolant flow rate. Feedwater flow rate and feedwater temperature to the steam generator are automatically controlled. See Figure (13) below for a diagram of the steam and feedwater system. Steam pressure at the turbine throttle is held constant by a power pressure valve, which dumps excess steam directly to the condenser.
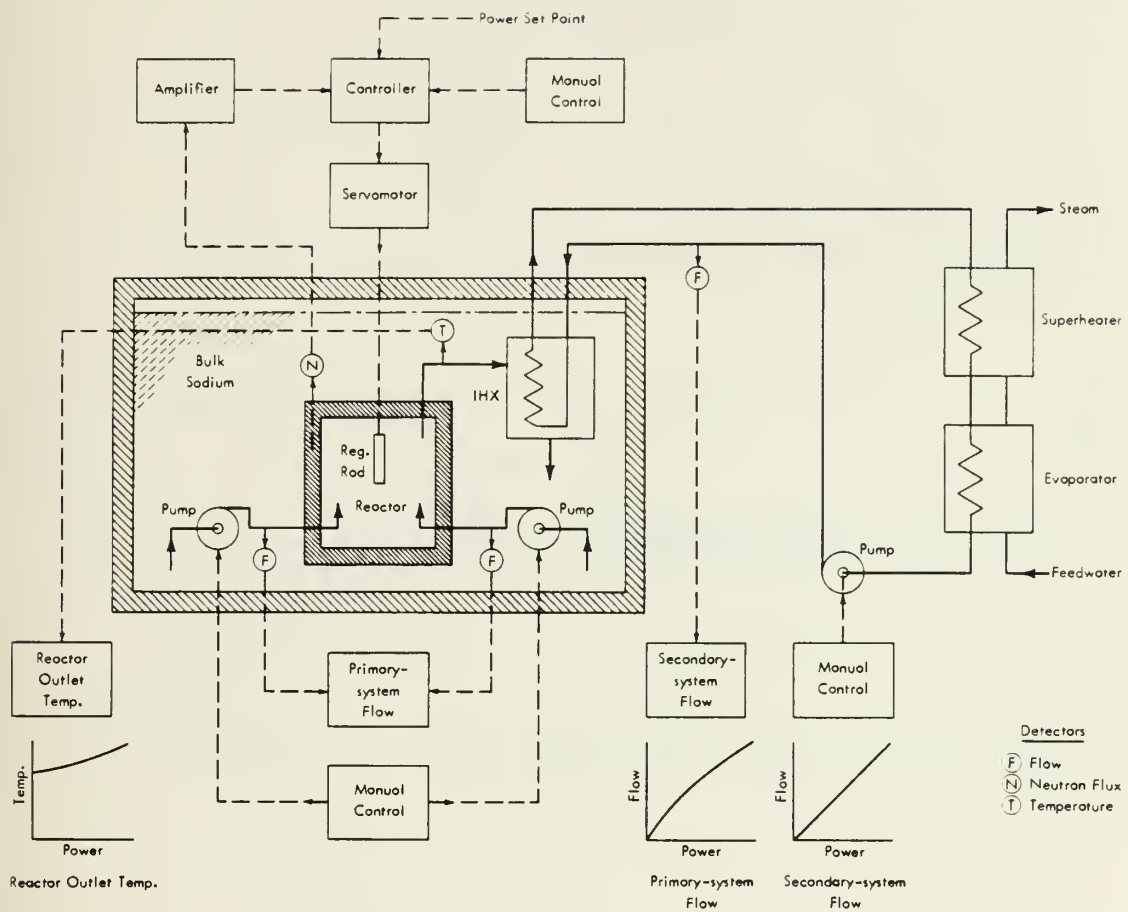
Figure (11) EBR-II Primary and Secondary Control System [22]

63
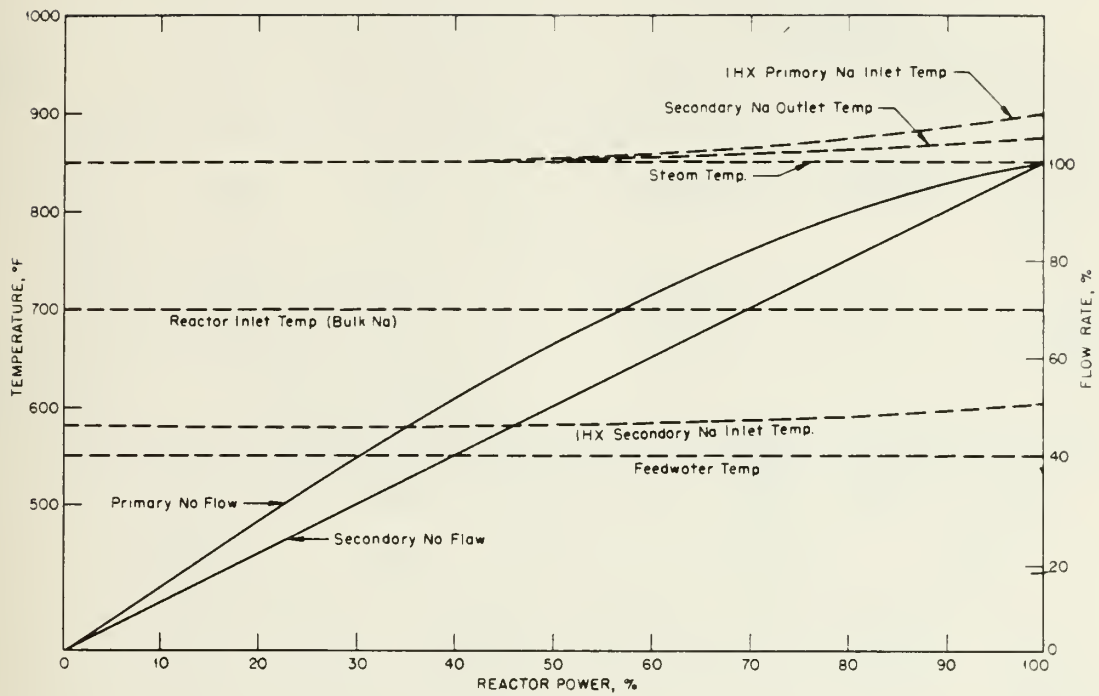
Figure (12) EBR-II Temperature and Flow Program [23]
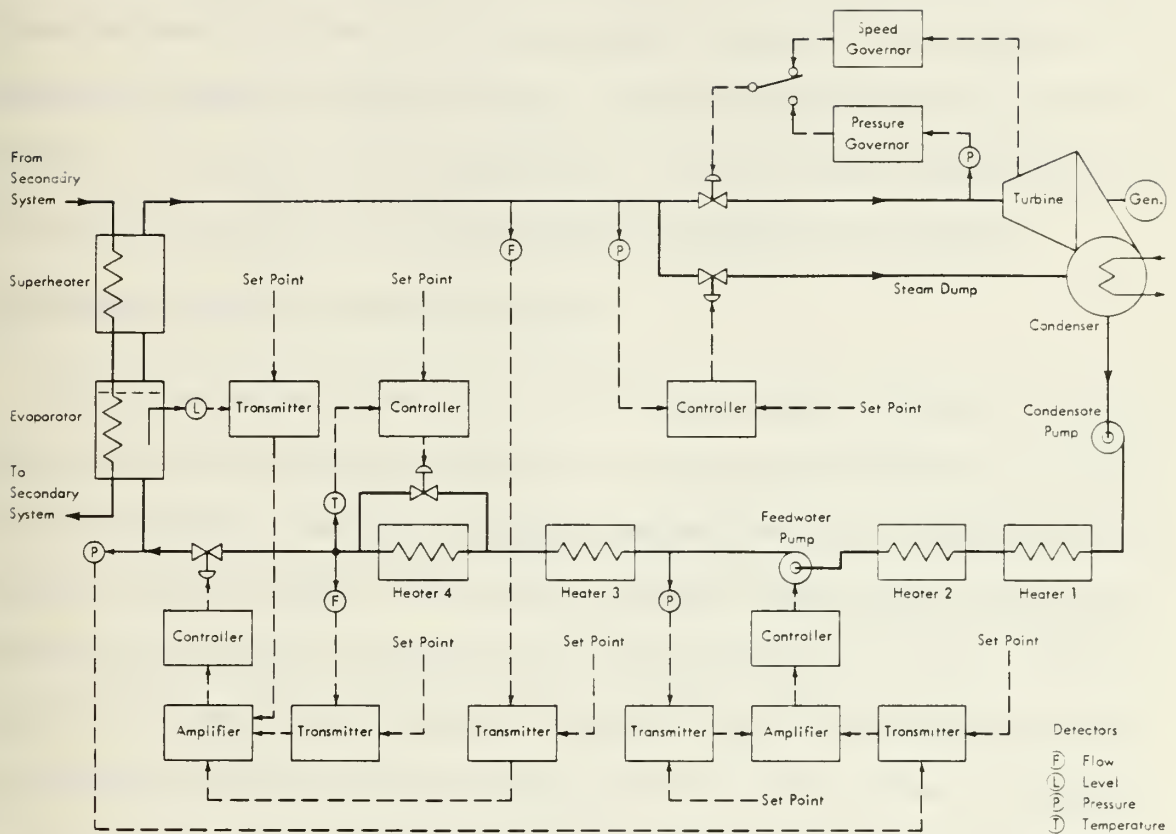
Figure (13) EBR-II Steam and Feedwater System [24]

65

An important feature of the EBR-II in regard to reactor stability is the virtual isolation of the reactor from the effects of changes in power system changes external to the reactor. There is no automatic control link between reactor power and the electrical load demand. The steam system incorporates a full flow steam bypass around the turbine to the condenser, a turbine generator load limiting device, and a regenerative feedwater system, which delivers constant temperature feedwater to the steam generator under all load conditions. This arrangement eliminates any effect of change in turbine generator load upon reactor inlet temperature. The primary system employed has a very large thermal capacity due to its pool-type design, thus the reactor inlet temperature can change only very slowly.

3.3.3 Hallam Sodium Graphite Reactor

Although the Sodium Graphite Reactor (SGR) built at Hallam, Nebraska, is not a fast reactor, it uses sodium as coolant and therefore its control system is of interest here [25] [26]. The plant is designed to automatically supply demanded steam flow at rated pressure and temperature over the range from 15% to 100% of rated load. Primary sodium inlet and outlet temperatures are held fairly constant to minimize thermal stresses in the reactor. Maximum design rate of change of load is 5 MW$_e$/min. To achieve this load following capacity, primary and secondary sodium flow rates are varied as a function of steam demand. This control concept provides operation comparable to that of a conventional fossil fuel steam power plant. The plant temperature program is shown in Figure (14).

The control system is divided into the following subsystems:

    1) Plant power control

    2) Sodium flow control

    3) Neutron flux control

    4) Convection flow control

    5) Feedwater and steam control
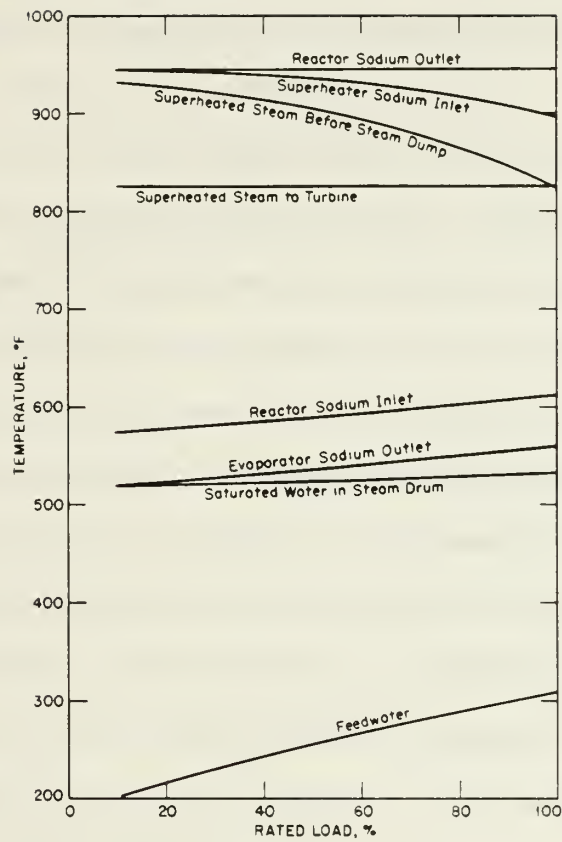
Figure (14) Hallam (SGR) Plant Temperature Program [27]

67

When all subsystems are on automatic, a variation in load causes the turbine governor to open or close the steam throttle valve, causing steam flow and pressure to change. The power plant control system detects the change in steam flow and commands a corresponding change in sodium flow from the division of load computer. Steam pressure acts as a trim signal on the steam flow signal to maintain correct turbine pressure. Sodium flow demand signals for the three primary and three secondary heat transport loops are generated in the division of load computer to match the demanded total steam flow from the plant power control system. Circuit flow ratios are set manually by the operator.

The secondary sodium flow control system detects the error between measured and demanded flow rate and adjusts the pump accordingly. Similarly, the primary sodium flow control system regulates the primary flow rate in response to demanded flow from the division of load computer. In addition, the reactor inlet temperature is maintained (at a value dependent upon load) by trimming primary flow with a temperature error signal. Sodium flow rates in the three primary loops are summed and multiplied by the desired temperature rise across the reactor (as set by the operator) to provide the power demand signal to the neutron flux control system. A power trim signal is also generated in the nuclear power computer as a function of outlet temperature errors. Both the reactor outlet plenum temperature and fuel channel outlet temperature are used to provide temperature compensation to the power demand signal.

The neutron flux control system operates on power demand from the nuclear power computer and the actual measured neutron flux. The difference between these two signals operates the rod drive relays, which drive the shim regulating rods at constant speeds in the proper direction to reduce the error to zero. The signal to the relays is gain compensated by the demanded neutron flux and the number of rods on automatic control. An inner loop with velocity feedback is used for improved stability and for generation of proportional reset actions. Travel limits on the inner loop automatically limit reactivity insertion.

The convection flow control system operates only upon a reactor SCRAM. Pump speeds are automatically reduced to zero. The ensuing natural convection flow in the primary is greater than necessary to remove reactor decay heat. The convection flow control system throttles the natural convection flow to maintain the fuel channel outlet temperature at a constant value.

Steam drum water level is maintained constant by the conventional three element feedwater control system principle, operating on drum level, feedwater flow rate, and steam flow rate. Constant pressure is maintained at the input of the feedwater control valve by the feedwater pressure control system. Superheater outlet temperature varies with load, but turbine steam temperature is maintained at a set value by the attemperator control system. This is accomplished through bypassing saturated steam around the superheater and mixing it with superheated steam to obtain the desired temperature.

The steam dump control system provides a means for conserving feedwater while dissipating reactor when a turbine generator outage occurs during periods of low power testing. It also serves to remove decay heat from the primary following a shutdown.

All controllers have deviation alarms, which are actuated upon excessive error between the controlled variable set point and measured value. Temperature changes are limited to 10 °C/hr, sodium flow changes to 20% of rated flow per minute.

3.3.4 Clinch River Breeder Reactor

The Clinch River Breeder Reactor (CRBR) represents a recent, advanced design of a large liquid metal cooled fast breeder reactor. Though never built, the control system design for the CRBR provides useful information on methods of implementing automatic controls, using advances in technology [28].

69

The plant control system provides overall control and coordination of the reactor, heat transport system, auxiliary systems, turbine and balance of plant systems for all normal plant operating modes. This system integrates the manual and automatic controls provided to maintain the plant at the desired power, temperature, pressure, and flow conditions for startup, load changing, rated power, standby, and shutdown conditions. Automatic control of the power, sodium and steam temperatures, steam pressure, sodium flows, steam and water flows is provided for load changing and power operation above 40% rated power. Robust signal validation and fault detection measures are implemented to ensure reliable control of the plant. The automatic control includes two modes:

1) Reactor-follow mode, in which the plant is operated based upon a reactor power level established by the plant operators. This could be used during reactor startup testing or when the plant is base-loaded.

2) Load-follow mode, in which the plant responds to the electrical load demand from the utility automatic load dispatch system. This makes plant operation much more flexible from an electric utility point of view.

The automatic control system maintains the temperatures, flows, and pressures according to a specified program shown in Figure (15).

The plant control system accomplishes the functions described above by using a two level feedback control system. The top level "supervisory " controller uses the automatic load dispatch demand signal or the plant operator determined reactor power signal as input. From this input, the temperature, power, flow, and pressure setpoints are established electronically according to the control program. These setpoints are the inputs for the reactor and sodium flow (bottom level) controllers which maneuver the control rods and sodium pump drives as necessary to attain the desired plant conditions. Figure (16) is a functional block diagram of

SYSTEM OPERATING TEMPERATURES (°F)

SYSTEM OPERATING TEMPERATURE (°F)

960
940
920
900

740
720
700
680
660
640
620
600
580
560

PRI HOT LEG

INTER HOT LEG

STEAM

PRI COLD LEG

INTER COLD LEG

INTER FLOW

EVAP. INLET

1.0
0.9
0.8
0.7
0.6
0.5
0.4
0.3
0.2
0.1
0

INTER FLOW (Required/Design)

T-H DESIGN VALUES
PRIMARY   995°F
INTERMEDIATE   936°F
STEAM   900°F

OPERATING PARAMETER versus POWER LEVEL FOR CONSTANT STEAM PRESSURE AND TEMPERATURE AND CONSTANT PRIMARY FLOW TO POWER RATIO

0   20   40   60   80   100

PERCENT-DESIGN POWER

Figure (15) Clinch River Breeder Reactor Control Program [29]

71

this two level control system. Included on the diagram are the supervisory, reactor, primary and intermediate flow, feedwater flow and feedwater pump pressure controls which are described in detail below.

The supervisory control generates the setpoints for the heat transport system flow control, reactor control and turbine control loops. The demand signal (load or power) is transformed by function generators with the necessary dynamic terms to temperature, pressure, flow and power setpoints. Steam temperature, steam pressure, turbine load demand and heat transport system sodium temperatures as feedback variables. The supervisory control outputs are transmitted to the flow, turbine and reactor control loops as trim and feed-forward inputs.

The reactor controller adjusts control rod position to maintain the reactor power or core outlet temperature at a programmed value, depending upon whether the plant is operated in the reactor follow or load-follow mode, respectively. The temperature setpoint is generated either manually or by the supervisory control. Programmed temperature demand is determined from the control program, as a function of plant load. This programmed temperature signal is then added to the controlled output temperature trim demand and fed forward to the reactor temperature controller. The temperature demand trim signal is obtained from the turbine temperature controller to maintain superheated steam conditions. In the reactor-follow mode, rods are controlled according to the error generated by the difference by the power set point and the measured power. In the load follow mode, rods are controlled according to the error generated by the demanded temperature set point and the measured core outlet temperature. Both control signals are passed through a dead band circuit, which sets up a band of no control. This dead zone prevents excessive control rod movement and allows the negative temperature coefficient effect to regulate small transients. Rod withdrawal prevention blocks based on high neutron flux to flow ratio and high neutron flux are also provided to prevent the automatic control system from challenging the safety system.

72

Figure (16) Clinch River Breeder Reactor Control System [30]

73

The flow control system consists of six controllers used to drive the three primary and three secondary sodium pumps. Each sodium pump has a cascade system with an inner loop using speed as the feedback signal and an outer loop based on a flow feedback signal. Flow control range for normal operations is 20% to 100% of rated flow. Flow setpoints are generated either manually or by the supervisory control. A feed-forward secondary flow demand signal is produced by a flow demand program function of plant load. Feed-forward aids the plant in responding to load change transients. This program flow demand is then added to the controller output trim demand to obtain the net secondary flow demand for use by all three secondary flow controllers. Primary flow controls are trimmed on a dynamically compensated error signal composed of a reactor inlet temperature set point and measured reactor inlet temperature.

The steam pressure controller operates on the steam pressure error signal and provides a dynamic compensated pressure trim demand to the intermediate loop flow controllers. The error signal is obtained from the algebraic sum of the pressure set point and the feedback measured steam pressure signal from the inlet to the turbine control valve.

The feedwater flow control system is part of the automatic control in the steam generator system. Water level in the steam drum is controlled with a cascade loop using feed-steam flow mismatch in the inner loop and level in the outer loop. Since this loop automatically adjusts for load follow operation, no input is required from the supervisory control. Feedwater flow varies according to the position of the feed throttle valve, as controlled by the feedwater flow control system.

Feed pump pressure control drives the variable speed feed pumps to maintain the appropriate pressure differences across feedwater throttle valves. This loop automatically adjusts for load follow operation. In addition to all of the functions listed above, the supervisory controller also provides demand signals to the turbine control system.

74

The multi-variable control problem of plant control is handled in the CRBR by dividing control actions into two levels, with the lower level controllers designed as regulators to maintain the controlled variable at a demand set point. The top level supervisory controller has the task of determining what operating region the lower level controllers should be set to operate in. Since the lower level regulators could possibly introduce instabilities, the setpoints chosen by the supervisor must necessarily be in a region of stability. Dynamic simulation of the plant time domain response should prove to be a useful design tool for a control system of this type.

3.4 Power Block Supervisory Controller

In developing the control system for the multi-modular reactor plant, a multi-tiered structure similar to that used in the CRBR design could be used. The highest level of such a system would reside in the power block supervisory controller. As discussed above, a supervisory controller is designed to determine the region of operation for the plant, and lower level controllers regulate plant parameters within this region. Beneath the power block supervisor, independent module controllers and the steam turbine plant controller perform the necessary regulating and maneuvering actions as directed by the power block supervisory control.

The input to the module controller consists of a load demand signal from the power block supervisor, in addition to a steam pressure demand. A detailed analysis of the manner in which these demand signal from the power block supervisor should be determined is beyond the scope of this report, but the use of an electric circuit analogy provides some useful insight into the problem. Refer to Figure (17) for a diagram of such a circuit.

P_A, P_B, and P_C represent the pressures in the steam for modules A, B, and C, respectively. P_H represents the steam header pressure at some arbitrary reference point. P_T signifies the turbine inlet pressure, downstream of the turbine throttle valve, shown as R_T - a variable

75
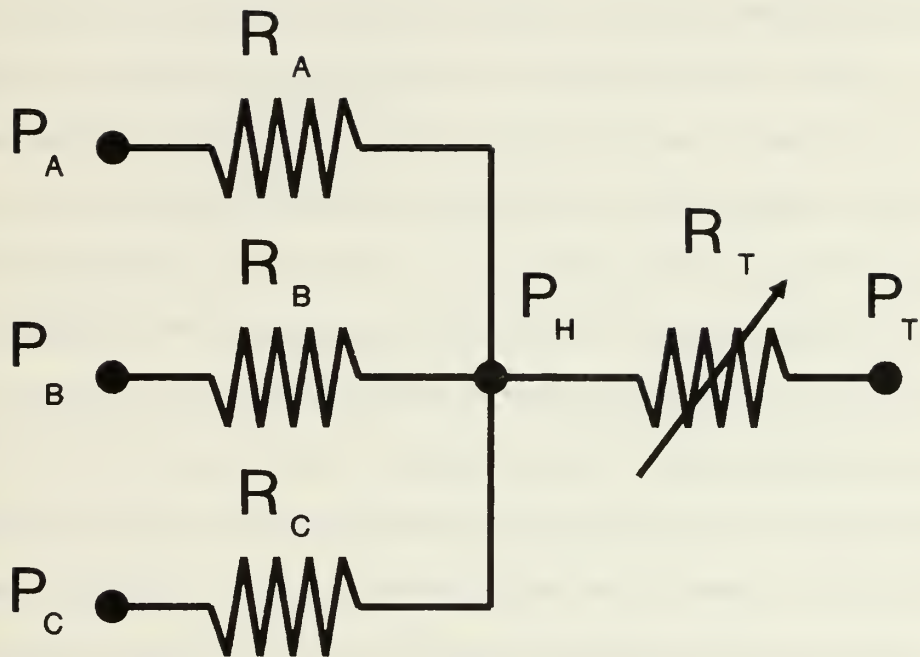
Figure (17) Steam System-Electric Circuit Analog

non-linear resistance to flow. R_A, R_B, and R_C represent non-linear flow resistances between each drum and the steam header. The pressure drop across a non-linear impedance takes on the form shown in Eq. (3-2), where Q_A represents the volumetric flow rate of steam through R_A.

$$P_A - P_H = R_A Q_A^2 \qquad (3-2)$$

With this simplistic model of the steam system, consider the process of sharing the turbine load between modules. For steady state conditions, the load demanded of each module would simply be a fraction of the total steam flow used by the turbine. If load is to be shared equally amongst the modules, P_A, P_B, and P_C would all be set at equal values (assuming $R_A=R_B=R_C$). Now, if the turbine throttle valve remains at a fixed position, header pressure and turbine inlet pressure remain constant as well. At this point, however, the designer must choose which pressure the control system should maintain constant at various loads.

For a strategy in which the turbine inlet or steam header pressure is to be held constant for any given load, the power block supervisory control would demand that the pressure generated in each steam drum be maintained at values appropriate for the given demand and load-sharing arrangement. The power block supervisory element would determine the pressure necessary in each drum based upon the (fixed) pressure reference, and the calculated pressure drops obtained from the electric circuit analog model or other method. This value of drum pressure then is converted to a pressure demand within the power block supervisor and sent to the module supervisory controller, along with the steam flow demand. The actions taken by the module supervisory controller upon receiving the demand signals are discussed below.

3.5 Module Supervisory Controller

The proposed PRISM nuclear steam supply module makes use of some of the ideas used on earlier LMR power plants and also applies a promising non-linear control technique, namely the "reactivity constraint approach". Some of the control system architecture from the Clinch River plant can be adapted for use on PRISM. The multi-level control concept, with a supervisory (top level) controller for the module, and lower level loop controllers offers attractive features. Modern control systems are using more distributed systems, with regulators on lower level control loops being supervised by a higher controller.

The module operating region is defined within the modular supervisory controller. Programmed values of plant parameters are determined from a map of equilibrium plant temperatures and flows, based upon the pressure and steam flow demand signals from the power block controller. With two demands placed upon it by the power block, the module supervisory controller calculates necessary plant parameters from a three-dimensional control program. Instead of entering with steam demand only, the necessary operating point is determined from the control program map by entering with both steam demand and pressure. Implementing such a control system requires a detailed analysis of required plant parameters necessary to sustain a given steam demand in a desirable load-sharing arrangement. Appendix B gives an analysis of the steady state plant temperatures within a PRISM steam supply module. This analysis is based upon the state equations developed from the plant model in Chapter 2. A control program generated from the steady state analysis provides the module supervisory controller with an estimate of the plant temperatures and flows which result in steam generation at the desired pressure and flow rate. Since the coolant temperatures are equilibrium values for a given power level in the reactor, power is effectively controlled by adjusting coolant temperatures as necessary to stay at the programmed operating points. A map of the programmed plant temperatures for maintaining a constant steam pressure of 6.7

78

MPa is presented below in Figure (18). A variable primary and secondary flow strategy to maintain a constant power-to-flow ratio has been chosen, as shown in Figure (19). Variable flow control allows for smooth load-following capability since induced thermal stresses in plant structures during load changes are minimized, allowing for more rapid transient response. Measures to prevent over-cooling of the plant upon a SCRAM should be implemented in the actual plant controller and safety system.

—
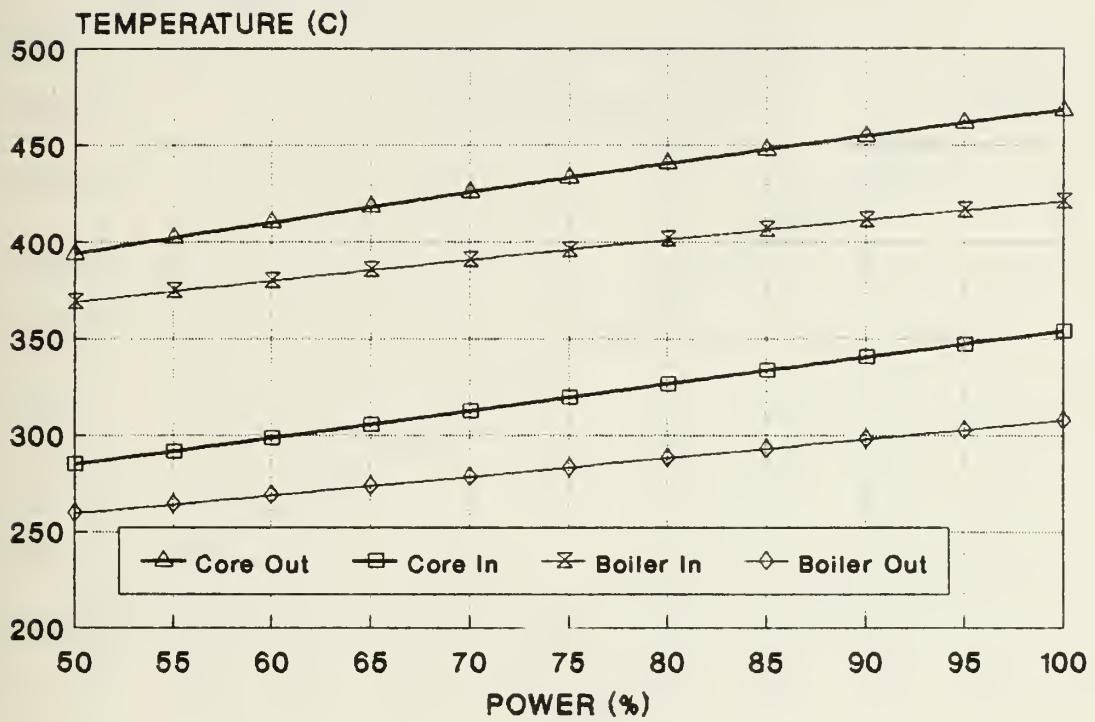
Figure (18) PRISM Temperature Control Program
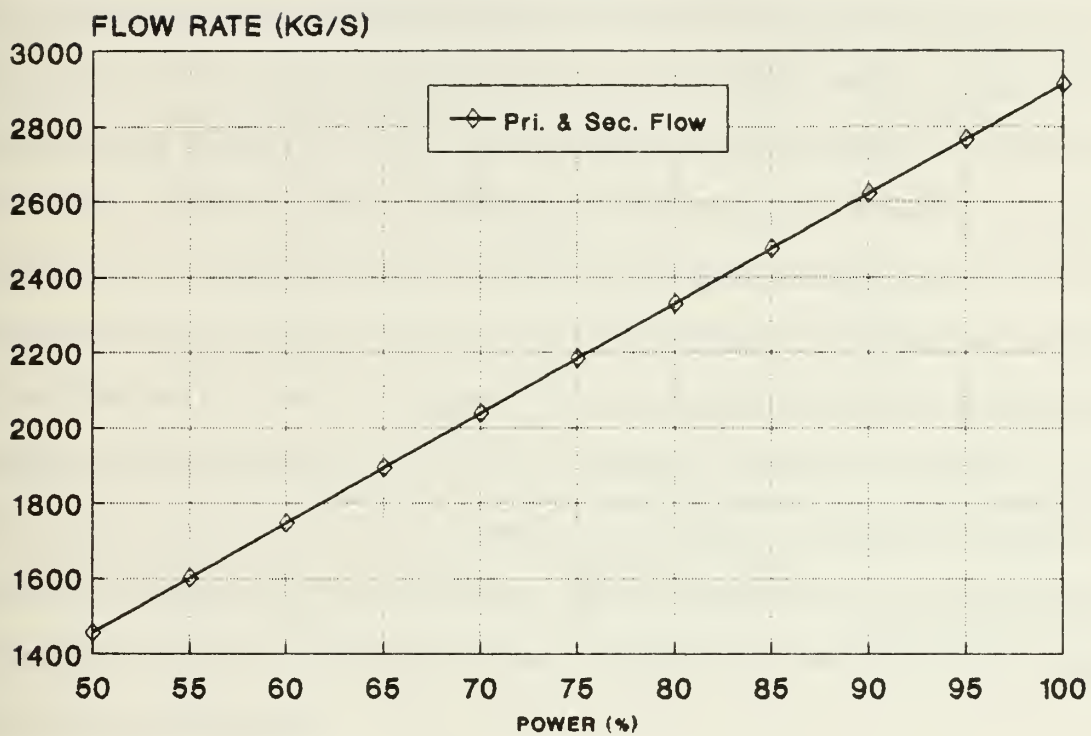
Figure (19) PRISM Flow Control Program

81

Having chosen a plant control principle and analyzed the associated steady state characteristics under such a control scheme, our attention must shift to the required task of the plant controller during transients and the need for supervisory control action.

3.6 Reactivity Constraint Approach to Reactor Control

Nuclear reactors behave as exponential devices. Linear system control techniques, though well developed, are unsuitable for unsupervised control of reactor temperature (power), owing to the non-linear and time-delayed behavior of the fission process. Traditionally, a control algorithm specifies the desired plant trajectory and, if the actual state of the plant differs from the specified one, uses a feedback signal to reduce the error. For safety-constrained systems, the control algorithm should also define the envelope of conditions in which it will be possible to halt the transient. Supervisory action then precludes operation beyond the safety envelope. The need for supervisory control is often unrecognized because it is generally only required if a system exhibits either non-linear or time-delayed behavior. One important goal of this report is to apply the reactivity constraint control method, discussed at length in [1], as part of a fault-tolerant supervisory controller. The use of the reactivity constraint approach towards closed-loop reactor control is designed to ensure that the controller will never challenge the plant safety system.

Basically, the reactivity constraint verifies "feasibility of control" before the control law is allowed to compute a control action. Feasibility of control requires that net reactivity be restricted so that it is always possible to stop the transient (make the reactor period infinite) by reversing the direction of motion of whatever control mechanism is associated with the controller [31]. If the control is feasible, that is, if the transient can be stopped before overshooting the desired power or temperature, using the maximum available control input rate, then the control law is allowed to compute the desired control action. If control is not feasible, that is, if the transient cannot be stopped before overshooting the desired power or temperature,

using the maximum available control input rate, then the supervisory element in the controller takes immediate action to restore feasibility of control. It is possible to implement such a supervisory element, which avoids overshoot at a future time, based only upon information available at the present time. The reactivity constraint-based controller is designed with the non-linearities of the system taken into account.

Deriving the reactivity constraint requires a description of reactor behavior in terms of the dynamic period. Remember that a nuclear reactor behaves as an exponential device, rather than a linear device. The instantaneous reactor period, $\tau(t)$, describes the rate of change of the neutron population (power) and is defined in Eqs. (3-3) and (3-4).

$$\tau(t) \quad = \quad \frac{1}{\omega(t)} \qquad\qquad (3-3)$$

where

$$\dot{N}(t) \quad \equiv \quad \omega(t)N(t) \qquad\qquad (3-4)$$

The dynamic period equation describes the instantaneous reactor period in terms of the reactivity and the rate of change of reactivity. Either the standard or alternate forms of the dynamic period equation may be used [1]. The standard equation is considered here, as shown in Eq. (3-5). Use of the standard form of the dynamic period equation leads to the presence of a derivative-containing term in the resulting expression, making the controller based upon the equation more sensitive to noise in measurements of standard effective decay parameter.

$$\tau(t) \quad \cong \quad \frac{\overline{\beta} - \rho(t)}{\dot{\rho}(t) \;+\; \lambda_e(t)\rho(t) \;+\; [\dot{\lambda}_e(t)/\lambda_e(t)]\,(\overline{\beta} - \rho(t))} \qquad (3-5)$$

83

$\rho(t)$ is net reactivity, $\dot{\rho}(t)$ is the rate of change of net reactivity, $\bar{\beta}$ is the effective delayed neutron fraction, $\bar{\beta}_i$ is the effective fractional yield of the ith delayed neutron group, λ_i is the decay constant of the ith precursor group, $\lambda_e(t)$ represents the standard effective multigroup decay parameter, and $\dot{\lambda}_e(t)$ its rate of change. The standard effective decay parameter is defined in Eq. (3-6) below.

$$\lambda_e(t) \equiv \frac{\sum\limits_{i=1}^{n} \lambda_i C_i(t)}{\sum\limits_{i=1}^{n} C_i(t)} \qquad (3-6)$$

$\lambda_e(t)$ cannot be directly measured, but several methods are available for estimating this parameter. Ref. [2] estimates both reactivity and the decay parameter using an extended Kalman filter. Ref. [32] describes another approach which does not restrict the sampling interval. This second approach rearranges Eq. (3-5) and makes some approximations to obtain a correlation between $\lambda_e(t)$ and net reactivity. Its use is restricted to transients for which the assumptions of small rates of reactivity change and near-asymptotic periods are reasonably valid. This correlation, though developed specifically for the MITR-II research reactor, is used in the implementation of the controller for the PRISM power plant model developed in this report. Of course, the use of this correlation between $\lambda_e(t)$ and reactivity means that the controller also needs an estimate of reactivity. Reactivity cannot be directly measured, but an approximate value can be obtained using a model for reactivity feedback in the plant and reactivity addition from control rod position.

For the controller used in this report, a very simple method of determining reactivity is used. Feedback reactivity from temperature changes and control rod movements is calculated from Eq. (3-7). ρ_0 represents reactivity contribution at beginning of transient, T_{av} is the average primary coolant temperature, and K_{fbk} is the feedback reactivity coefficient.

$$\rho - \rho_0 \ = \ (\rho - \rho_0)_{rod} \ + \ K_{fbk}(T_{av} \ - \ T_{av0}) \qquad (3-7)$$

Control rod reactivity is modeled as a function of rod height in the core. Reactivity from control rods is estimated from an integral rod worth curve similar to the one shown in Figure (20). Also illustrated is a typical differential rod worth curve. Note that reactivity estimates are related to measurable quantities, control rod height and average coolant temperature. Rod worths are determined from reactor physics testing, and are subject to change over the fuel cycle as poisons build up in the core. The effects of fuel burnup on the robustness of this method of control require investigation, but assuming the rod worth curves used in the controller are periodically verified against physics testing results, variations between actual and assumed rod worths should not seriously hamper control effectiveness.

Maintenance of feasibility of control implies that the contribution of the delayed neutrons to the period must be limited so that, upon attainment of the desired power level, the insertion of the control rod will make the rate of change of the prompt neutron population sufficiently negative so as to offset the continued rise in the delayed neutrons. This objective can be realized if the net reactivity is constrained so that the denominator of Eq. (3-5) can be made less than or equal to zero (note that the numerator - for safety reasons - is always positive). In mathematical terms, the condition of Eq. (3-8) must be met. $\dot{\rho}_f$ represents the rate of change of feedback reactivity, and $\dot{\rho}_c$ is the rate of change of control reactivity.

85
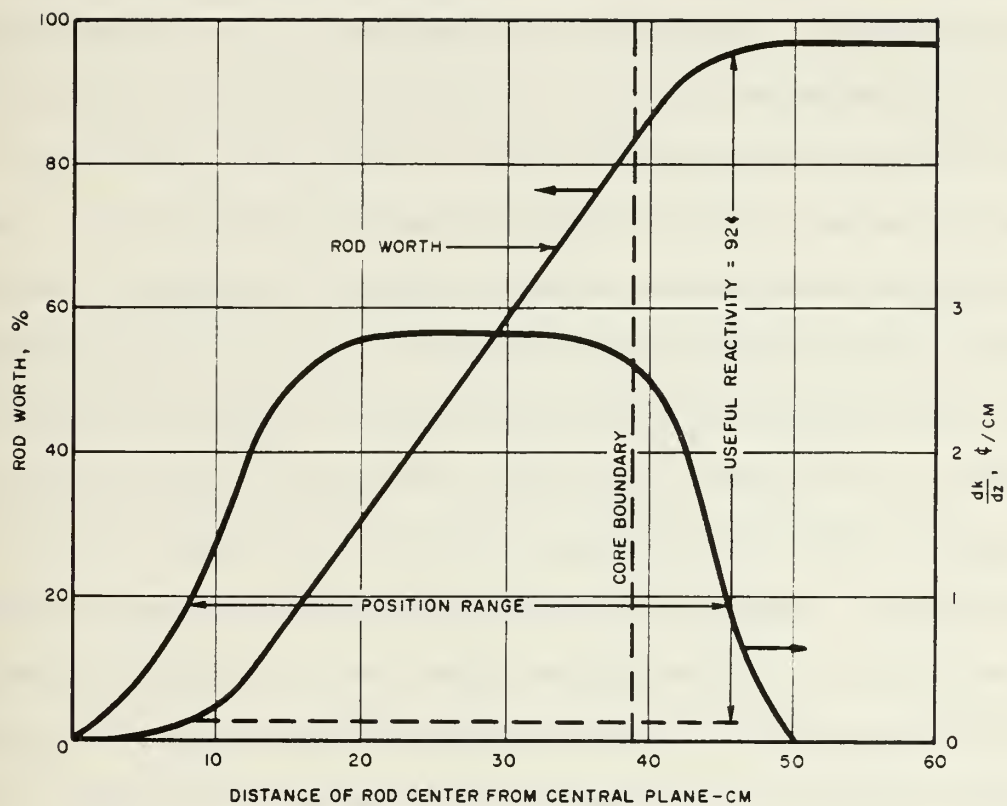
Figure (20) Control Rod Worth Curves

Integral Worth (on left) and Differential Worth (on right) [33]

86

$$\left[\lambda_e(t)\rho(t) \;+\; \frac{\dot{\lambda}_e(t)}{\lambda_e(t)}(\bar{\beta} - \rho(t)) \;+\; \dot{\rho}_f \right] \;=\; |\dot{\rho}_c| \qquad (3-8)$$

Note that $\rho(t)$ is the net reactivity, made up of reactivity which has been added deliberately, and also that present indirectly from feedback effects. The quantity $|\dot{\rho}_c|$ denotes the maximum available rate of change of reactivity that could be obtained were a control rod to be moved, and is a physical characteristic of the control system. It is always a non-zero, finite number, regardless of whether or not the mechanism is actually being moved. If the relation given by Eq. (3-8) is continuously observed, then it will be possible to drive the reactor period to infinity (steady state) and halt a power change by reversal of the direction of travel of the control mechanism. This methodology is referred to here as the "reactivity constraint" approach.

Cabral, in Appendix K of [2], takes the reactivity constraint control methodology and generalizes the approach, using it to control the position of a simple servo motor mechanism. The constraint can be implemented in many different forms, but in general, implementation depends upon information obtained from a plant model. The basic idea is to define two different times: the available time (τ_A), and the required time (τ_R). Available time denotes the time until the desired state is attained, given the present rate of change. Required time represents the time required to halt the transient using the available control input rate. The supervisory control element is then formulated to guarantee that the constraint in Eq. (3-9) is always met. If the constraint is satisfied, then the control law is free to maneuver control rods as if it had full control.

$$\tau_R \;\leq\; \tau_A \qquad (3-9)$$

Now that the concept of the reactivity constraint approach has been presented, let us consider how to obtain values for the required and available times which are so important for proper supervisory action. While required time (τ_R) depends upon reactor physics, the available time (τ_A) can be defined in several ways. The discussion to follow will define an available time for power overshoot and a time for a temperature overshoot.

3.6.1 Calculating Required Time

Assuming a prompt-jump approximation and an effective decay parameter for delayed neutrons [2], the reactor point kinetics equations result in the relationship shown in Eq. (3-10).

$$\frac{dN}{dt} = \frac{1}{\overline{\beta} - \rho}[\rho\lambda_e + \dot{\rho}]N \qquad (3-10)$$

N represents the reactor neutronic power, $\overline{\beta}$ is the total delayed neutron fraction, λ_e is the effective one-group decay parameter for delayed neutron precursors, and $\dot{\rho}$ is the rate of change of total reactivity.

It can be seen that to halt the transient, it is necessary to satisfy Eq. (3-11).

$$\rho\lambda_e + \dot{\rho} = 0 \qquad (3-11)$$

The condition of Eq. (3-11) can be met at any time for which reactivity is restricted by Eq. (3-12).

$$|\rho| \leq |\frac{\dot{\rho}}{\lambda_e}| \qquad (3-12)$$

Eq. (3-12) represents the absolute reactivity constraint. Its use in reactor power control schemes is discussed at length in [1]. If this constraint is observed, then by reversing the control rods, $\dot{\rho}$ will take on the value of $\dot{\rho}_{rod}$ and the condition of Eq. (3-11) will be satisfied. However, this absolute constraint is needlessly conservative since it stipulates that it be possible to halt the transient at any time. All that is actually required is the ability to stop the

transient at the termination point. A less stringent and more efficient constraint can be written which permits the presence of additional reactivity beyond the amount allowed by the absolute constraint in Eq. (3-11). This less stringent condition requires that there be sufficient time remaining to eliminate whatever reactivity is present beyond the amount that can be immediately removed by the reversal of direction of the control rods. Of course, this required time must be less than or equal to the available time before the transient termination point is exceeded. The amount of time required to reduce reactivity to a level which will allow control reversal to halt the transient is given by Eq. (3-13).

$$\tau_R = \frac{|\rho + \frac{\dot{\rho}_{rod}}{\lambda_e}|}{|\dot{\rho}_{rod}|} \qquad (3-13)$$

Note that Eq. (3-13) neglects the contribution of reactivity feedback to the quantity of $\dot{\rho}$.

As mentioned above, the control constraint is derived by comparing the required time (τ_R) to the available time (τ_A) in the inequality from Eq. (3-9). With the calculation of τ_R, this inequality takes the form of Eq. (3-14).

$$\frac{|\rho + \frac{\dot{\rho}_{rod}}{\lambda_e}|}{|\dot{\rho}_{rod}|} \leq \tau_A \qquad (3-14)$$

The expression in Eq. (3-14) serves as the basis for the non-linear reactivity constraint-based supervisory controller used in this report. Of course, to be used, the controller must know τ_A, the differential rod worth ($\frac{d\rho}{dz}$), and available rod speed ($\frac{dz}{dt}$) to obtain available reactivity insertion rate ($\dot{\rho}$). Estimates of reactivity (ρ), and effective one-group delayed neutron decay parameter ($\overline{\lambda}_e$). The methods used to obtain these quantities is discussed further in the following section.

3.6.2 Calculating Available Time

Now that the reactivity constraint has been defined and the required time to halt the transient, given the available rate of reactivity insertion, has been quantified, the available time until the end of the transient is reached must be quantified. In a power reactor, where the temperature is the controlled quantity, we are interested in preventing a temperature overshoot. Also, since the reactor core is designed to produce a rated power, and because the controller should never challenge the safety system, we also wish to control the plant in such a way to prevent a power overshoot.

Having the possibility of both power and temperature overshoots during transients in a power plant reactor, two different available times can be calculated. The first available time considered is the time until a maximum safe power level is reached (τ_1) [1] and is defined in Eq. (3-15). The reactor period ($\tau(t)$) can be obtained from the rate of change of power and the present power level.

$$\tau_1 \;=\; \tau(t)\ln\!\left(\frac{P_{safe}}{P(t)}\right) \qquad\qquad (3-15)$$

P_{safe} is a maximum power level not to be exceeded during the transient, and $P(t)$ is the present power level. The constraint to be satisfied now takes the form of Eq. (3-16).

$$\frac{\left|\rho \;+\; \frac{\dot{\rho}_{rod}}{\lambda_e}\right|}{|\dot{\rho}_{rod}|} \;\leq\; \tau(t)\ln\!\left(\frac{P_{safe}}{P(t)}\right) \qquad\qquad (3-16)$$

If Eq. (3-16) is always satisfied, reactor power will not increase beyond the allowed safe power level, regardless of the decision made by the control law.

To prevent the reactor from exceeding thermal limits, we can define another constraint. This additional supervisory constraint monitors the rate of change of coolant temperature and prevents overshooting the desired value during a transient. Two alternate methods are used

to calculate the available time until temperature overshoot occurs. The first calculation is based simply upon the existing rate of change of the average temperature, $\dot{T}_{av}$, and results in an available time denoted as τ_2. Average primary coolant temperature, T_{av} is defined in Eq. (3-17).

$$T_{av} = \frac{T_h + T_c}{2} \tag{3-17}$$

The first available time for the temperature constraint, τ_2, is defined in Eqs. (3-18) and (3-19).

$$\text{If } T_{prog} \leq T_{av} \Rightarrow \begin{cases} \text{If } \dot{T}_{av} \geq 0 & \text{then } \tau_2 = \infty \\ \text{If } \dot{T}_{av} < 0 & \text{then } \tau_2 = \dfrac{T_{prog} - T_{av}}{\dot{T}_{av}} \end{cases} \tag{3-18}$$

$$\text{If } T_{prog} > T_{av} \Rightarrow \begin{cases} \text{If } \dot{T}_{av} \leq 0 & \text{then } \tau_2 = \infty \\ \text{If } \dot{T}_{av} > 0 & \text{then } \tau_2 = \dfrac{T_{prog} - T_{av}}{\dot{T}_{av}} \end{cases} \tag{3-19}$$

T_{prog} represents the programmed average coolant temperature, calculated as a function of load demand and steam pressure demand by the module supervisor.

Another value for temperature constraint available time, τ_3, can be obtained from a calculation based upon an energy balance of the primary system. This balance results in Eq. (3-20), with MC representing the total heat capacity (J/°C) of the fuel, cladding, and coolant in the primary system. $\dot{Q}_{core}$ represents the heat production rate of the reactor core, $\dot{Q}_{load}$ is the heat removal rate from the primary coolant system, and $\overline{T}$ symbolizes the primary system average temperature of fuel, cladding, and coolant. Pumping power is neglected.

$$\frac{d\overline{T}}{dt} = \frac{\dot{Q}_{core} - \dot{Q}_{load}}{MC} \tag{3-20}$$

Assuming the fuel, cladding, and coolant temperatures vary asymptotically at the same rate, Eq. (3-20) can also be used to quantify the rate of change of primary coolant temperature,

$\dot{T}_{av}$, caused by an overshoot or undershoot in reactor power. When such a power mismatch occurs, the available time for the temperature constraint, denoted by τ_3, is calculated by Eqs. (3-21) to (3-23).

$$\text{If} \quad T_{prog} \leq T_{av} \quad \text{and} \quad \dot{Q}_{core} < \dot{Q}_{load} \quad \Rightarrow \quad \tau_3 = MC \frac{T_{prog} - T_{av}}{\dot{Q}_{core} - \dot{Q}_{load}} \qquad (3-21)$$

$$\text{If} \quad T_{prog} > T_{av} \quad \text{and} \quad \dot{Q}_{core} > \dot{Q}_{load} \quad \Rightarrow \quad \tau_3 = MC \frac{T_{prog} - T_{av}}{\dot{Q}_{core} - \dot{Q}_{load}} \qquad (3-22)$$

$$\text{Otherwise,} \quad \tau_3 = \infty \qquad (3-23)$$

An infinite value for available time can be physically interpreted as a condition in which the temperature will never reach the desired value. If reactor power has overshot the load power and the rate of change of temperature is a positive value, temperature will never reach the desired point. Because the supervisory constraint for temperature should be conservative, the smaller of the two values calculated, τ_2 or τ_3, is taken for the available time when evaluating the temperature constraint, as shown in Eq. (3-24).

$$\tau_A = \min\{\tau_2, \tau_3\} \qquad (3-24)$$

With the quantities now defined, the supervisory element of the reactor controller is able to determine:

1) Time required to stop the transient given the maximum rate of reactivity inertion available.

2) Time available until the final power level, or allowable maximum power level, is reached given the present reactor period (rate of change of power).

3) Time available until the desired temperature is reached, given the existing rate of change of temperature, or given the existing mismatch between heat generation rate and heat removal rate along with information about the heat capacity of the plant.

Now, our attention shifts to the controller logic needed to implement the reactivity constraint for power and temperature, using a simple control law.

3.7 Reactor Controller Logic and Implementation

The Non-Linear Temperature Controller (NLTC) is the implementing algorithm for the reactivity constraint approach to reactor control and is an extension of the MIT-CSDL Non-Linear Digital Controller (NLDC) [1]. The NLTC has a multi-tiered structure consisting of supervisory and predictive routines. The supervisory algorithm uses a sufficient reactivity constraint to provide a method for determining if the control signal should be changed at the present time in order to avoid an overshoot at some future time. This is the unique feature of the reactivity constraint approach. It permits the on-line determination of the proper moment for initiation of reactivity removal during a transient. Figure (21) provides a schematic of the NLTC.

The sufficient reactivity constraint, Eq. (3-14), is used to evaluate the decision of an associated control law and to verify that no challenge will be made to the safety of the plant as a result of implementing that decision. This arrangement permits changes in the demanded coolant temperature (a function of power) to be readily and safely accomplished. For example, suppose the control law were simply to move the control mechanism at a fixed speed should the deviation between the desired and actual temperature exceed a specified band. Then suppose a temperature increase is desired. Initially, the reactor is at steady state with the control law maintaining the temperature within the allowed deadband. Once the temperature set point is changed, the control law signals for the withdrawal of the control rod. The reactivity constraint is initially satisfied, and withdrawal is permitted. Rod withdrawal continues until the constraint is no longer satisfied. Once the constraint is violated, rod withdrawal is halted, even if the control law is signaling for its continuation. The reactor period then lengthens from its dynamic to its asymptotic value. The constraint is again satisfied, and further rod
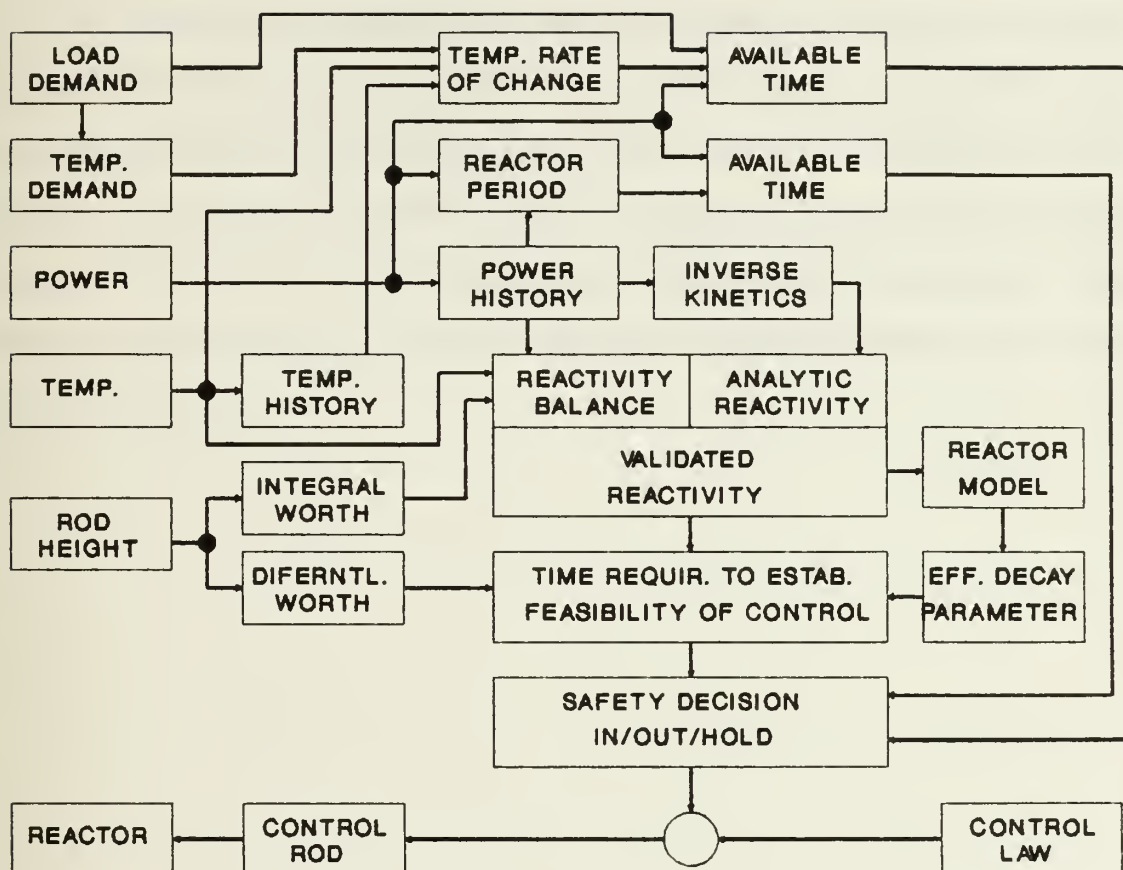
Figure (21) Non-Linear Temperature Controller

Schematic Diagram

94

withdrawal is possible. This process continues until the constraint cannot be satisfied simply by a cessation of rod withdrawal. Rod insertion begins. The reactor period lengthens, the constraint is satisfied, and rod insertion is halted until the constraint is once again violated. The net effect is that the rod is initially withdrawn continuously, then held more or less constant, and finally inserted in a stepwise fashion.

Now that we have discussed various plant control schemes used on other LMR plants, reviewed the reactivity constraint approach towards reactor control, and outlined the logic used in implementing the module supervisory controller, coolant flow controller, and reactor controller, we can apply the controller to the plant model and observe plant response to transients. In the next section, results obtained from simulated transients are presented. These results show great promise for solving the non-linear temperature control problem of the multi-modular reactor plant.

Chapter 4 - Evaluation of Proposed Controller

4.1 Implementation of Simulation

Now that the plant model and supervisory controller have been clearly defined, they can be implemented on a digital computer for simulation studies. The purpose of the simulation studies is to determine the stability of the proposed control system during transients and the effectiveness of the supervisory constraints on power and temperature overshoots.

As mentioned before, the plant model is implemented using the DSNP, Ver. PC/A, simulation language. Recall that the DSNP precompiler takes the DSNP statements and expands them to FORTRAN statements which are compatible with the FORTRAN compiler. The controller algorithm is implemented in FORTRAN as well, with special care taken to incorporate the controller with the DSNP generated model. Listings of all computer codes used are contained in Appendix D. Information on the DSNP simulation language is contained in Appendix A. The Microsoft Optimizing Compiler, Ver. 4.01, is used to compile the FORTRAN codes. A DELL Model 310 personal computer, running at 20 MHz is the machine used to execute the simulations.

In order to demonstrate the effectiveness of the power level and temperature constraints which comprise the supervisory elements of the Non-Linear Temperature Controller (NLTC), a very simple control law is chosen for use in the following simulated transients. The logic of this control law is as follows: if the actual value of average primary coolant temperature is greater than the programmed (desired) value, the control rods are inserted. If the actual value of average coolant temperature is less than the programmed value, control rods are withdrawn. Both movements occur at the maximum speed of the control mechanism. The control rod used has three times the worth of the regulating rod in the MITR-II, so reactivity insertion rates are relatively large. In addition, the transients simulated below began with the position of the rod near its maximum differential rod worth. With such simple controller logic

96

and large reactivity insertion rates available, an oscillatory response is to be expected. However, with the NLTC supervisory logic in place to ensure that programmed limits are not exceeded, the simulated plant will not exceed "safe" operating conditions. A better control law could be devised using variable rod speed dependent upon the magnitude of the temperature error [2]. Even without a more sophisticated control law, the results presented below exhibit satisfactory plant temperature response.

Using the NLTC as configured in this report, only the temperature and power constraints prevent challenges to the safety system. When implemented on an actual power reactor, the NLTC supervisory algorithm should perform additional checks to limit the reactor period to a reasonable values. Also recommended are limits on the amount of net reactivity present in the reactor. Such safety checks will not impede normal reactor plant operations, and will enhance reactor safety by preventing the automatic controller from challenging the reactor protection system.

4.2 Unsupervised Control Law Transient Response

Figure (22) below illustrates the response of average primary coolant temperature to a transient in which demanded power increased from 340 MW to 420 MW. Temperature overshoots the programmed value since control rod insertion does not occur until overshoot actually occurs. The control law, on its own, has no anticipatory capability and is unable to turn the transient until well after the programmed temperature has been exceeded. Large oscillations occur, in part due to the high rod worth used for the simulation. The small perturbation of the temperature near the beginning of the transient is caused by the programmed change in flow. The flow increase is illustrated in Figure (23) below and is representative of flow changes in all the other transient simulations presented.

97
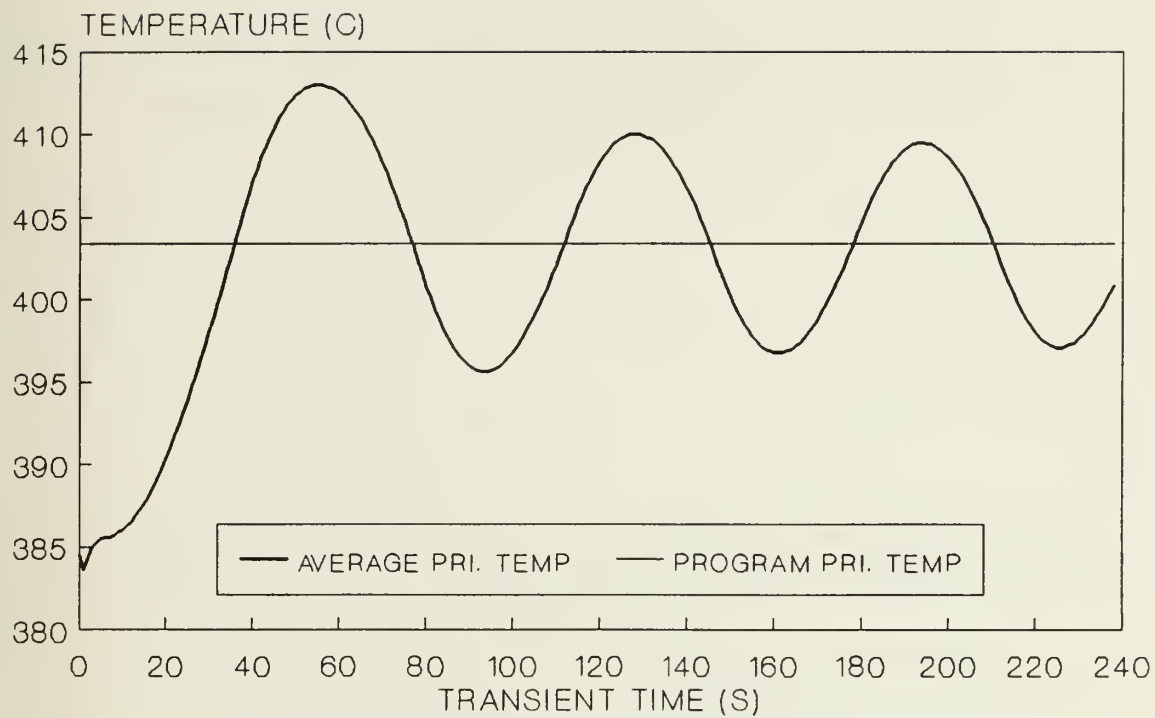
Figure (22) Unsupervised Temperature Response
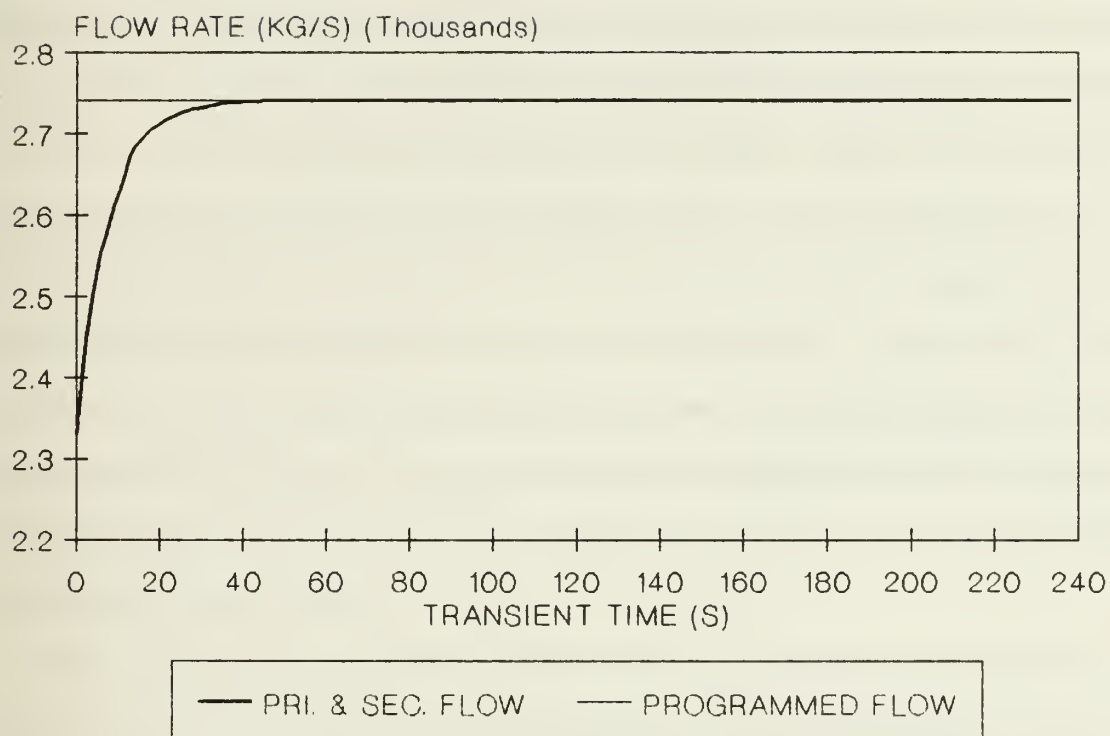
Figure (23) Coolant Mass Flow Rate Response

4.3 Transient Response with Temperature Constraint

Having observed the undesirable response of the plant using the simplistic control law, the NLTC is modified to supervise the temperature response, and take action to prevent overshoot. As discussed in Section 3.6, when the available time until temperature overshoot occurs, τ_A, is exceeded by the required time to turn the transient, τ_R, the supervisory algorithm takes action to stop the transient before overshoot occurs. Figure (24) illustrates the temperature response during the transient. Again, the elementary control law is used, but with the supervisory constraint, temperature never exceeds the desired value. Even with a poorly conceived control law, the supervisor guarantees no overshoot. Figure (25) illustrates the response of reactor power and reactivity during the transient. The oscillatory behavior occurs due to the logic of the control law used. Note the peak value of power reached early in the transient, and the time at which the reactivity curve sharply dips. Power exceeds a "safe" value since no constraint is placed on power level or period. The time at which reactivity dips sharply corresponds to the time at which the temperature constraint can no longer be satisfied, as shown in Figure (26), and the supervisory algorithm takes action to turn the temperature rise in time to prevent overshoot.

Again, it should be emphasized that these transients demonstrate the effectiveness of the supervisory element of the NLTC control algorithm. A more sophisticated control law, in an actual power plant implementation, would be used to control of the plant once inside the allowed operating envelope. This improved control law could be used to eliminate the large variations in plant response caused by the simple control law chosen here deliberately to test the supervisory algorithm.
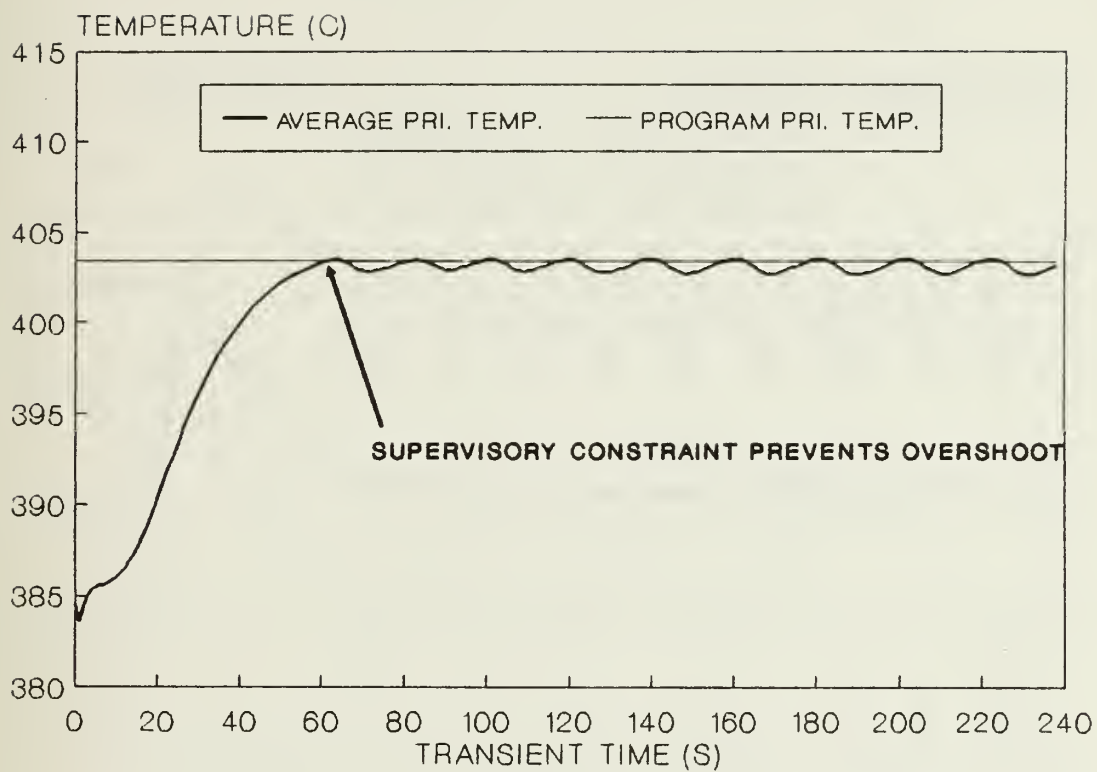
Figure (24) Temperature Response with

Temperature Constraint
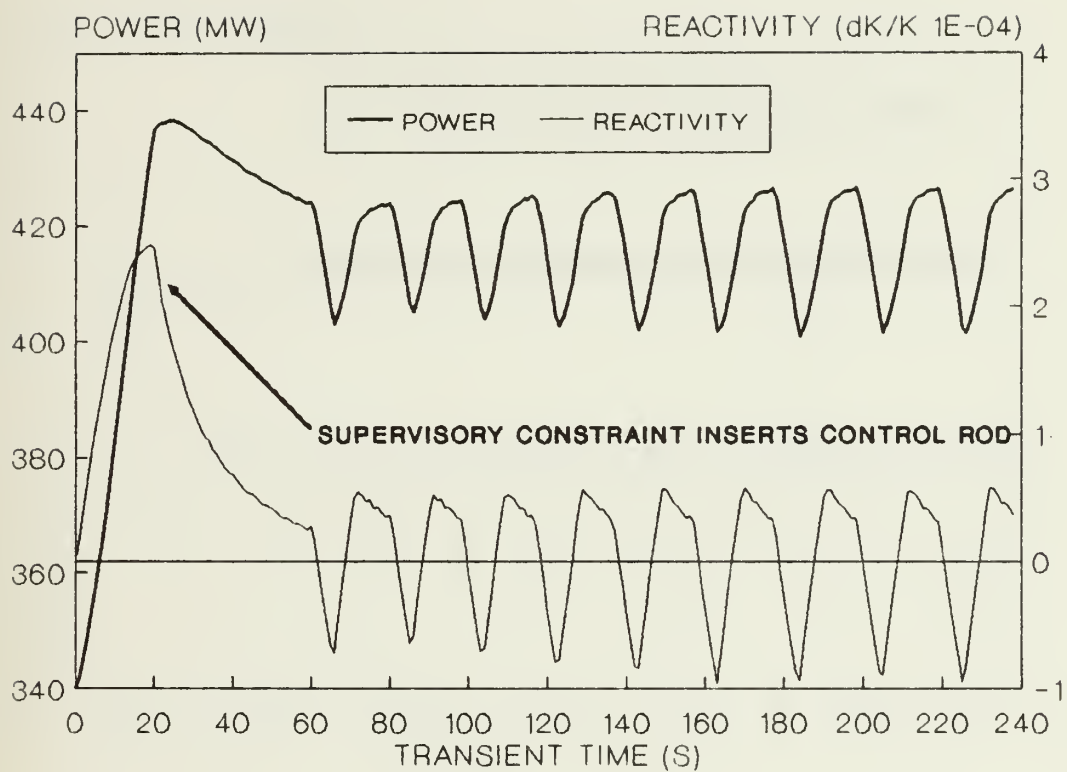
Figure (25) Power and Reactivity Response with
Temperature Constraint
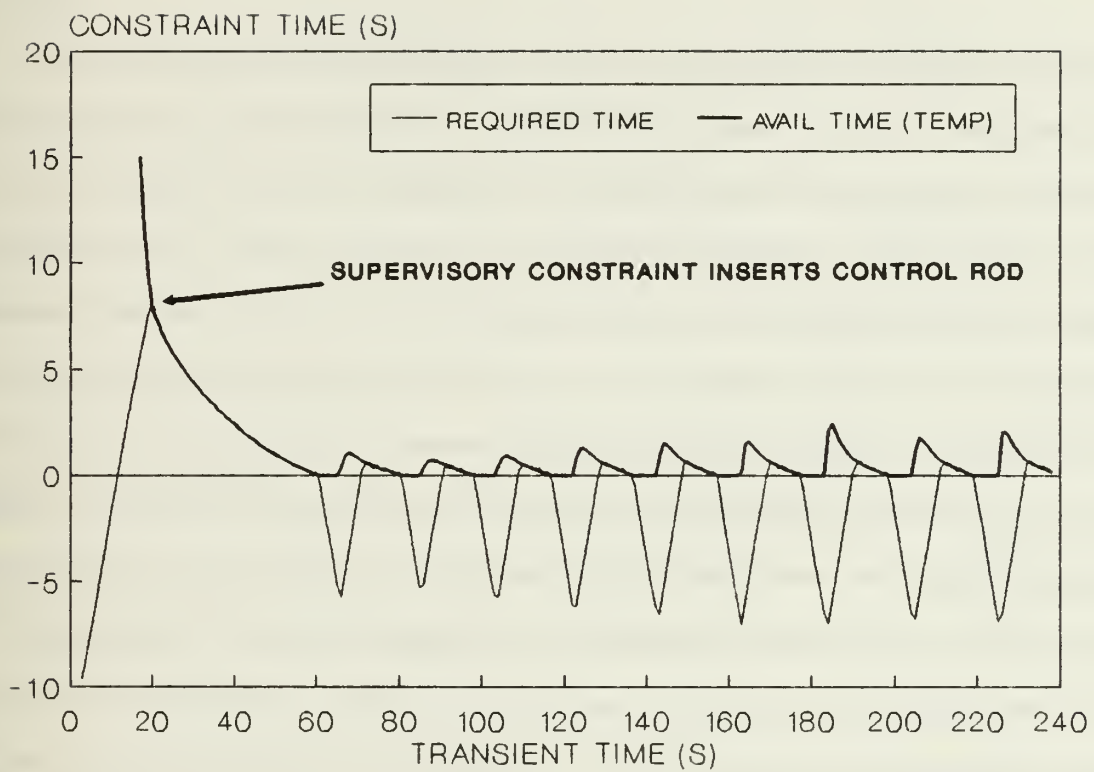
Figure (26) Required and Available Times with

Temperature Constraint

4.4 Transient Response with Power Constraint

The use of the temperature constraint has been shown to prevent overshooting the desired temperature value during transient conditions in the plant. However, without any constraint on the power level, large reactor power excursions are permitted by the supervisory algorithm. To demonstrate the effectiveness of the reactivity constraint approach towards reactor power control, the NLTC is modified to substitute a power level constraint for the temperature constraint.

In the transient studied, load demand is raised from 340 MW to 420 MW. The power level constraint is implemented in such a manner to allow power to reach a maximum value of 425 MW without overshoot. Temperature is controlled only by the elementary control law discussed earlier. Figure (27) presents the temperature response to the increase in load transient. Note that the rise time is greater than in the previous transient and that overshoot is still prevented by the supervisory element of the controller. The lack of temperature overshoot can be explained by the choice of temperature setpoint made by the module control program. Recall that this temperature is calculated for equilibrium conditions in the reactor for given flow and load conditions. Temperature lags behind power, and before temperature has the opportunity to exceed the programmed (equilibrium) value, the power level has been reduced by the power level constraint. Temperature then falls below the programmed value, and the control law signals for rod withdrawal. Power increases, with temperature lagging shortly behind, until the supervisory constraint once again takes action to prevent overshoot of the maximum allowable power.

Figure (28) shows the power and reactivity response, and Figure (29) illustrates the behavior of required and available times, as defined in the control logic for this transient. As before, whenever the available time is less than or equal to the required time to stop the

transient, the supervisory algorithm of the NLTC takes action to turn the transient by holding or inserting control rods. This transient demonstrates the utility of the power constraint in preventing excessive power overshoots.
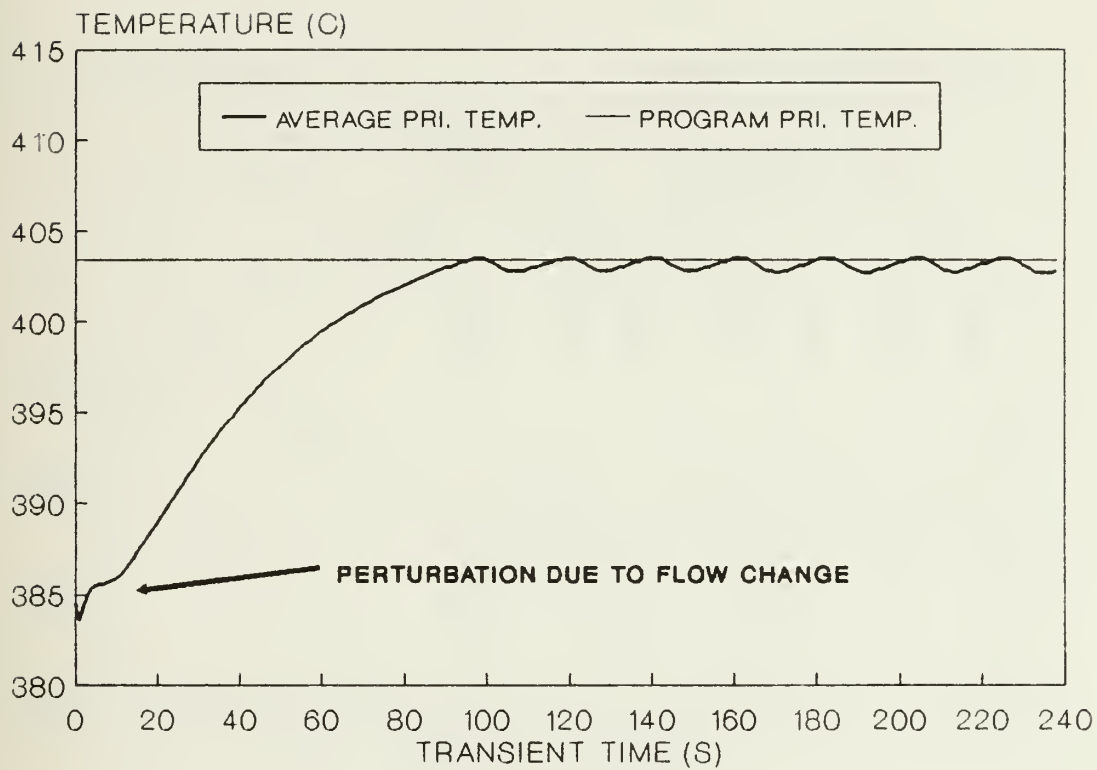
Figure (27) Temperature Response with

Power Constraint

106
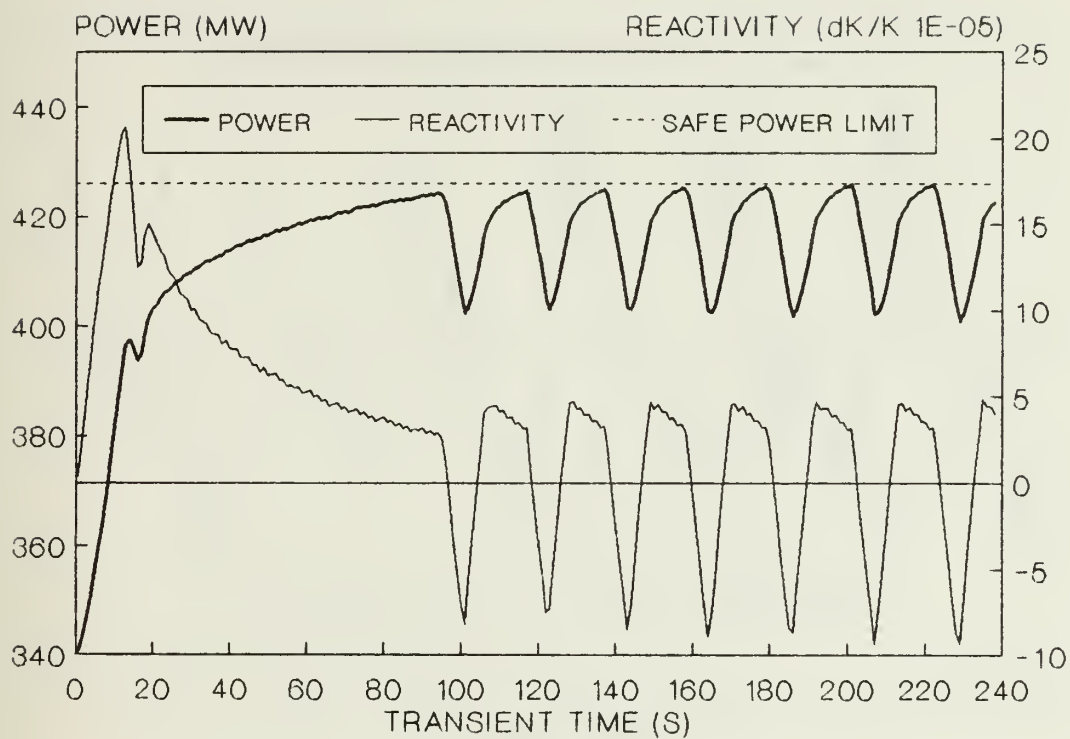
Figure (28) Power and Reactivity with

Power Constraint
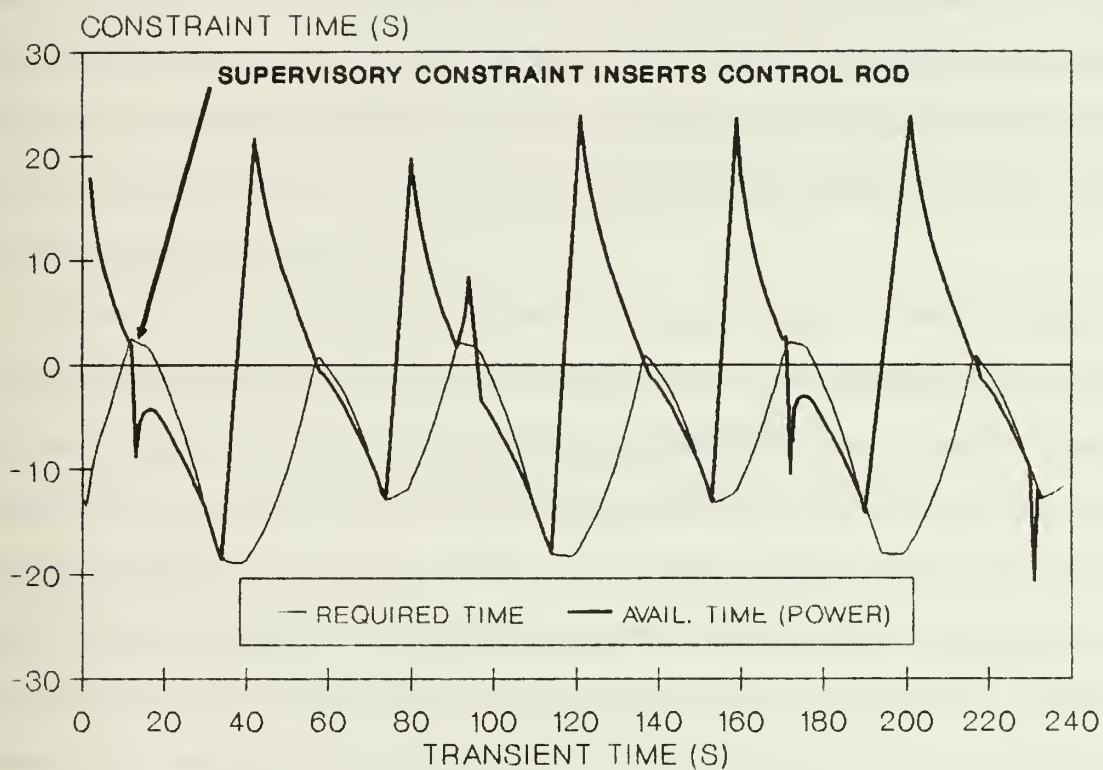
Figure (29) Required and Available Times with

Power Constraint

108

4.5 Transient Response with Power and Temperature Constraints

Since both the power and temperature constraints have been shown to be useful in preventing overshoots during transients, both of them are incorporated in the final NLTC supervisory controller for the reactor. In the simulated transient presented here, the load is increased from 340 MW to 400 MW, with maximum allowable power set at the PRISM rated value of 425 MW. By defining the controller limit in this manner, the necessity for and effectiveness of both constraints can be illustrated. Power is allowed to exceed the equilibrium power for the given load demand, and yet remain bounded by a reasonably safe level. This allows for a rapid temperature increase, with the temperature constraint algorithm preventing overshoot during the transient.

Figure (30) shows the response of temperature, again with no overshoot. Figure (31) plots the power and reactivity response. Power never exceeds the allowable maximum power level even though the same elementary control law described above is used to adjust the position of the control rods. Figure (32) illustrates the behavior of the required and available times used to define the constraints. Note that early in the transient, the available time until power overshoot dips below the required time to turn the transient. This initiates a supervisory action to insert control rods, as shown by the sharp dip in the reactivity curve. Later in the transient, when temperature in the reactor has reached the desired value, the temperature constraint takes action to prevent a temperature overshoot due to the mismatch between reactor power and load. The temperature constraint supervisory action occurs when the available time until temperature overshoot occurs dips below the required time to turn the transient. Careful observation of the constraint time curve shows that the in the later portions of the transient, the temperature constraint is the limiting case. In the initial portion of the transient, the power constraint is limiting. So, in the transient simulated here, the utility of both constraints is demonstrated.
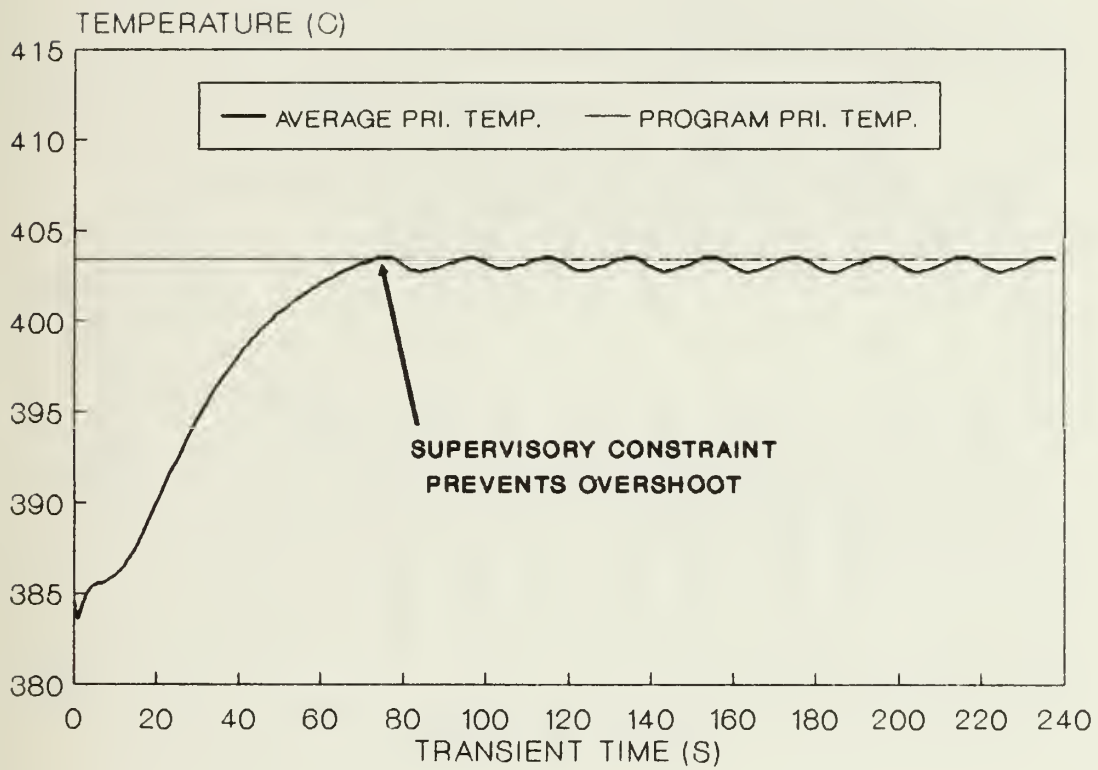
Figure (30) Temperature Response with

Power and Temperature Constraints

110
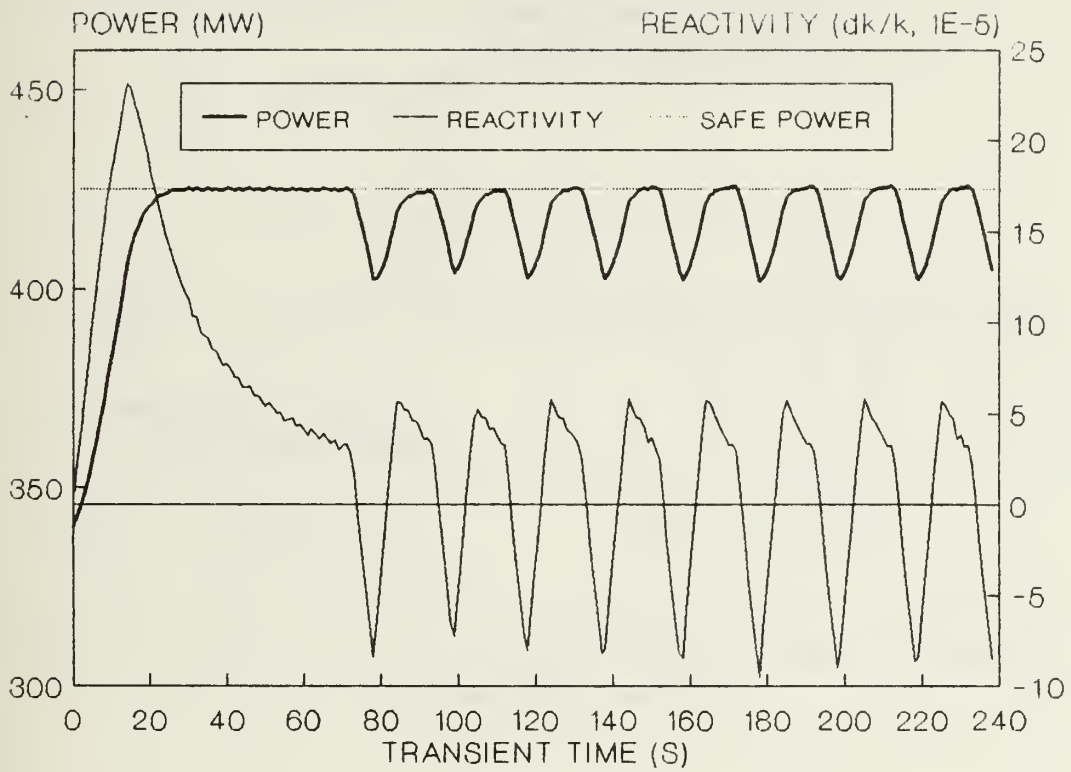
Figure (31) Power and Reactivity with

Power and Temperature Constraints
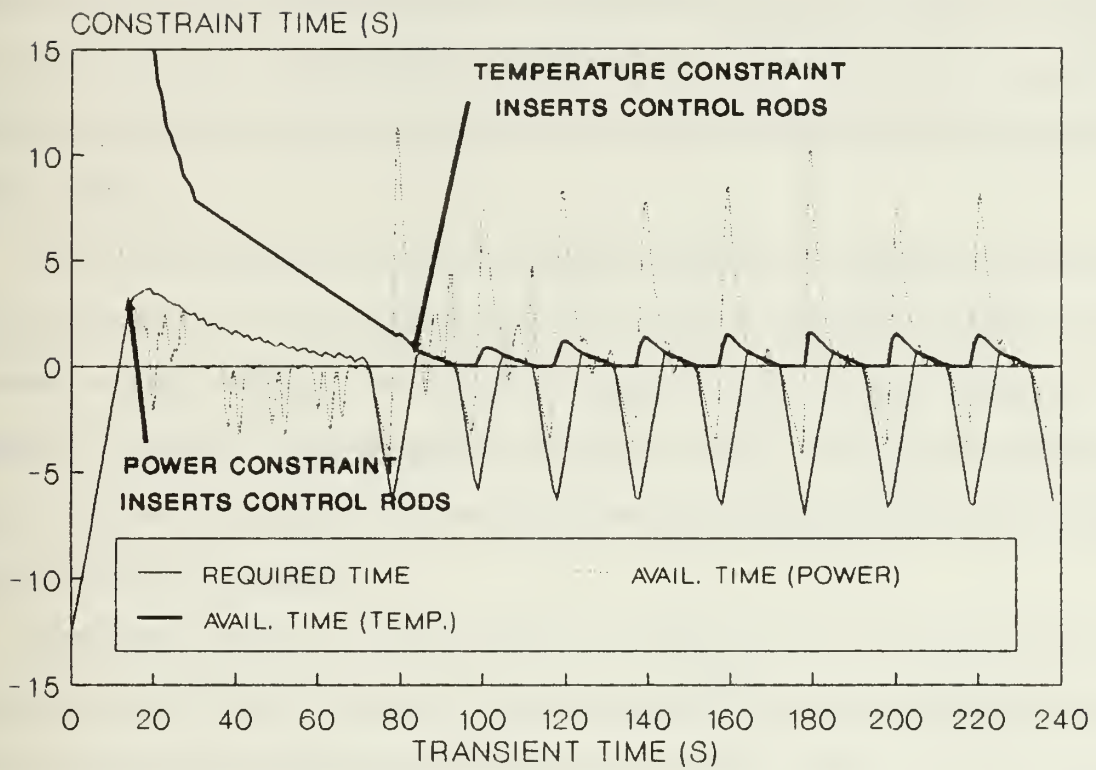
Figure (32) Required and Available Times with
Power and Temperature Constraints

112

4.6 Summary of Simulation Results

Through the careful development of a plant model, and the applied use of the reactivity constraint approach, the control of nuclear power plant temperatures has been demonstrated. The steady state equilibrium values of required temperatures for given coolant flows, demanded steam flows, and demanded steam pressure have also been calculated and mapped into a control program. Under transient conditions, the non-linear temperature controller (NLTC) has shown that required temperatures can be attained within reasonable time periods without overshoot.

The transient response to demanded power and temperature is quite good considering the non-linear behavior of the nuclear heat source. In addition, temperature transients can be completed without overshoot even though the control law used to move control rods is deliberately formulated to be inadequate for the purpose at hand. The reason the controller is able to prevent temperature excursions lies in the supervisory algorithm of the NLTC, namely the reactivity constraint.

Although the operation of multi-modular reactor plants involves control of more than reactor plant power, coolant temperature, and coolant mass flow rate, a large portion of the problem has been solved in this report. Even though the dynamic behavior of steam pressure has not been simulated during the transients studied here, the plant control program has been designed to supply steam at a desired pressure, so after the transient, pressure could be expected to return to its equilibrium value. Possible transient instabilities between coupled steam supply systems should be explored, using the control method presented in this report.

113

Chapter 5 - Summary and Conclusions

5.1 Control of Multi-Modular Reactors

Multi-modular reactors provide an innovative alternative to the current generation of large, light water reactors (LWRs). In the multi-modular design, clusters of smaller reactors supply steam to a single turbine-generator. Such an arrangement allows for simpler and less expensive implementation of advanced reactor safety features. Through the use of passive means of decay heat removal from the smaller, modular reactor cores, multiple layers of active safety systems can be eliminated. If these so-called "inherent safety measures" can be demonstrated through an actual plant test, it may be possible to regain public acceptance of nuclear power.

A new generation of nuclear power plants, whether of multi-modular design or not, must cost no more to operate than present reactor designs. Automatic control of nuclear power plants promises to maintain or even reduce operating costs. The multi-modular reactor plant could prove expensive to operate if licensed human operators are required to monitor and control each reactor module. However, if the newer designs are more forgiving in operation than LWRs, the present doctrine which relegates automatic reactor control mechanisms to advisory or non-safety related functions may shift towards acceptance of automatic adjustment of reactivity.

The Massachusetts Institute of Technology has embarked upon an integrated program to develop a fault-tolerant, robust methodology for the control of nuclear reactors. A unique and distinguishing characteristic of this program is that the concepts developed are tested on the 5 MW_t M.I.T. Research Reactor (MITR-II). The results presented in this report are based directly upon simulation studies, but are extensions of previous work which has been thoroughly tested on the MITR-II [1]. Given the encouraging results of this work, the next logical

114

step is the implementation of closed-loop digital control on a nuclear power plant. An implementing algorithm for reactor power control, the MIT-CSDL[4] Non-Linear Digital Controller (NLDC), has been licensed for unrestricted use on MITR-II by the Nuclear Regulatory Commission. In experiments with the NLDC a novel controller, in the form of a control law, is allowed to control power within the normal operating range. The decision of the control law is reviewed for safety by the NLDC supervisory element. This supervisory review is based upon the "reactivity constraint" concept. The NLDC is programmed to intervene if a decision made by the control law could result in power exceeding some maximum allowed power, usually 4.5 MW$_t$. This arrangement is designed to assure that the control law will not challenge the reactor safety system, while allowing it to act as if it had full control.

Multi-modular nuclear reactor plant operating criteria are different than those of research reactors, yet still share common requirements. The most important shared requirement is that any automatic control mechanism used to operate the reactor must be designed to avoid challenging the safety system. In a reactor plant with an associated steam system operating in a thermodynamic cycle for power production, temperature is controlled rather than power [2]. Indirect control of the reactor power is achieved by controlling reactor thermal conditions because of the negative temperature coefficient of reactivity. At equilibrium, the thermal power of the reactor plant matches the load demanded by the turbine-generator. Reactor power is determined by steam demand unless special measures are taken to isolate feedback from the steam plant. Control rods adjust temperatures in the reactor plant, which are maintained at levels determined by weighing desired steam plant conditions against desired reactor plant conditions.

---

4 Developed jointly by M.I.T. and the C.S. Draper Laboratory.

Steam plant conditions require special consideration in the multi-modular nuclear power plant design due to the parallel operation of the steam generators. Although each module may be producing steam at different demanded flow rates, the pressure of the steam produced must be compatible with the steam pressure existing in the balance of the steam plant. If steam generator pressure is too low, the module will not supply steam at the demanded flow rate. If pressure is not properly controlled, thermal loading will shift back and forth between modules, setting up undesirable instabilities. Therefore, each module must be designed to supply steam at a demanded flow rate and a demanded pressure.

5.2 Nuclear Steam Supply Module Control Program

Equilibrium reactor plant temperatures necessary for maintenance of desired steam plant pressures and flows can be "mapped" into a plant control program. The shape of this map depends upon the characteristics of and the operating strategy chosen for the power plant. A controller which keeps plant parameters on this map could be used to maintain module steam flow and pressure at their desired values.

A proposed multi-modular reactor plant, the General Electric Co. Power Reactor Inherently Safe Module (PRISM), utilizes three liquid metal cooled reactor (LMR) modules in a "power block" of three modules. The reactor in each module operates with a fast-neutron spectrum, and is cooled by liquid sodium coolant. Since the sodium becomes radioactive when circulated through the neutron flux in the core and is hazardous to personnel, a secondary loop of liquid sodium transports the heat from the primary system to the steam generator. Heat between the primary and secondary sodium coolant loops passes through an intermediate heat exchanger (IHX). Because sodium exhibits a large temperature change across the reactor core and heat exchangers, variable flow control is typically employed in LMR power plants. By maintaining a constant power-to-flow ratio, the temperature difference across the core and heat exchange components is maintained at a nearly constant value for various power levels.

116

Although a variable flow strategy complicates the plant control system, it allows for changing plant loads without creating undesirable thermal cyclic stresses on plant components. Because the PRISM plant analyzed in this study is designed for flexibility and ease of operation, a variable flow control scheme is selected for evaluation of the module control program.

For operation of the modular steam plant in parallel with other modules, a constant steam pressure program is selected here for consideration. The rationale for this decision considers that if all three PRISM modules are equally sharing the total load, then each should be at the same pressure, assuming equal head loss between the steam generator and the load. If all three modules continue to share equal fractions of the total load as the load increases and decreases, and constant steam pressure is maintained during the load change on the turbine-generator, then the load will still be equally shared during and after the transient. Otherwise, the load will shift between modules, possibly setting up undesirable oscillations. If load is to be shared unequally between modules, steam generator pressures must be maintained at levels necessary to provide desired steam flows into the steam header (see Section 3.4). Therefore, a modified version of the constant steam pressure program is needed for operation of the multi-modular nuclear reactor plant.

In order to calculate the values of the equilibrium temperatures on the module control program, a model of the plant must be developed. The approach taken here is to lump the distributed parameters of the plant components into nodes. Each node acts as an energy storage element and, by performing an energy balance on the node, the state of the node can be evaluated. If temperature is chosen as the state of the node, the energy equation is derived in terms of temperature. By considering a transient energy balance, a dynamic determination of plant thermal conditions can be obtained. For the plant control program, only the steady state conditions are needed. The module control program, showing the equilibrium values of

117

plant temperatures which will be maintained by the module controller is shown in Figure (33).
The flow control program, to maintain a constant power-to-flow ratio, is also shown in Figure
(34).
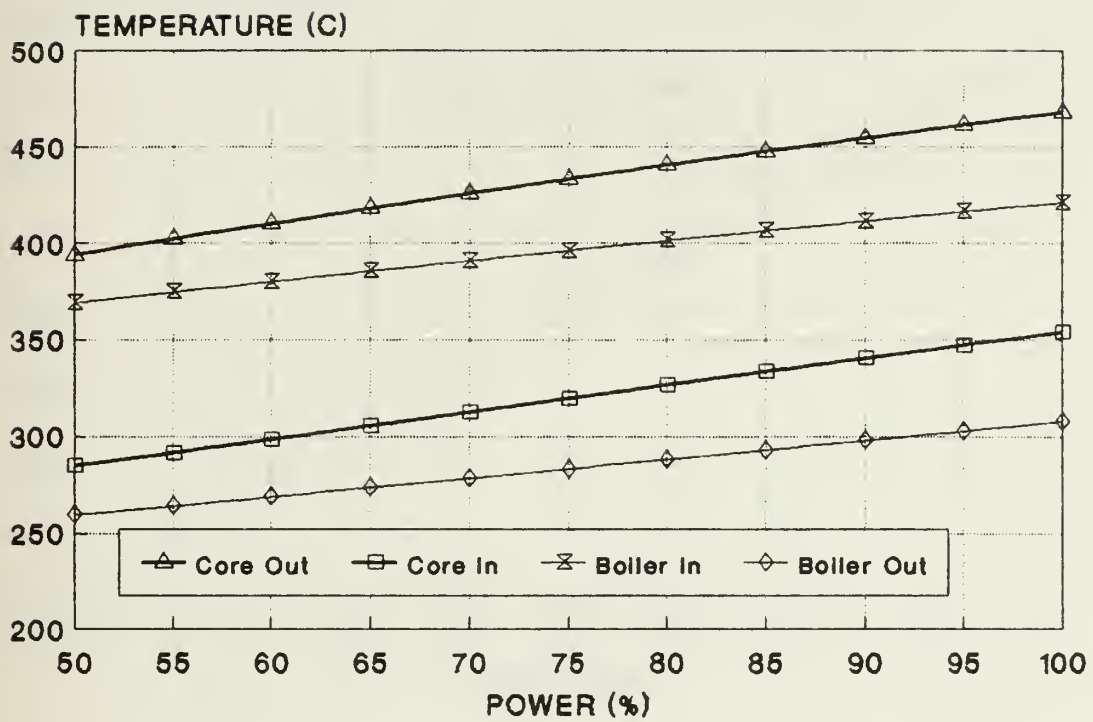
Figure (33) Module Temperature Control Program
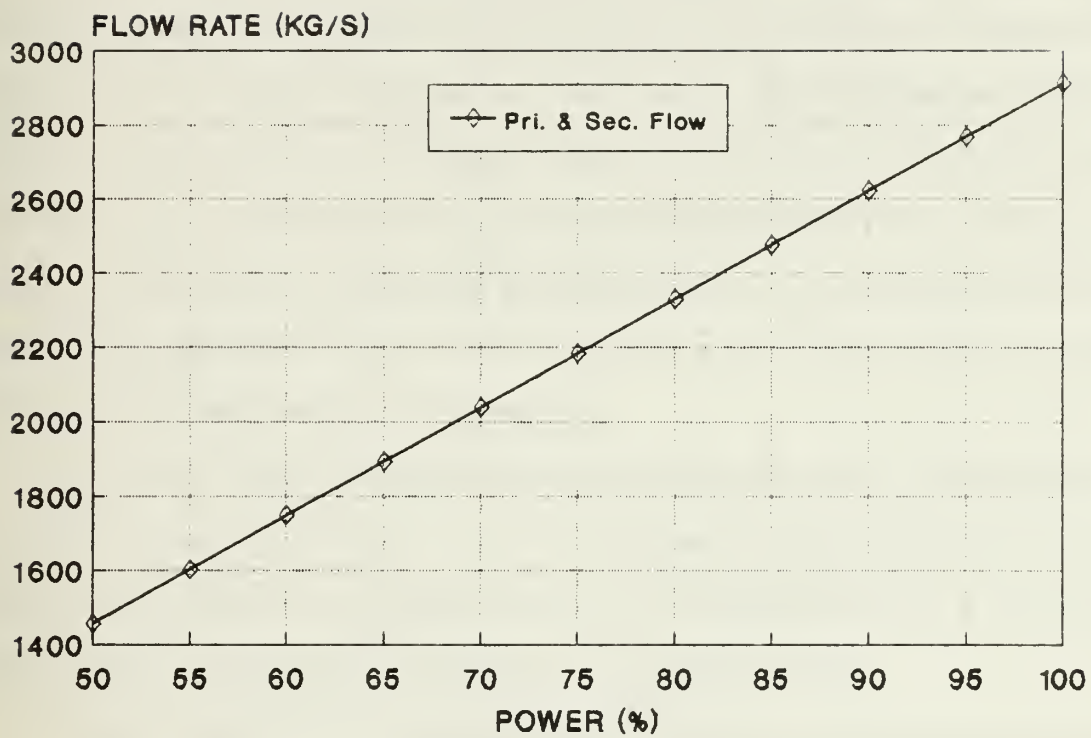
Figure (34) Module Flow Control Program

120

5.3 Reactivity Constraint Approach to Automatic Reactor Control

The objective of the "reactivity constraint approach" [1] is to provide a means for the closed-loop digital control of reactor plant temperature (or power) during transients so that there will not be a challenge to the reactor safety system. It is part of the basis for the Non-Linear Temperature Controller's (NLTC)[5] supervisory algorithm. The approach functions by restricting the effect of the delayed neutron populations to that which can be balanced by an induced change in the prompt population. This is done by limiting the net reactivity to the amount that can be offset by reversing the direction of motion of the automated control mechanism. Also constrained is the rate of change of temperature to a value such that a given temperature limit will not be exceeded during the transient. The necessary constraints are obtained from the dynamic period equations and from a conservative estimate of available time until the temperature limit will be reached.

The first step requires a definition of those conditions for which it is possible to control the reactor temperature (or power). That is, it is necessary to define those combinations of reactivity and available rate of change of reactivity for which temperature (or power) can be leveled. This is accomplished by identifying the desired reactor states.

A reactor, together with a specified control mechanism is defined here as constituting a system that is "feasible to control" if the system can be transferred from a given temperature (or power level) and rate of change of temperature (or power) to a desired steady state temperature (or power level) without overshooting a specified tolerance band, if any. This concept has two important attributes. First, it applies to a reactor and to the specific control mechanism designated for use in accomplishing a given transient. Second, not all states are allowable intermediates through which the system may pass while transiting from some initial to some

---

5 An extension of the MIT-CSDL Non-Linear Digital Controller (NLDC).

final state. Excluded are both those states that represent actual overshoots and those from which overshoots could not be averted by manipulation of the specified control mechanism[6]. It is important to realize why certain intermediate states must be avoided. The rate of rise of reactor power is a function of the rates of change of both the prompt and delayed neutrons. The former are directly controllable. The latter are not, owing to the delay in their production from fission products. Power changes can only be halted if the rate of rise of the delayed neutrons can be offset by making the rate of change of the prompt neutrons negative. Physically, this means that it must be possible to counter positive reactivity with a negative reactivity inertion rate. Therefore, a need exists to restrict operation to only certain combinations of reactivity and available reactivity insertion rates.

Having defined the allowable reactor states, the next step in the development of a supervisory controller is to describe those states mathematically. This can be accomplished using the dynamic period equation. The standard form of this equation is considered here.

Neglecting prompt terms, the standard dynamic period equation takes the form of Eq. (5-1). $\tau(t)$ represents the dynamic reactor period (time required for power to change by a factor of "e"), $\overline{\beta}$ is the total effective delayed neutron fraction, $\rho(t)$ is net reactivity, and $\lambda_e(t)$ is the standard effective delayed neutron decay parameter.

$$\tau(t) \cong \frac{\overline{\beta} - \rho(t)}{\dot{\rho}(t) + \lambda_e(t)\rho(t) + [\dot{\lambda}_e(t)/\lambda_e(t)] (\overline{\beta} - \rho(t))} \qquad (5-1)$$

Maintenance of "feasibility of control" implies that the contribution of the delayed neutrons to the period must be limited so that, when the desired power level is reached, the insertion of the control mechanism will make the rate of change of the prompt neutron population

---

6 It should be recognized that the concept of "feasibility of control" is distinct from the more general property of "controllability." A system is controllable if any initial state can be transferred to any final state in a finite time by some control sequence; no restrictions are placed on any intermediate conditions.

sufficiently negative so as to offset the continued rise in the delayed neutron population. This objective can be realized if the net reactivity is constrained so that the denominator of Eq. (5-1) can be made less than or equal to zero. Note that the numerator of Eq. (5-1) is, for safety reasons, always positive. Mathematically, the condition of Eq. (5-2) must be met.

$$\left[\lambda_e(t)\rho(t) \ + \ \frac{\dot{\lambda}_e(t)}{\lambda_e(t)}(\overline{\beta} - \rho(t)) \ + \ \dot{\rho}_f \right] \ \leq \ |\dot{\rho}_c| \qquad (5-2)$$

The net reactivity, $\rho(t)$, accounts for both the reactivity added deliberately through movement of a control mechanism and for reactivity present due to feedback effects. The quantity $\dot{\rho}_f$ denotes the rate of change of reactivity that results from temperature feedback effects, and $|\dot{\rho}_c|$ represents the maximum available rate of change of reactivity that could be obtained from movement of control rods.

Implementation of a controller based upon Eq. (5-2) is difficult because of the derivative term, $[\dot{\lambda}_e/\lambda_e]\,(\overline{\beta} - \rho)$. However, studies have shown that this term may be neglected. The $\dot{\rho}_f$ term from thermal reactivity feedback aids the control mechanism in turning up power transients, so the difficulty in measuring this quantity can be circumvented by neglecting it altogether. With these two assumptions, the required condition for stopping a transient takes the form of Eq. (5-3).

$$[\lambda_e(t)\rho(t)] \ \leq \ |\dot{\rho}_c| \qquad (5-3)$$

Eq. (5-3) is the standard form of the absolute reactivity constraint. Under this constraint, reversal of the direction of motion of the specified control mechanism will negate the effect of the reactivity present and make the period infinite at any time during a transient.

The absolute reactivity constraint is needlessly conservative because it stipulates that it be possible to level reactor power at any time during a transient when all that is required is that it be possible to level power at the termination point. A less stringent and more efficient condition specifies that there be sufficient time to eliminate whatever reactivity is present

123

beyond the amount that can be immediately negated by reversal of direction of the control mechanism before the desired power level is attained. This condition, the sufficient reactivity constraint, is given by Eq. (5-4) for power increases.

$$\frac{\rho(t) \;-\; |\dot{\rho}_c|/\lambda_e(t)}{|\dot{\rho}_c|} \;\leq\; \tau(t)\ln\!\left(\frac{P_f}{P(t)}\right) \qquad (5-4)$$

P_f and $P(t)$ refer to final desired power level, and present power level, respectively. Eq. (5-4) can be physically interpreted as two times. The left hand side of Eq. (5-4) represents required time to establish feasibility of control, τ_R, and the right hand side represents available time until the desired power level is exceeded, τ_A.

The concept of available time until the desired state is reached can be extended towards control of temperature. Since temperature lags behind reactor power, if the power transient can be stopped within a required time which is always less than or equal to an available time until temperature overshoot, then the same sort of constraint can be applied to temperature. If the reactor coolant average temperature is denoted by T_{av} and the programmed average temperature is represented by T_{prog}, then an available time until temperature overshoot occurs can be defined by Eqs. (5-5) and (5-6).

$$\text{If } T_{prog} \leq T_{av} \Rightarrow \begin{cases} \text{If } \dot{T}_{av} \geq 0 \quad \text{then} \quad \tau_1 = \infty \\[2mm] \text{If } \dot{T}_{av} < 0 \quad \text{then} \quad \tau_1 = \dfrac{T_{prog} - T_{av}}{\dot{T}_{av}} \end{cases} \qquad (5-5)$$

$$\text{If } T_{prog} > T_{av} \Rightarrow \begin{cases} \text{If } \dot{T}_{av} \leq 0 \quad \text{then} \quad \tau_1 = \infty \\[2mm] \text{If } \dot{T}_{av} > 0 \quad \text{then} \quad \tau_1 = \dfrac{T_{prog} - T_{av}}{\dot{T}_{av}} \end{cases} \qquad (5-6)$$

$\dot{T}_{av}$ is the existing rate of change of average coolant temperature. Another rate of change of average coolant temperature could be created by a mismatch between reactor power and load.

124

The equation used to calculate this rate of change is given in Eqs. (5-7), (5-8) and (5-9). $\dot{Q}_{core}$ represents the core thermal output, $\dot{Q}_{load}$ is the demanded thermal power, and MC is the total heat capacity of the fuel, clad, and coolant in the reactor primary system.

$$\text{If} \quad T_{prog} \leq T_{av} \quad \text{and} \quad \dot{Q}_{core} < \dot{Q}_{load} \quad \Rightarrow \quad \tau_2 = MC \frac{T_{prog} - T_{av}}{\dot{Q}_{core} - \dot{Q}_{load}} \qquad (5-7)$$

$$\text{If} \quad T_{prog} > T_{av} \quad \text{and} \quad \dot{Q}_{core} > \dot{Q}_{load} \quad \Rightarrow \quad \tau_2 = MC \frac{T_{prog} - T_{av}}{\dot{Q}_{core} - \dot{Q}_{load}} \qquad (5-8)$$

$$\text{Otherwise,} \quad \tau_2 = \infty \qquad (5-9)$$

The available time is taken as the minimum value of the two calculated times, as shown in Eq. (5-10).

$$\tau_A = \min\{\tau_1, \tau_2\} \qquad (5-10)$$

The constraint which must be satisfied then takes the form of Eq. (5-11)

$$\tau_R \leq \tau_A \qquad (5-11)$$

Required time, τ_R, as obtained from the sufficient reactivity constraint in Eq. (5-4), is calculated from Eq. (5-12).

$$\tau_R = \frac{|\rho + [\dot{\rho}_c/\lambda_e]|}{|\dot{\rho}_c|} \qquad (5-12)$$

Information from a plant model is used to evaluate both the required and available times within the controller. The controller supervisory logic takes action to restore feasibility of control whenever the constraint of Eq. (5-11) is violated. If the constraint is met, then the control law used for control of the reactor is allowed to take action. In order to thoroughly test the constraints used, a very simplistic control law is deliberately chosen for evaluation during simulated transients with the dynamic plant model.

5.4 Transient Response

Figure (35) shows the reactor plant average primary coolant temperature response during an increase in load transient from 340 MW to 400 MW. Note that even though the control law is not designed to take action to reduce temperature until the programmed temperature value is exceeded, temperature overshoot does not occur due to the action of the supervisory algorithm in the reactor controller. Figure (36) plots the response of reactor power and reactivity to the increase in load transient. Power exceeds the demanded power, but does not overshoot the maximum allowed power, defined as 425 MW for this transient. The decision made by the supervisory algorithm can be observed by studying Figure (37), which shows the required time, τ_R, and available times, τ_A, for both power and temperature constraints. During the early portion of the transient, the power constraint takes action to prevent a power excursion above the maximum allowable power. Later in the transient, as temperature reaches the programmed value corresponding to the equilibrium temperature for the demanded load, the temperature constraint takes action to prevent a temperature overshoot. This occurs because reactor power is allowed to increase above its equilibrium value, and temperature follows power. The temperature constraint is defined so as to prevent overshoot beyond the programmed average coolant temperature.
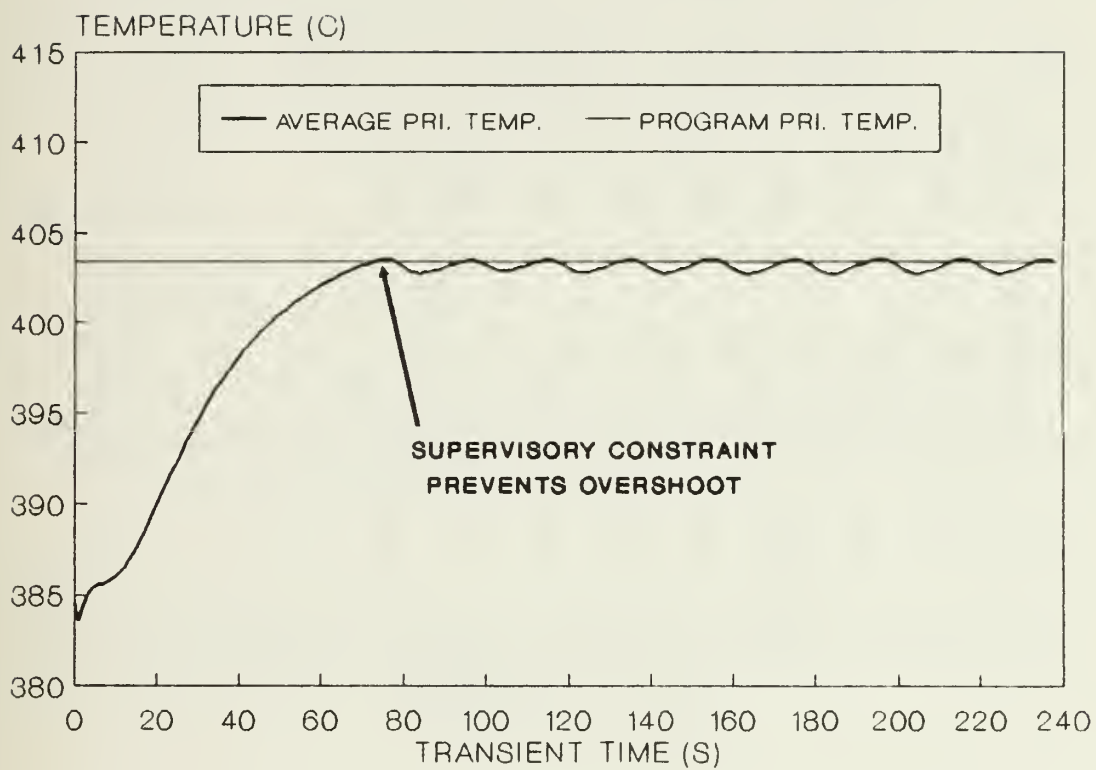
Figure (35) Temperature Response with

Non-Linear Temperature Controller

127
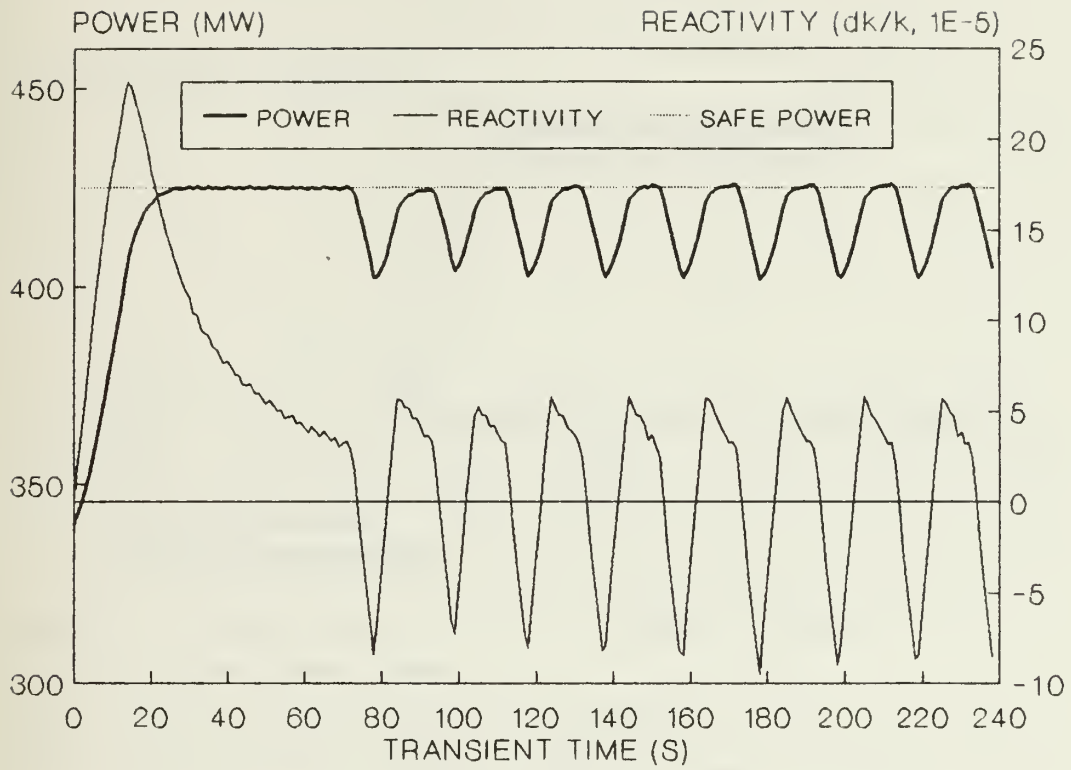
Figure (36) Power and Reactivity Response with

Non-Linear Temperature Controller

128
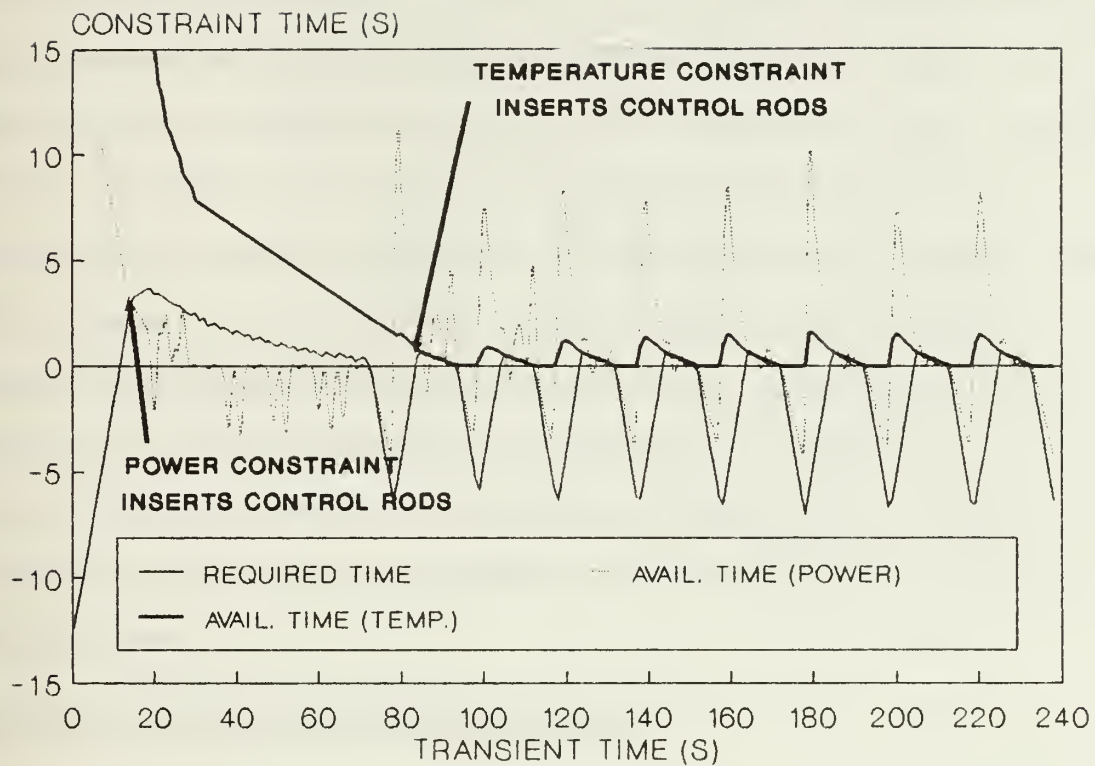
Figure (37) Required Time and Available Time

with Non-Linear Temperature Contoller

129

Other definitions for the temperature constraint could be formulated, perhaps relaxing the definition given here and substituting some maximum allowable coolant temperature instead. Regardless, even with an inadequate control law, the supervisory constraint as formulated effectively prevents overshooting allowed power and temperature. This result, in conjunction with the choice for the plant control principle, goes a long way toward solving the multi-modular control problem. A solution for the non-linear reactor plant temperature control problem has been proposed and demonstrated through simulation. Further work could involve evaluation of a suitable control law to operate within the supervisory constraints provided by the NLTC. Requirements for load-sharing and load-shifting between modules have been defined. A suitable control principle which is compatible with parallel steam supply module operation, has also been analyzed. A control program, which determines necessary reactor plant temperatures and flows, based upon steam flow and steam pressure demands, is implemented in a dynamic plant model and acceptable transient response of average coolant temperature has been demonstrated through simulation. Also demonstrated is the fault-tolerant capability of the reactor supervisory controller, and its ability to keep the plant within a safe operating envelope.

5.5 Recommendations for Further Research

In this report, a non-linear reactor plant temperature controller has been developed and demonstrated on a simulated plant model. The results are encouraging, with the ability to safely control reactor power and coolant temperature during transients demonstrated through simulation. Temperature is controlled at a level predicted to generate steam at a desired pressure. However, modeling of dynamic changes in steam pressure is beyond the scope of this report. Therefore, no strong statements about the effectiveness of the proposed multi-modular controller for closed-loop control of steam pressure and flow are possible. Only the effective control of reactor plant coolant temperature has been demonstrated.

Nevertheless, implementation of the controller proposed here in a more detailed multi-modular plant simulator may establish further confidence in the automatic control methodology presented here. More investigation is needed to attain closed-loop control of steam generator pressure. Load-following transients and load-shifting between modules also require further study. Such research requires a dynamic simulation of multiple modules, each with steam drums which respond to pressure variations in the steam header. The steam system should also have a turbine to simulate the load variations. With a simulator of this complexity, the structure of the power-block controller discussed in Section 3.4 could also be studied. More research is needed to decide upon the appropriate logic needed to shift loads between modules.

Also, experimental demonstration of the temperature constraint on the MITR-II research reactor or another test facility would help further establish the reactivity constraint approach to reactor control. More study on applying and implementing constraint control methodology in ways closely related to power plant thermal limits is also warranted. One possible scenario questions whether a thermal limit involving fuel centerline temperature would be violated during a transient if average primary coolant temperature exceeds the equilibrium value for the given load. If thermal-hydraulic limits could be formulated in the form of a constraint, that is, an available time until the specified limit is exceeded, then the supervisory element of the reactor controller would be exercising more realistic supervision of automatic control decisions.

With new reactor power plants promising enhanced safety, and automatic control of nuclear reactors being demonstrated, the era of manual operation of reactors may be coming to an end.

Appendix A - The DSNP Simulation Language

Introduction

The Dynamic Simulator for Nuclear Power plants (DSNP) is a special purpose, block-oriented, higher-level simulation language. It is designed to be set up directly from block diagrams of reactor systems and permits easy exchange of any of its modules. These modules describe the plant or the reactor component at different levels of complexity. This is a significant feature which permits portions of the plant requiring intense study to be modeled in finer detail than the remainder of the plant, with attendant cost of computing economy.

A computer program to simulate a nuclear power plant might contain between a thousand and a hundred thousand FORTRAN statements, depending on the degree of sophistication and complexity involved. The corresponding human effort invested in such a program ranges from one man-year to perhaps twenty man-years for a complex and detailed one. Many of these programs have a major drawback in that they were developed for a specific power plant or reactor type, and for a particular type of transient. The adaptation of any of these simulation programs to a different reactor type or transient consumes more time. The reason for this difficulty is the inflexible coupling among the various plant components, especially those with hydraulic couplings. Different thermal hydraulic elements will result in a different set of differential equations. In addition, the many numerical constants and thermal hydraulic correlations usually built into the program add to the complexity of program modifications.

The difficulties described above and the huge cost of software development provide the incentive for developing a higher-level, modular approach to the simulation of nuclear plants. The DSNP language is, in principle, a modular modeling system to solve the problem of plant simulation. It contains libraries of modules, with each module containing a programmed mathematical model of a plant component or a process. A statement of the module name will cause the cause the inclusion of the desired component or process into the simulation program.

The differential equations in the mathematical models of all the included components are grouped into a subroutine for solution by the integration routine(s) selected by the user. The proper links between a particular module and other parts of the plant are also established by the simulation software, and the necessary constants and correlations are included as required.

By using the DSNP language, therefore, a relatively small number of statements can produce a large simulation program. As a result, the programming effort to generate a FORTRAN program with DSNP is measured in man-days; even large modifications require only a number of man-hours. Also, the inherent flexibility of the language permits the simulation of a large variety of different power plants. Execution times are longer with the higher-level language, but are offset by the shorter development time.

The original version of DSNP was developed by Argonne National Laboratory in 1975-78 under the LMFBR program sponsored by DOE. In the following eleven years, many extensions and improvements have been made by DSNP users and incorporated into subsequent versions. All versions use the FORTRAN-77 compiler to compile the DSNP precompiler and also the FORTRAN programs generated by DSNP. The version of DSNP used in this report (version PC/A) runs on IBM compatible personal computers with the MICROSOFT FORTRAN compiler (version 4.01) and can be obtained from:

> John T. Madell
> Head, DSNP Users' Group
> System Simulation & Analyses, Inc.
> P.O. Box 199
> Western Springs, IL 60558
> (312) 246-0640

Basic Elements of the DSNP Language

Since DSNP is a language at a higher level than FORTRAN, a compiler is required to translate the DSNP statements into FORTRAN, Just as a FORTRAN compiler translates its

statements into machine language. The DSNP compiler, referred to as the "precompiler" to avoid confusion with the FORTRAN compiler, translates each DSNP statement into corresponding FORTRAN statements.

DSNP is a free field language except for the first column, which may only contain a control identifying character or symbol. Several statements can be placed in a record from column 2 through 72. Each statement must be terminated by a semicolon (;). The DSNP statements are subdivided into the following subgroups:

1)   control identification symbols (1st column)

2)   control statements, e.g., definition of a program segment

3)   structural statements, e.g., performance of an integration

4)   input-output statements, e.g., selection of output variables

5)   definitions, e.g., specification of additional COMMON blocks

6)   component module statements, e.g., inclusion of a neutron point kinetics module

7)   material properties statements, e.g., incorporation of a coolant density subroutine

8)   auxiliary function statements, e.g., inclusion of a user supplied subroutine

9)   MACRO statements, e.g., insertion of debugging statements

A full discussion of the DSNP statements can be found in the DSNP User's Manual [34]. Note that FORTRAN statements are a subset of DSNP statements and can be placed anywhere in the simulation program.

The basic structure of a DSNP program consists of at least three and as many as six types of segments. The BEGIN, SIMULATE and TERMINATE segments, which are the three required ones, specify the steady state initializing segment, the dynamic simulation segment, and the simulation termination time, respectively. The program may have a Declaration segment which interrelates component modules and defines other special features, a Function segment which adds special functions, and a Level-zero-library segment which includes user supplied modules or subroutines.

134

Writing a DSNP Program

Since DSNP is a block oriented simulation language, the first step in simulating a nuclear plant is the construction of a detailed block diagram of the system. Next, one should identify the blocks with components which correspond to modules in the DSNP libraries and prepare a new flowchart in which the names of physical components are replaced by those of DSNP modules. If modules are not available for a component, one is written and added to the appropriate library. The modules requiring a definition should be identified, and the appropriate information provided in the Declaration segment. A definition gives information needed to generate the FORTRAN program, such as the names of materials whose thermodynamic properties will be needed for the simulation, the number of nodes to be used for energy balances, or the arrangement of hydraulic flow paths. All the components and processes for which steady state calculations are necessary are included in the BEGIN segment. Here, one or more iteration loops are set up using absolute or relative convergence criteria to compute initial conditions prior to starting the transient. The SIMULATE segment contains the modules and other statements necessary for describing the dynamics of the system. More than one dynamic segment can be specified. If all the modules are closely coupled, a single dynamic segment is specified, with the differential equations solved using the selected numerical integration routine. If different parts of the system or plant are weakly coupled, it is more efficient to include each in its own segment with the appropriate numerical technique and relative time step.

The first statement in the next segment, the TERMINATE segment, specifies the simulation termination time. Post processing statements may follow the time statement. Although input/output statements can be placed anywhere in the program, they are usually located in this program segment. The DSNP input statements are similar to FORTRAN data statements

135

and cause a data block or input data file to be written. The output variables and printing frequencies are defined by "P" and "BYTO" statements, respectively. Segments in which the user supplies his own functions, modules, and subroutines follow the TERMINATE segment.

Sample DSNP Problem

A block diagram illustrating the relationship between the components of an LMFBR primary system is shown below in Figure (38).
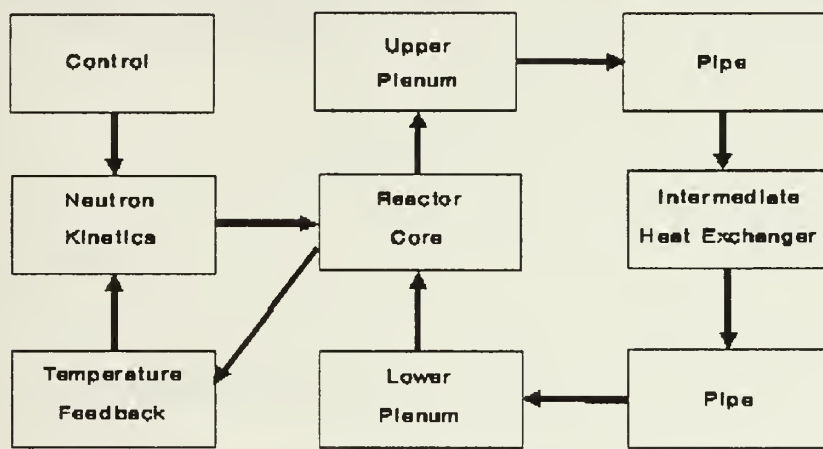
Figure (38) DSNP Block Diagram of an LMFBR Primary System

A sample DSNP file is listed below to illustrate some of the salient features of the code in simulating a LMFBR primary system. Components of this plant include a core, upper and lower mixing plenums, pipes connecting the plenums to an intermediate heat exchanger, and a source of external reactivity to initiate the transient.

```
C***************** DECLARATION SECTION ******************
.       CNCTCU(TENI,TECX);
.       DFIHXMAI(3,SO,SO,SS);
.       DFPIPELC(TEMX,TECI,ZFLCOR/ZROPXA,50);
.       DFPIPEUI(TENX,TEAPI,FPAI/ZROCX,25);
.       DFPIPEIL(TEAPX,TEMI,FPAI/ZROPXA,25);
C***************** INITIAL CONDITIONS ******************
BEGIN AT 0.D0
 1  CONTINUE
.       FDBEK1;
.       NEUTP1;
.       CNTRL1
```

136

```
       FPAI=ZFLCOR
   2   CONTINUE
   .       TPOWR1;
   .       LPLEN1;
   .       PIPELC;
   .       CORTP1(LMFBR);
   .       CNCTCU;
   .       UPLEN1;
   .       PIPEUI;
   .       IHXMA1;
   .       PIPEIL;
   .       CONVERGR(TECX,1.0D-3,2,10,P);
   .       CONVERGA(TEAPX,1.0D-1,1,10,P);
C****************** DYNAMIC SECTION **********************
SIMULATE LOOP01 STIFF1 TDV=2
   .       FDBEK1;
   .       NEUTP1;
   .       CNTRL1;
   .       TPOWR1;
   .       LPLEN1;
   .       PIPELC;
   .       CORTP1(LMFBR);
   .       CNCTCU;
   .       UPLEN1;
   .       PIPEUI;
SIMULATE LOOP02 TRAPZ1 TDV=1
   .       IHXMA1;
   .       PIPEIL;
C****************** TERMINAL SECTION *********************
TERMINATE AT 60.0D0
```

In the declaration section above, the intermediate heat exchanger is defined as having sodium coolant (SO) on both sides of a stainless steel tube (SS) with 3 axial nodes. Pipe "LC" connects the lower plenum to the core in terms of the energy equation only. Hydraulics are not included in this simulation. Pipe "UI" connects the upper plenum to the intermediate heat exchanger, "IL" connects the intermediate heat exchanger to lower plenum, etc. These pipes produce time delays in energy flow. The core is directly connected to the upper plenum by the .CNCTCU(TENI,TECX); statement. The flow path is short enough not to merit a time delay.

137

In the initial condition section, modules are listed in the desired order. In this problem, the CONVERGR(TECX...) statement will transfer control to statement label 2 and calculate the core exit temperature given the input data for the thermal conditions in the core. Then, if TECX does not differ from its initial value by more than the 0.1% error specified, the program will transfer to statement label 1 and calculate TEAPX for the value of TECX previously calculated. If TEAPX does not converge to the absolute error criteria of ±0.1 degree, then a new value of TECX will be calculated and the process repeated. The two iteration loops calculate steady state values for core exit temperature (TECX) and intermediate heat exchanger primary exit temperature (TEAPX). Notice that TECX will be varied as necessary to get a steady state value for TEAPX. So, set up the initial condition section with values we want to hold steady in the outer iteration loop (or loops). Place values which we are not sure of in the inner loop (or loops), and the simulation will force them to converge to steady state values. The user can experiment with ordering the modules in different ways and using different convergence loops in order to get the simulation to converge. Note that the modules can be in completely different orders in the initial condition section and dynamic section.

Two dynamic simulation iteration loops are used to improve the efficiency of execution in the dynamic section. The first loop uses a stiff algorithm with variable time steps, with the second loop making use of a trapezoidal integration algorithm. This helps to make up for the inefficiency in calculations caused by modular programming. Remember to experiment in order to find the best results.

Data input and output statements have been neglected from this example problem, but they are normally included after the termination section of the DSNP program. User supplied subroutines or modules are also included after the Termination section.

Inserting a User Supplied Subroutine

To include a user supplied subroutine, function or module in the simulation, use the "
.INCLUDE CONTR0; " statement in the declaration section for a subroutine named CONTR0.
Choose a function or subroutine name six characters long, the last of which should be "0". If
placing the subroutines within the DSNP problem file, on one line after the termination phase,
place an "L" in the first column to mark the Level-zero library. Then, place an "*" in the first
column followed immediately by the subroutine name. Now the FORTRAN or DSNP
statements used in the subroutine may be listed. If subroutines have been debugged and will
be used frequently, place them in a file called LIB0.FOR. The "L" marker in the first column
is no longer needed. Several statements must be inserted as shown below in subroutine
CONTR0 to ensure proper integration with the remainder of the DSNP generated FORTRAN
listing of the simulation code:

```
L
C***************** LEVEL ZERO LIBRARY ***********************
*CONTR0
      SUBROUTINE CONTR0
.     TICIL;
.     COMON/CONTR5/ ....(List of COMMON variables used in CONTR0 subroutine);
.     COMIN CONTR5;     (Includes COMON block just defined in subroutine)
      CHARACTER*8 SNAME
.     TASNA('CONTR0');
        •
        •
      (Any number of FORTRAN or DSNP statements)
        •     •
      KSUBST=KSUBST-1
      RETURN
      END
```

The statements included above are used to keep track of the subroutine under execution in
order to identify the source of simulation time errors. KSUBST is a stack counter. The
TASNA statement places the name of the subroutine in the stack. Without the counter and
name, the simulation may become "stuck" at some point, leading to an aborted simulation

run. TICIL ensures that variables are specified as double precision, since all DSNP routines use double precision arithmetic. Functions follow the same naming convention as subroutines, but do not require insertion of the special statements shown above.

A user may wish to define a module which has dynamic properties which require solution by the DSNP integration routine. Again, some special procedures must be followed which are listed in the DSNP User Manual, but are repeated here for clarity.

1) The variable "LOOP" must be one of the subprogram parameters.

2) The ".DYMOD;" statement must preceed any executable statement.

3) There must be a ".STATIC;" statement followed by whatever initial condition calculations are requested by the module.

4) There must be a ".DYNAMIC;" statement followed by the dynamic simulation statements executed in the module.

5) The dynamic segment must be terminated by the ".TERMINAL;" statement.

6) The range of allowed labels is from 1 to 900.

In the dynamic simulation, one must define the time derivative of the state variable which describes the system. In our power plant model, these derivatives are related to the mass or energy of the system. Once this derivative is defined, one merely uses the ".INTRGL=....;" OR ".VCTRGL=....;" statement in DSNP which ensures that the state will be integrated in the designated numerical integration routine. A stiff algorithm and a fourth-order Runge-Kutta algorithm are used in the PRISM power plant simulation. Once the new state is determined, other related values can be calculated in the user defined module and execution passed back to the main program.

Thermal Hydraulic Models

The three conservation equations - mass, energy, and momentum - for a plant component are given in not one, but two DSNP modules. One is called a component module, and the

other a hydraulic module. The energy equations are defined in the component module, and the momentum and mass equations in the hydraulic module. For example, the steam generator component modules, BOILR1 and DRUMS1, contain the equations simulating the transfer of energy from the reactor coolant through the tubes to the feedwater and steam. The flow rates and pressures are determined from the hydraulic modules HPIPE1 and FLOW, which are used to simulate the flow passages and secodary sides of the steam generator.

Component Modules

The component modules contain the energy equations for the fluid, the structures contacting the fluid, and any heat sources or sinks under both steady state and transient conditions. The steady state equations are algebraic in form and are located in the part of the module which is entered only during the calculation of the initial conditions. The energy equations in the dynamic section may be algebraic and/or differential. A constant mass condition is implied in the energy equations. Any time dependency of the mass in a component is modeled explicitly in the hydraulic equations. Modules reside in various DSNP libraries for the components in the primary system of LWRs, HTGRs, and LMFBRs. Some balance of plant components are also included. Modules of various levels of detail exist for components such as core channels, steam generators, pressurizers, and heat exchangers, but all are interchangeable with other component modules. For example, one steam generator module uses a lumped parameter model with single nodes for the primary side, secondary side and tubes. Another module uses a three region, multi-node representation with moving boundaries based on the boiling regimes.

Hydraulic Modules

The hydraulic modules are combined in a DSNP program to define a hydraulic network. A pipe module, HPIPExx, gives the flow characteristics (length, hydraulic diameter) in a

section of the network. The flow module, FLOWxx, describes the arrangement of the pipe sections and pumps which carry a particular flow. Modules for pumps (HPUMP1), junctions (JUNCxx), cavities (CAVTxx) and other hydraulic elements complete the description of the network. Three methods for solving the momentum equations are available: an integral method, a staggered mesh approximation, and a quasi-static approximation.

The hydraulic modules in the DSNP libraries model one-dimensional flows, but the structure of the language would allow, in principle, modules with multidimensional flow models. Two-phase flows are simulated with a single set of momentum equations which are supplemented with functional equations between the phases, such as slip ratio and two-phase multiplier relationships. In a recent development, special one-dimensional modules were developed for two component flow, e.g., helium and steam.

Neutronic Models

The neutronic processes are separated into individual DSNP modules. A typical simulation of the core neutronics uses six types of modules describing:

1)   feedback reactivity

2)   external reactivity due to control rods

3)   scram reactivity

4)   point kinetics

5)   decay heat

6)   core power deposition

As is the case for other thermal hydraulic engineering simulation software, DSNP inputs values for the reactivity coefficients and power and power distribution rather than calculating them from the core's neutronic parameters. The DSNP libraries contain several modules for each of the six processes noted above, allowing the user to select the level of detail and special features needed for the problem at hand. If the user wishes to speed computation of transients

not involving a reactor scram, for example, the scram reactivity module could be eliminated. The three neutron point kinetics modules use different assumptions and/or numerical techniques for solving the point kinetics equations. Decay heat generation can be obtained by solving one to eight differential equations, obtaining the level of detail desired by the user.

Physical Properties Models

Steam properties can be obtained in several ways, depending upon the version of DSNP. The data used in this report is obtained by solving the Helmholtz equations over the range of pressures and temperatures expected in the problem and generating a look-up table for thermodynamic properties. The physical properties of other materials are given in subroutines which are called from the component and hydraulic modules.

Solution Techniques

The steady-state solution which initializes the plant prior to beginning the transient is obtained by iterating sets of linear algebraic equations. The user places the module statements in an order and arranges them in iteration loops to achieve a fast convergence. Most orders and arrangements lead to rapid convergence of the energy equation. Fast convergence of the momentum equations is more difficult to assure, but the process is helped considerably by solving the hydraulic equations separately, as discussed above.

Once the selected parameters have converged in the initial condition calculations, the dynamic equations are calculate at time zero. Ideally, all rates of change of variables will be zero. In a large simulation, as the one used in this report, a few time steps are required for values to settle out during a null transient.

143

For the dynamic segments, the user selects the module order and numerical integration technique for up to five separate iteration loops. The time step for integration in each loop is set as a multiple of the basic time step. The experience gained in making these selections allows the users to write programs which perform efficient integrations.

The numerical integration techniques used in this simulation include a "stiff" algorithm for the neutronic point kinetic equations, and a fourth-order Runge-Kutta algorithm for the balance of the PRISM module components.

Transient Simulation

The modules currently in the DSNP libraries provide the capability of simulating most operational transients, such as control rod withdrawal, loss of reactor coolant pump, etc. A wide variety of transients in all types of reactors have been simulated with DSNP and reported in the literature. See Refs. [35] and [36] for more details.

144

Appendix B - Derivation of Steady State Control Program

Once a plant control principle has been selected, determination of the temperature control program becomes the central element in the design of the module supervisory controller. This map for the chosen control principle represents the steady state values of coolant flows within the reactor plant necessary for generating a given steam pressure and steam flow. These temperatures can be determined by applying the chosen control principle to the state equations presented in Chapter 2.

The first step involves setting the time derivatives of all the states to zero. Then, the equations are arranged as a system of linear algebraic equations. Plant heat transfer coefficients involve quantities dependent upon the temperature of the fluid being analyzed, and actually make the resulting state equations non-linear. However, the heat transfer coefficients are not extremely sensitive to temperature and can be calculated at the temperature for a nearby condition, making the equations linear. The system can be solved using linear algebra techniques, or if a dynamic model has been implemented, temperatures can be found by initializing the system and running a null transient. Both approaches have been used to obtain and verify an accurate control map for use with the PRISM plant model.

Equilibrium state mapping defines the plant system as described by the state equations, with core power output ($\dot{Q}_{core}$), saturation temperature (T_{sat}), and riser temperature (T_r) as input variables. Then, the feedwater temperature and saturation temperature (pressure) are held at some desired value, and the core power is varied. Another approach maps temperatures in the plant as pressure varies and power is held constant. A combination of these maps, accounting for feedwater variations with power or pressure, is needed in the module supervisory controller to properly estimate the equilibrium temperatures in the module necessary for sharing thermal loads in a multi-modular array.

Core Temperatures

Beginning in the reactor core, under steady state conditions, the reactor power ($\dot{Q}_{core}$) is related to coolant flow rate (W_p), specific heat (C_p), and coolant temperature (T_{core}) by Eq. (B-1).

$$\dot{Q}_{core} = W_p C_p (T_{core}^{in} - T_{core}^{out}) \qquad (B-1)$$

Intermediate Heat Exchanger Temperatures

Within the intermediate heat exchanger at steady state, the primary side coolant node energy balance is described by Eq. (B-2). Refer to Figure (39) for a diagram of the IHX, with nodes labeled according to the convention used here.
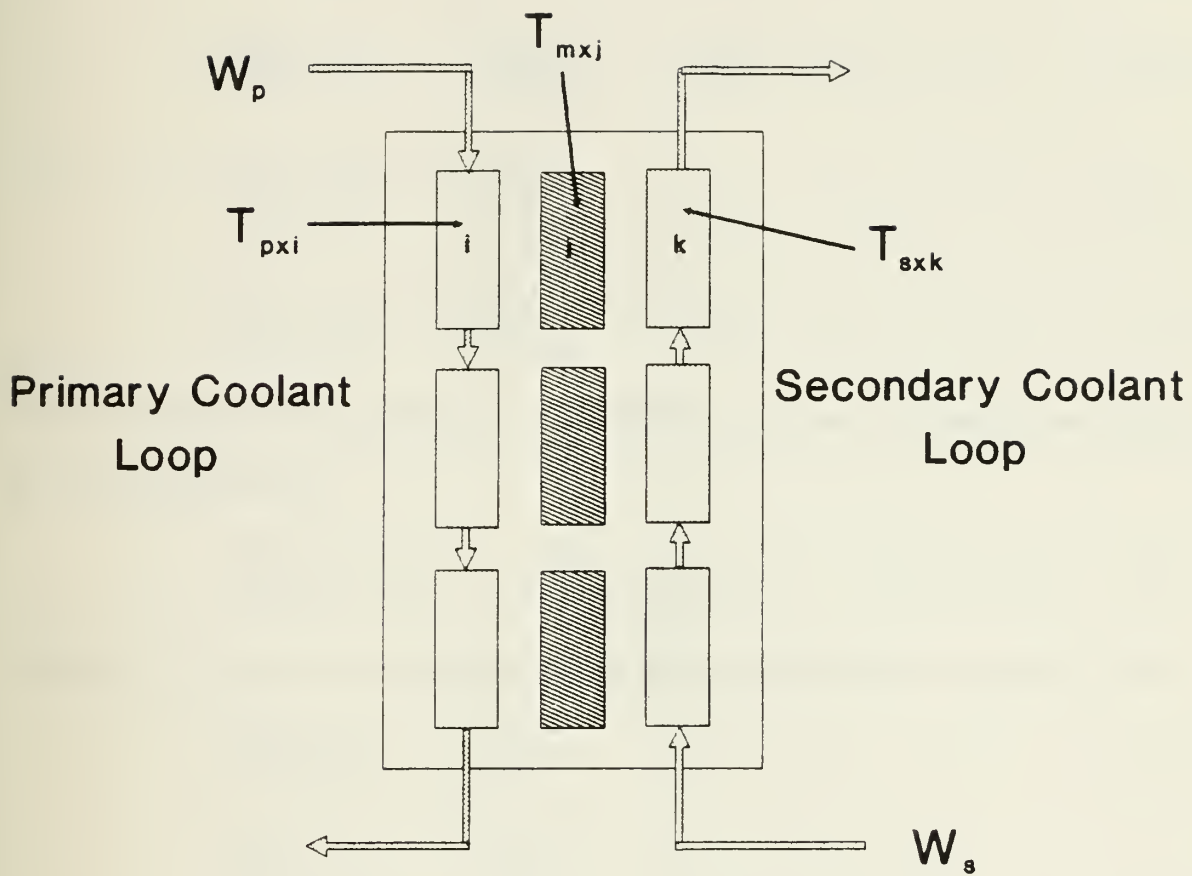
Figure (39) Intermediate Heat Exchanger Nodal Diagram

$$0 \;=\; \frac{W_p}{M_{pxi}}(T_{pxi}^{\text{in}} - T_{pxi}) \;-\; \frac{H_{pmx}}{(MC)_{pxi}}(T_{pxi} - T_{mxj}) \qquad (i = j = 1, 2, 3) \quad (B-2)$$

Given that the IHX is connected to the core, with the primary side inlet temperature being equal to the core outlet temperature, the three primary nodes are described by Eqs. (B-3) to (B-5).

$$\left[\frac{W_p C_{px1}}{H_{pmx}}\right]T_{core}^{out} \;-\; \left[\frac{W_{px1}C_{px1}}{H_{pmx}} + 1\right]T_{px1} \;+\; T_{mx1} \;=\; 0 \qquad (B-3)$$

$$\left[\frac{W_p C_{px2}}{H_{pmx}}\right]T_{px1} \;-\; \left[\frac{W_p C_{px2}}{H_{pmx}} + 1\right]T_{px2} \;+\; T_{mx2} \;=\; 0 \qquad (B-4)$$

$$\left[\frac{W_p C_{px3}}{H_{pmx}}\right]T_{px2} \;-\; \left[\frac{W_p C_{px3}}{H_{pmx}} + 1\right]T_{core}^{\text{in}} \;+\; T_{mx3} \;=\; 0 \qquad (B-5)$$

Moving to the secondary coolant nodes of the IHX at steady state, the energy balance gives the relationship in (B-6).

$$0 \;=\; \frac{W_s}{M_{sxk}}(T_{sxk}^{\text{in}} - T_{sxk}) \;-\; \frac{H_{mxs}}{(MC)_{sxk}}(T_{sxk} - T_{mxj}) \qquad (j = k = 1, 2, 3) \quad (B-6)$$

Writing Eq. (B-6) for each of the three secondary coolant nodes results in Eqs. (B-7) to (B-9).

$$\left[\frac{W_s C_{sx3}}{H_{mxs}}\right]T_{pg3} \;-\; \left[\frac{W_s C_{sx3}}{H_{mxs}} + 1\right]T_{sx3} \;+\; T_{mx3} \;=\; 0 \qquad (B-7)$$

$$\left[\frac{W_s C_{sx2}}{H_{mxs}}\right]T_{sx3} \;-\; \left[\frac{W_s C_{sx2}}{H_{mxs}} + 1\right]T_{sx2} \;+\; T_{mx2} \;=\; 0 \qquad (B-8)$$

$$\left[\frac{W_s C_{sx1}}{H_{mxs}}\right]T_{sx2} \;-\; \left[\frac{W_s C_{sx1}}{H_{mxs}} + 1\right]T_{sx1} \;+\; T_{mx1} \;=\; 0 \qquad (B-9)$$

Regarding the tubes of the IHX, each metal node is described at steady state conditions by Eq. (B-10).

$$\frac{H_{pmx}}{H_{mxs}}(T_{pxi} - T_{mxj}) \;-\; (T_{mxj} - T_{sxk}) \;=\; 0 \qquad (i = j = k = 1, 2, 3) \quad (B-10)$$

148

Writing Eq. (B-10) for each of the three metal tubing nodes results in Eqs. (B-11) to (B-13).

$$\left[\frac{H_{pmx}}{H_{mxs}}\right]T_{px1} \quad - \quad \left[\frac{H_{pmx}}{H_{mxs}} + 1\right]T_{mx1} \quad + \quad T_{sx1} \quad = \quad 0 \qquad (B-11)$$

$$\left[\frac{H_{pmx}}{H_{mxs}}\right]T_{px2} \quad - \quad \left[\frac{H_{pmx}}{H_{mxs}} + 1\right]T_{mx2} \quad + \quad T_{sx2} \quad = \quad 0 \qquad (B-12)$$

$$\left[\frac{H_{pmx}}{H_{mxs}}\right]T_{core}^{in} \quad - \quad \left[\frac{H_{pmx}}{H_{mxs}} + 1\right]T_{mx3} \quad + \quad T_{sx3} \quad = \quad 0 \qquad (B-13)$$

Steam Generator Temperatures

In the steam generator, equilibrium conditions exist in the primary side coolant nodes when Eq. (B-14) is satisfied. See Figure (40) for a diagram of the steam generator.

$$0 \quad = \quad \frac{W_s}{M_{pgi}}(T_{pgi}^{in} - T_{pgi}) \quad - \quad \frac{H_{pmg}}{(MC)_{pgi}}(T_{pgi} - T_{mgj}) \qquad (i = j = 1, 2) \qquad (B-14)$$

By writing the equilibrium condition for each of the two primary side coolant nodes, Eqs. (B-15) and (B-16) are obtained.
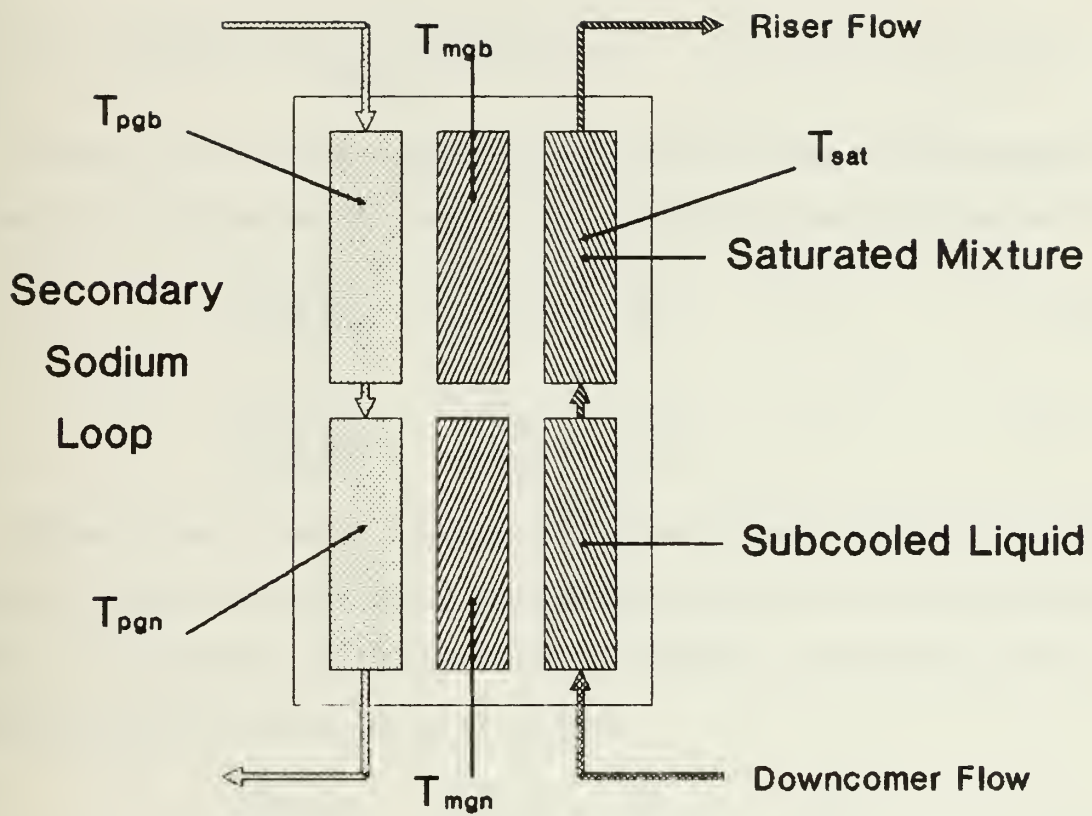
Figure (40) Steam Generator Nodal Diagram

$$\left[\frac{W_s C_{pg1}}{H_{pmg}}\right] T_{sx1} \quad - \quad \left[\frac{W_s C_{pg1}}{H_{pmg}} + 1\right] T_{pg1} \quad + \quad T_{mg1} \quad = \quad 0 \qquad (B-15)$$

$$\left[\frac{W_s C_{pg2}}{H_{pmg}}\right] T_{pg1} \quad - \quad \left[\frac{W_s C_{pg2}}{H_{pmg}} + 1\right] T_{pg2} \quad + \quad T_{mg2} \quad = \quad 0 \qquad (B-16)$$

The metal nodes, in both the boiling and non-boiling regions, are in equilibrium when Eq. (B-17) is satisfied.

$$0 \quad = \quad \frac{H_{pmg}(T_{pgi} - T_{mgj}) \quad - \quad H_{mgk}(T_{mgj} - T_{sk})}{(MC)_{mgj}} \qquad (i = j = 1, 2) \quad (k = b, n)(B-17)$$

Of course, we may write two equations using Eq. (B-17), one for the boiling region, and one for the non-boiling region. The results are shown in Eqs. (B-18) and (B-19), respectively.

$$\left[\frac{H_{pmg}}{H_{mgb}}\right] T_{pg1} \quad - \quad \left[\frac{H_{pmg}}{H_{mgb}} + 1\right] T_{mg1} \quad = \quad -T_b \qquad (B-18a)$$

$$\left[\frac{H_{pmg}}{H_{mgn}}\right] T_{pg2} \quad - \quad \left[\frac{H_{pmg}}{H_{mgn}} + 1\right] T_{mg2} \quad = \quad -T_r \qquad (B-19)$$

The temperatures on the secondary side of the steam generator tubes correspond to the temperature of the water in the boiling and non-boiling regions. The boiling region temperature, T_b, corresponds to the saturation temperature for the secondary side pressure, T_{sat}. This changes Eq. (B-18a) to (B-18b) as shown below.

$$\left[\frac{H_{pmg}}{H_{mgb}}\right] T_{pg1} \quad - \quad \left[\frac{H_{pmg}}{H_{mgb}} + 1\right] T_{mg1} \quad = \quad -T_{sat} \qquad (B-18b)$$

The temperature in the riser, T_r, is a function of feedwater temperature, T_{fdw}, as well as saturation temperature since the feedwater mixes in the steam drum with saturated liquid.

151

Solving for the Steady State Temperature Vector

Having obtained the set of equilibrium temperature equations, we are now ready to solve them as a system. First, choose a temperature vector, $\vec{T}$, and write out the equations in a fashion so as to form a coefficient matrix, $\vec{A}$, and an input vector, $\vec{U}$, as shown below.

$$\vec{A}\,\vec{T} \;=\; \vec{U} \qquad\qquad (B-20)$$

$\vec{T}$ is a 14 x 1 column vector given by:

$$\vec{T} = [T_{core}^{out} \quad T_{px1} \quad T_{px2} \quad T_{px3} \quad T_{mx1} \quad T_{mx2} \quad T_{mx3} \quad T_{sx1} \quad T_{sx2} \quad T_{sx3} \quad T_{pg1} \quad T_{pg2} \quad T_{mg1} \quad T_{mg2}]^T$$

$$(B-21)$$

The input vector, $\vec{U}$, is also a 14 x 1 column vector composed of elements given by:

$$\vec{U} = [\dot{Q}_{core} \quad 0 \quad 0 \quad 0 \quad 0 \quad 0 \quad 0 \quad 0 \quad 0 \quad 0 \quad 0 \quad 0 \quad -T_{sat} \quad -T_r]^T \qquad (B-22)$$

$\vec{A}$ is a 14 x 14 square matrix with most elements on or along the diagonal. Unless otherwise specified, $\vec{A}_{ij} = 0$. Other elements are given below in (B-23).

$$A_{11} \;=\; W_p C_c \qquad\qquad A_{14} \;=\; -\; W_p C_c$$

$$A_{21} = \frac{W_p C_{px1}}{H_{pmx}} \qquad A_{22} = -\left[\frac{W_p C_{px2}}{H_{pmx}} + 1\right] \qquad A_{25} = 1$$

$$A_{32} = \frac{W_p C_{px2}}{H_{pmx}} \qquad A_{33} = -\left[\frac{W_p C_{px2}}{H_{pmx}} + 1\right] \qquad A_{36} = 1$$

$$A_{34} = \frac{W_p C_{px3}}{H_{pmx}} \qquad A_{44} = -\left[\frac{W_p C_{px3}}{H_{pmx}} + 1\right] \qquad A_{47} = 1$$

$$A_{52} = \frac{H_{pmx}}{H_{mxs}} \qquad A_{55} = -\left[\frac{H_{pmx}}{H_{mxs}} + 1\right] \qquad A_{58} = 1$$

$$A_{63} = \frac{H_{pmx}}{H_{mxs}} \qquad A_{66} = -\left[\frac{H_{pmx}}{H_{mxs}} + 1\right] \qquad A_{69} = 1$$

$$A_{74} = \frac{H_{pmx}}{H_{mxs}} \qquad A_{77} = -\left[\frac{H_{pmx}}{H_{mxs}} + 1\right] \qquad A_{710} = 1$$

$$A_{85} = 1 \qquad A_{88} = -\left[\frac{H_{pmx}}{H_{mxs}} + 1\right] \qquad A_{89} = \frac{W_s C_{sx1}}{H_{mxs}}$$

$$A_{96} = 1 \qquad A_{99} = -\left[\frac{W_s C_{sx1}}{H_{mxs}} + 1\right] \qquad A_{910} = \frac{W_s C_{sx2}}{H_{mxs}}$$

$$A_{107} = 1 \qquad A_{1010} = -\left[\frac{W_s C_{sx3}}{H_{mxs}} + 1\right] \qquad A_{1012} = \frac{W_s C_{sx3}}{H_{mxs}}$$

$$A_{118} = \frac{W_s C_{pg1}}{H_{pmg}} \qquad A_{1111} = -\left[\frac{W_s C_{pg1}}{H_{pmg}} + 1\right] \qquad A_{1113} = 1$$

$$A_{1211} = \frac{W_s C_{pg2}}{H_{pmg}} \qquad A_{1212} = -\left[\frac{W_s C_{pg2}}{H_{pmg}} + 1\right] \qquad A_{1214} = 1$$

$$A_{1311} = \frac{H_{pmg}}{H_{mgb}} \qquad A_{1313} = -\left[\frac{H_{pmg}}{H_{mgb}} + 1\right]$$

$$A_{1412} = \frac{H_{pmg}}{H_{mgn}} \qquad A_{1414} = -\left[\frac{H_{pmg}}{H_{mgn}} + 1\right]$$

$$(B - 23)$$

Determining the values of the elements in the $\vec{A}$ matrix depends upon the flowrate, W_p

and W_s, specific heat capacity of the sodium coolant, C_{xxx}, and overall heat transfer coefficient,

H_{xxx}. For the reasons discussed in Chapter 3, a variable flow program to maintain a constant

power-to-flow ratio in the reactor is chosen for this study. Specific heat for sodium coolant

can be calculated using an algebraic curve fit to experimental data. Heat transfer coefficients

are by far the most difficult quantity to obtain when analyzing steady state temperatures in

the plant. The reasons for this difficulty will be discussed further below.

Programmed flow conditions are controlled to maintain a constant power-to-flow ratio in the reactor. Both primary and secondary sodium coolant loops follow the same program, as defined in Eq. (B-24).

$$W_p \;=\; W_s \;=\; W_{rated} \;+\; \left[\dfrac{W_{rated}}{\dot{Q}_{rated}}\right](\dot{Q} \;-\; \dot{Q}_{rated}) \qquad (B-24)$$

$\dot{Q}_{rated}$ and W_{rated} represent maximum rated values of core thermal power and rated mass flow rate, respectively. Values used can be found in Appendix C of this report.

The specific heat of sodium is calculated from an algebraic fit of available experimental data as a function of temperature [37]. This correlation is given in Eq. (B-25), with specific heat in units of (J/kg°C) and temperature in units of degrees Celsius (°C).

$$C_p \;=\; (1.43605 \times 10^3) \;+\; T[-0.5802 \;+\; T(4.62506 \times 10^{-4})] \qquad (B-25)$$

Obtaining a value for the overall heat transfer coefficient, H, proves to be more involved than simply using a correlation which is a function of a single variable. H is related to the heat transfer coefficient by Eq. (B-26), with A_s representing the area of the heat transfer surface.

$$H \;=\; UA_s \qquad (B-26)$$

In calculating U, several dimensionless quantities are used, the first of which is the Nusselt number, Nu, defined in Eq. (B-27).

$$Nu \;=\; \dfrac{UD_e}{K} \qquad (B-27)$$

D_e is the equivalent diameter of the channel in meters, defined in Eq. (B-28), and K is the thermal conductivity of the coolant in units of (W/m°C), given by the correlation [38] in Eq. (B-29) as a function of temperature.

$$D_e = \frac{4A}{P} \qquad (B-28)$$

A is the cross-sectional area of the flow channel, and P is the wetted perimeter.

$$K = 92.948 - T(5.809 \times 10^{-2}) + T^2(1.1727 \times 10^{-5}) \qquad (B-29)$$

Nusselt numbers are obtained from empirical correlations obtained from experimental data. One should choose the correlation used to calculate the Nusselt number carefully, ensuring that its use is consistent with the conditions for which it has been derived. For sodium coolant, Nusselt correlations all depend upon the Peclet number, Pe, which is defined in Eq. (B-30) below.

$$Pe = \frac{VD_e\rho C_p}{K} \qquad (B-30)$$

V represents the flow velocity across the heat transfer surface. Once the total cross-sectional area of the flow channel, A, is known, and the mass flow rate, W, is determined, the average flow velocity can be calculated from the continuity relationship in Eq. (B-31). Density of the sodium coolant is determined by a correlation [39] shown in Eq. (B-32), with density in units of (kg/m^3) and temperature in degrees Celsius.

$$V = \frac{W}{\rho A} \qquad (B-31)$$

$$\rho = 950.076 + T\{-0.2297 + T[(-1.46049 \times 10^{-5}) + T(5.63788 \times 10^{-9})]\} \qquad (B-32)$$

Once the Peclet number is known for the flow conditions in the heat exchanger, the appropriate Nusselt number correlation can be used to calculate Nu. For heat transfer from the primary sodium on the shell side of the intermediate heat exchanger (IHX) to the metal tubes, Eq. (B-33) gives the Nusselt correlation [40].

$$Nu = 0.313 + 0.2(Pe)^{0.613} \qquad (B-33)$$

155

For flow through the tubes on the secondary side of the IHX, the appropriate correlation is given in Eq. (B-34). P/D represents the dimensionless pitch-to-diameter ratio, where pitch, P, is the spacing between the tube centers, and D is the tube diameter.

$$Nu \;=\; 4.0 \;+\; 0.33(P/D)^{3.8}(Pe/100)^{0.86} \;+\; 0.16(P/D)^{5.0} \qquad (B-34)$$

Use Eq. (B-33) for the primary (shell) side of the steam generator evaporator section in both the boiling and non-boiling regions.

On the secondary (tube) side of the steam generator, the coolant is water, and the dimensionless numbers already defined are calculated in terms of the water properties, flows, etc. For the boiling region, the Nusselt number is calculated [41] by Eq. (B-35). Re represents the Reynolds number, defined in Eq. (B-36) and Pr represents the Prandtl, another dimensionless quantity, defined in Eq. (B-37).

$$Nu \;=\; 0.0193(Re)^{0.8}(Pr)^{1.23}\left(\frac{\beta}{\alpha}\right)^{0.68}\left[X \;+\; (1 \;-\; X)\frac{\beta}{\alpha}\right]^{0.68} \qquad (B-35)$$

$$Re \;=\; \frac{D_e V \rho}{\mu} \qquad (B-36)$$

$$Pr \;=\; \frac{C_p \mu}{K} \qquad (B-37)$$

The symbol μ represents fluid viscosity, α represents the vapor volume fraction, β is the liquid volume fraction, and X is the quality of the saturated steam mixture.

In the non-boiling region of the steam generator secondary side, the Nusselt number is calculated using the Dittus-Boelter correlation, shown in Eq. (B-38).

$$Nu \;=\; 0.023(Re)^{0.8}(Pr)^{0.4} \qquad (B-38)$$

Now, knowing the heat transfer coefficients, U, and with the size of the heat transfer area, one can calculate the overall coefficient, H_{xxx}, for each node in the plant model. With the additional knowledge of desired flows, and the specific heat capacity of the fluids, we are

at last in a position to calculate all of the quantities in $\vec{A}$ and solve for $\vec{T}$, the vector of steady state temperatures in the plant. By selecting the input parameter of interest, either power level, $\dot{Q}$, or T_{sat} (P_{sat}) in the steam generator, the plant control program for pressure and power level can be calculated. This map will be used by the module supervisory controller described in Chapter 3 to decide upon the plant temperature control points for given pressure and power level demands on the module. A map of plant primary temperatures to maintain a constant pressure can be implemented using an algebraic curve fit from calculated data. The appropriate plant set points can then be calculated on-line. This approach towards control of steam pressure and flow is not closed-loop. The predicted pressure is not guaranteed since errors in the calculation of the heat transfer coefficients could occur due to plant aging, scale buildup on heat exchanger tubes, or inaccuracies in correlations used. However, use of this implementation of the control principle for the plant should cause steam to be produced at or near the desired values during steady state.

Appendix C - PRISM Plant Data

PRISM Plant Data	
PARAMETER	VALUE
POWER BLOCK	
Number of PRISM modules	3
Rated turbine-generator output (MW_e)	415
Rated thermodynamic efficiency (%)	32.5
Rated thermal output (MW_t)	1275
Rated steam flow to turbine (kg/sec)	622.4
Turbine throttle steam pressure (MPa)	6.653
Turbine throttle steam temperature ($^\circ$C)	282
Feedwater temperature at steam drum ($^\circ$C)	216
MODULE	
Number of primary pumps (EM type)	4
Number of intermediate heat exchangers	2
Number of steam generators	1
Rated thermal output (MW_t)	425
Primary sodium hot leg temperature ($^\circ$C)	468
Primary sodium cold leg temperature ($^\circ$C)	321
Primary flow rate through core (kg/sec)	2913
Average linear power (KW/m)	18.37
Peak linear power (KW/m)	31.17
Core height (m)	1.2

Rated steam flow (kg/sec)	207.9

The data listed below was provided by the Oak Ridge National Laboratory in .

PRISM Plant Modeling Data [42]	
Overall eat transfer coefficient, clad-to-primary coolant (W/°C)	5.195122×10^6
Overall heat transfer coefficient, primary coolant-to-IHX tube wall (W/°C)	71.0×10^6
Overall heat transfer coefficient, IHX tube wall-to-secondary coolant (W/°C)	71.0×10^6
Overall heat transfer coefficient, secondary coolant-to-SG tube wall (W/°C)	5.1695203×10^6
Overall heat transfer coefficient, SG tube wall-to-water (W/°C)	5.1695203×10^6
Primary hot leg coolant mass (kg)	46,989.0
Primary cold leg coolant mass (kg)	94,886.0
Core coolant mass (kg)	10,442.0
Core fuel mass (kg)	30,000.0
IHX primary coolant mass (kg)	40,860.0
IHX secondary coolant mass (kg)	36,774.0
IHX tube metal mass (kg)	25,197.0
Secondary sodium hot leg coolant mass (kg)	38,700.0
Secondary sodium cold leg coolant mass (kg)	33,097.0
SG primary coolant mass (kg)	305,088.0
SG tube metal mass (kg)	273,762.0
Steam drum volume (m³)	30.0

Appendix D - Steam Drum Model

The steam drum collects wet steam from the evaporator section of the steam generator and can be modeled as a single node, containing a saturated mixture of liquid and vapor phases. This model is sometimes referred to as the "boiling pot" representation [43]. It assumes that pressure is uniform throughout the drum. Incoming feedwater mixes instantly with the saturated liquid and is recirculated as subcooled fluid to the boiler through the downcomer. The two phases of saturated water are assumed to be in thermodynamic equilibrium at all times. See Figure (41) for a schematic diagram of the steam drum, showing incoming and outgoing flows.

By performing a mass balance on the steam drum, we can obtain a differential equation describing drum fluid mass. This result is presented in Eq. (D-1).
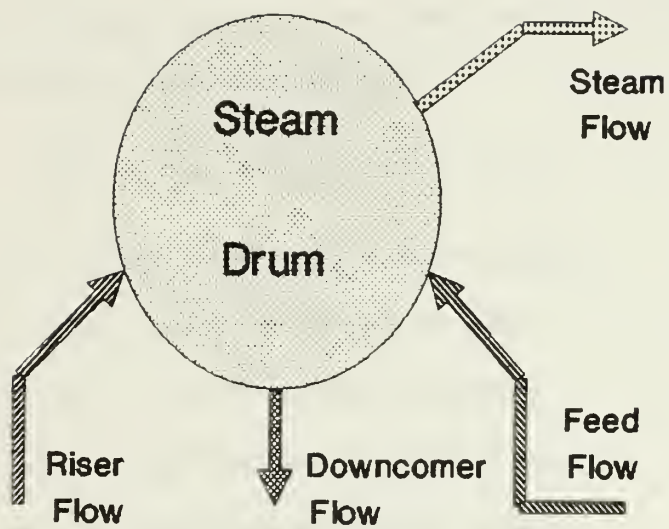
Figure (41) Steam Drum Model Schematic

$$\frac{dM}{dt} = W_r + W_{fdw} - W_s - W_d \qquad (D-1)$$

M = total control volume mass

W_r = riser fluid mass flow rate

W_{fdw} = feedwater mass flow rate

W_s = steam mass flow rate

W_d = downcomer fluid mass flow rate

By accounting for the energy brought into the drum by each of the flows, we can also write an energy balance equation, as shown in Eq. (D-2).

$$\frac{dE}{dt} = W_r h_r + W_{fdw} h_{fdw} - W_s h_s - W_d h_d \qquad (D-2)$$

E = total control volume internal energy

h_r = riser fluid specific enthalpy

h_{fdw} = feedwater specific enthalpy

h_s = saturated vapor specific enthalpy

h_d = downcomer fluid specific enthalpy

Pressure, P, and vapor volume fraction, α, are chosen as the states of the steam drum, where the latter is defined in Eq. (D-3).

$$\alpha = \frac{V_v}{V} \qquad (D-3)$$

V = total drum volume

V_v = total vapor phase volume

The model requires initial conditions for P and α. All of the thermodynamic properties of the saturated mixture are taken to be functions of pressure. We shall see below how this allows us to expand the energy balance and rewrite it in terms of pressure. For numerical simulation,

162

it is desirable to use a form of Eq. (D-2) that is independent of the arbitrary reference point for enthalpy and internal energy. This may be accomplished by multiplying Eq. (D-1) by any reference enthalpy (we shall choose $h_{ref} = h_s$ for convenience) and subtracting the result from Eq. (D-2). The result is presented in Eq. (D-4). See Ref. [44] for details on this procedure, as well as an algebraic fit for saturated steam properties as a function of pressure based upon the TRAC code.

$$\frac{dE}{dt} - h_s \frac{dM}{dt} = W_r(h_r - h_s) + W_{fdw}(h_{fdw} - h_s) - W_d(h_d - h_s) \qquad (D-4)$$

The control volume energy and mass can be expressed in terms of the state variables in Eq. (D-5) and (D-6).

$$M = [\rho_l(1 - \alpha) + \rho_v \alpha]V \qquad (D-5)$$

$$E = [\rho_l u_l(1 - \alpha) + \rho_v u_v \alpha]V \qquad (D-6)$$

$$\rho_l = \text{saturated liquid density}$$

$$\rho_v = \text{saturated vapor density}$$

$$u_l = \text{saturated liquid specific internal energy}$$

$$u_v = \text{saturated vapor specific internal energy}$$

Note that ρ_l, ρ_v, u_l, u_v are all functions of pressure. The time derivatives of M and E are given by Eq. (D-7) and (D-8).

$$\frac{dM}{dt} = \left(\frac{\partial M}{\partial p}\right)_\alpha \frac{dp}{dt} + \left(\frac{\partial M}{\partial \alpha}\right)_p \frac{d\alpha}{dt}$$

$$= \left[\frac{d\rho_l}{dp}(1 - \alpha) + \frac{d\rho_v}{dp}\alpha\right]V\frac{dp}{dt} + (\rho_v - \rho_l)V\frac{d\alpha}{dt} \qquad (D-7)$$

$$\frac{dE}{dt} = \left(\frac{\partial E}{\partial p}\right)_\alpha \frac{dp}{dt} + \left(\frac{\partial E}{\partial \alpha}\right)_p \frac{d\alpha}{dt}$$

$$= \left[\frac{d(\rho_l u_l)}{dp}(1-\alpha) + \frac{d(\rho_v u_v)}{dp}\alpha\right]V\frac{dp}{dt} + [\rho_v u_v - \rho_l u_l]V\frac{d\alpha}{dt} \qquad (D-8)$$

Substituting Eq. (D-7) and (D-8) into (D-1) and (D-4) produces the set of state equations in the form we wish to use, as shown in Eq. (D-9).

$$\vec{A}\frac{d}{dt}\begin{bmatrix} P \\ \alpha \end{bmatrix} = \begin{bmatrix} W_r & + & W_{fdw} & - & W_s & - & W_d \\ W_r & (h_r - h_v) & + & W_{fdw} & (h_{fdw} - h_v) & - & W_d & (h_d - h_v) \end{bmatrix} \qquad (D-9)$$

$\vec{A}$ is a 2 x 2 vector with the following entries:

$$A_{11} = \left[\alpha\frac{d\rho_v}{dp} + (1-\alpha)\frac{d\rho_l}{dp}\right]V \qquad (D-10)$$

$$A_{12} = [\rho_v - \rho_l]V \qquad (D-11)$$

$$A_{21} = \left\{\alpha\left[\rho_v\frac{du_v}{dp} - \frac{p}{\rho_v}\frac{d\rho_v}{dp}\right] + (1-\alpha)\left[\rho_l\frac{du_l}{dp} + \frac{d\rho_l}{dp}(u_l - u_v) - \frac{p}{\rho_v}\frac{d\rho_l}{dp}\right]\right\}V \qquad (D-12)$$

$$A_{22} = \left[(u_v - u_l)\rho_l + \left(\frac{\rho_l}{\rho_v} - 1\right)p\right]V \qquad (D-13)$$

Eq. (D-9) may be represented in the form of Eq. (D-14).

$$\vec{A}(\vec{x})\frac{d\vec{x}}{dt} = \vec{f}(\vec{x},\vec{u}) \qquad (D-14)$$

The state vector is defined as shown in Eq. (D-15).

$$\vec{x} = \begin{bmatrix} p \\ \alpha \end{bmatrix} \qquad (D-15)$$

The input vector consists of the elements given in Eq. (D-16).

$$
\vec{u} = \begin{bmatrix} W_{fdw} \\ W_s \\ W_r \\ W_d \\ h_r \\ h_{fdw} \end{bmatrix}
\qquad\qquad (D-16)
$$

The vector which combines the inputs and states is defined in Eq. (D-17).

$$
\vec{f}(\vec{x},\vec{u}) = \begin{bmatrix} W_r & + & W_{fdw} & - & W_s & - & W_d \\ W_r \; (h_r - h_v) & + & W_{fdw} \; (h_{fdw} - h_v) & - & W_d \; (h_d - h_v) \end{bmatrix} (D-17)
$$

For simulation purposes, one must evaluate the terms in the $\overrightarrow{A}$ at each time step, invert

the matrix to obtain $\overrightarrow{A}^{-1}$, and multiply $\overrightarrow{A}^{-1}\vec{f}(\vec{x},\vec{u})$ to obtain the state derivative vector. The

derivative can then be integrated with an appropriate numerical integration procedure to find

the state.

Unfortunately, the boiling pot model developed here exhibits unstable behavior above

3 MPa pressure. Stability is determined by the eigenvalue of the linearized system. It can be

shown that the two eigenvalues for the steam drum system are given by Eq. (D-18), (D-19a),

and (D-19b).

$$
\lambda_1 = 0 \qquad\qquad (D-18)
$$

$$
\lambda_2 < 0 \qquad\qquad \text{for } p < 3 \text{ MPa} \qquad\qquad (D-19a)
$$

$$
\lambda_2 > 0 \qquad\qquad \text{for } p > 3 \text{ MPa} \qquad\qquad (D-19b)
$$

The first eigenvalue, $\lambda_1 = 0$, corresponds to an open integrator. This open integrator

occurs because when the boiling pot model is an equilibrium condition, the vapor volume

fraction α can take on any value between 0 and 1 for given pressure and given inputs.

The second eigenvalue, λ_2, is a function of P and α. It causes instability above 3 MPa because steam flow and feedwater flow are chosen as model inputs. When the system is in steady state with the pressure above 3 MPa, and steam flow, feedwater flow, and other inputs are fixed, a small increase in pressure causes a decrease in the specific enthalpy of the steam vapor phase, h_v. This decrease causes the energy input to the steam drum to exceed the energy removed. The energy imbalance causes the pressure to rise further and, since the rate of change of steam vapor enthalpy with respect to pressure is negative, the imbalance increases. Such a process is unstable. In a real plant, the steam flow would not remain fixed. The rising pressure would cause the steam flow to increase and bring the steam drum thermal power mismatch back into balance. One method of creating a stable model would involve adding a model of the steam header of the multi-modular plant to the boiling pot steam drum. Pressure increases and decreases should then stabilize under the influence of the adjoining component. Creating such an extended model is beyond the scope of this report, but this information is provided to help other investigators pursue related work.

Appendix E - Listing of Computer Codes

```
C------------------------------------------------------------
C This file implements the modified non-linear digital
C temperature controller (NLTC) on the PRISM module.
C A simple control law adjusts control reactivity to control
C temperature.  All variable names defined for use with the
C controller are defined by COMMON Block.  Other variable names
C are defined by the DSNP simulation language.  See the DSNP
C User's Manual for more information.
C
C      All units are SI.
C      length = meters
C      press. = pascals
C      temp.  = centigrade
C      power  = watts or megawatts
C      energy = joules
C      mass   = kilograms
C      time   = seconds
C
C      /DUMMY5/
C
C      TAUFP    primary flow control time constant
C      TAUFS  = secondary flow control time constant
C
C      /RXCON5/
C
C      DELKRF = reference reactivity
C      POWR   = demanded thermal power (MW)
C      VRMAX  = maximum rod speed (in/sec)
C      TSAM   = sampling period (sec)
C      XBETA  = delayed neutron fraction
C      TPC    = average primary coolant temperature (C)
C      TPCREF = avg. pri. coolant temp. reference value (C)
C      RN     = reactor power (W)
C      HRR    = height of regulating rod (in)
C      HRRREF = height of reg. rod reference value (in)
C      HRRSAV = height of reg. rod previous value (in)
C      SETSTO = setpoint stored value of temp. demand (C)
C      RNREF  = reactor power ref. value (C)
C      TSAV   = avg. pri. coolant temp. previous value (C)
C      PSAV   = reactor power previous value (W)
C      SIGSAV = control signal previous value (+1/-1)
C      SIGNAL = control signal (+1/-1)
C      DKRR   = regulating rod reactivity
C      DKT    = temperature reactivity
C      DELK   = net reactivity
C      TAUEST = reactor period estimate (sec)
C      DKS    = reactivity estimate for determining delayed
C               neutron decay parameter
C      DC     = delayed neutron decay parameter
```

167

```
C      XSAM  = controller sampling counter
C      TPROG = programmed avg. pri. temperature (C)
C      ZMC   = heat capacity of fuel, clad, coolant (MJ/C)
C      DTPCDT = avg. pri. coolant temp. rate of change (C/SEC)
C      PSAFE = maximum allowed power (W)
C      VAL1  = required time (sec)
C      VAL2  = available time - power - (sec)
C      VAL3  = available time - temperature - (sec)
C      QREM  = heat removed from primary loop (MW)
C      VROD  = control rod speed (in/sec)
C
C      /SUPER5/
C
C      POWER = module power demand (MW)
C      PRESS = demanded steam pressure (Pa)
C      TPHZ  = primary hot leg programmed temp. (C)
C      TPCZ  = primary cold leg programmed temp. (C)
C      FPZ   = primary programmed flow (kg/sec)
C      FSZ   = secondary programmed flow (kg/sec)
C
C-----------------------------------------------------------------
C PRISM MODULE SIMULATION
C-----------------------------------------------------------------
.      COMON/DUMMY5/TAUFP,TAUFS;
.      COMON/KPRNT5/TITLE(15);
.      COMON/TPRNT5/BYTO(20);
.      INCLUDE HSSPT1; INCLUDE VSSPH1;
.      INCLUDE RXCON0;
.      INCLUDE RAISE0;
.      INCLUDE LOWER0;
.      INCLUDE ESTKN0;
.      INCLUDE ANALY0;
.      INCLUDE REACT0;
.      INCLUDE RKRRD0;
.      INCLUDE RKRRI0;
.      INCLUDE SUPER0;
.      DFBOILG1(SO,SS);
.      DESTROY;
.      DFIHXMA1(3,SO,SO,SS);
.      DESTROY;
.      CNCTCU(TENI,TECX);
.      CNCTLC(TECI,TEMX);
.      CNCTUI(TEAPI,TENX);
.      CNCTIL(TEMI,TEAPX);
.      CNCTIG(TEBPIG,TEAHX,ZFBPG,FHAI);
.      CNCTGI(TEAHI,TEBPXG);
.      INDAT1(07);
C-----------------------------------------------------------------
C INITIAL CONDITIONS
C-----------------------------------------------------------------
BEGIN AT 0.0D0
.      CNCTIG;
```
168

```
.    3 BOILG1;
.      CNCTGI;
.    2 IHXMA1;
.      CNCTIL;
.    1 FDBEK1;
.      NEUTP1;
       FPAI=ZFLCOR
.      TPOWR1;
.      LPLEN1;
.      CNCTLC;
.      CORTP1(LMFBR);
.      CNCTCU;
.      UPLEN1;
.      CNCTUI;
.      CONVERGR(TECX,1.D-3,1,15,N);
.      CONVERGR(TEAHX,1.D-3,2,15,N);
.      CONVERGR(TEAPX,1.D-3,2,15,N);
.      CONVERGR(TEBPXG,1.D-3,3,15,N);
       CALL SUPER0
C----------------------------------------------------------------
C FIRST DYNAMIC LOOP
C----------------------------------------------------------------
SIMULATE LOOP01 STIFF1 TDV=1
       IF((XSAM*TSAM - TIMEM) .LT. DTMIN) CALL SUPER0
       ZFLCOR=ZFLCOR+((FPZ-ZFLCOR)*DELTM/TAUFP)
       FHAI=FHAI+((FSZ-FHAI)*DELTM/TAUFS)
.      FDBEK1;
.      NEUTP1;
       FPAI=ZFLCOR
.      TPOWR1;
.      LPLEN1;
.      CNCTLC;
.      CORTP1(LMFBR);
.      CNCTCU;
.      UPLEN1;
C----------------------------------------------------------------
C SECOND DYNAMIC LOOP
C----------------------------------------------------------------
SIMULATE LOOP02 RUNGE1 TDV=1
.      CNCTUI;
.      IHXMA1;
.      CNCTIL;
.      CNCTIG;
.      BOILG1;
.      CNCTGI;
C----------------------------------------------------------------
C  TERMINAL SECTION
C----------------------------------------------------------------
C
TERMINATE AT 180.D0
C
C----------------------------------------------------------------
```

```
C PRINTING INSTRUCTIONS & DATA STATEMENTS
C----------------------------------------------------------------
P PWJ,REAK,RKCN,TPC,TPROG,ZEGIIA,ZEGIBG
P DTPCDT,VAL1,VAL2,VAL3
P ZFLCOR,FHAI,FPZ,FSZ
P TECX,TECI,TEAHX,TEAHI
P RN,HRR
P DKRR,DKT,RKFB,DELK,TAUEST,DKS,DC
P TPHZ,TPCZ,QREM
. DATA(KPRNT)=TITLE/'PRISM_MO','DULE_FOR','_TESTING','_NON-LIN',
. 'EAR_TEMP','ERATURE_','CONTROLL','ER_(NLTC',')_____',6*'_____'/;
. DATA(TPRNT)=BYTO/1.0D0,3.D2,18*1000.D0/;
. DATA(TIMER)=DTMAX/1.D-1/,DTMIN/1.D-6/,LETM/2/,DELT/1.D-1/,IPLOT/18/,
. ICRT/80/,TIMEDS/0.D0/,TIMEDE/0.D0/,TIMEF/180.D0/,IINPT/07/,ISCR1/0/;
. DATA(FDBEK)=RKDC/-3.D-3/,RKEC/-4.D-6/,RKSC/4.5D-6/;
. DATA(NEUTR)=BETA/8.723D-5,7.499D-4,6.648D-4,1.306D-3,5.95D-4,1.949D-4/
. ,ELAMDA/0.0129,0.0308,0.132,0.335,1.34,3.27/,EL/4.829D-7/,PN0/1.D0/;
. DATA(TPOWR)=PW0/425.D6/;
. DATA(LPLEN)=CM/4.6D2/,QLPF/2.0D3/,TEMI/339.D0/,TEMA/339.D0/,
. TEMFA/339.D0/,UMA/3.5D6/,VMC/8.D0/;
. DATA(CORTP)=CF/766.7D0/,CL/4.6D2/,GA/0.D0/,QMF/27.D3/,QML/3.D3/,
. TECI/326.6D0/,UCA/6.26D6/,ULA/5.195122D6/,ZFLCOR/2.3304D3/,
. ZFLCR0/2.913D3/,VC/6.0/,TECA0/404.5D0/,TECI0/339.0D0/,TECX/470.0D0/,
. TEFA0/554.2/;
. DATA(UPLEN)=QUPF/1.0D3/,TENI/470.D0/,TENA/470.D0/,TENFA/470.D0/,
. UNA/1.75D6/,VNC/4.D0/;
. DATA(IHXMA)=TEAPI/440.70D0/,TEAPX/338.94D0/,TEAHI/288.10D0/,
. TEAHX/421.37D0/,FPAI/2.913D3/,FHAI/2.3304D3/,ZAPDI/1.2D0/,
. ZERAIA/1.D-3/,ZERRIA/5.D-4/,ZPPAA/1.5D5/,ZPHAA/2.5D5/,ZPDIA/1.2/,
. ARPA/2.274D0/,XWLA/3.413D0/,RINA/.9875D-2/,REXA/.1112D-1/,FFA/.93D0/,
. NXWA/5580/,ITIMXA/15/,ITOMXA/20/;
. DATA(BOILG)=ZPBSG/6.7D6/,ZTEBSG/282.8468D0/,TEBPIG/401.3D0/,
. TEBPXG/290.45D0/,ZFDG/934.5D0/,ZFBPG/2.913D3/,TEBWBG/363.45D0/,
. TEBWNG/323.36D0/,ZXNBG/3.0D0/,TEBPBG/405.13D0/,ZHBIG/890.0D3/,
. ZXQXG/.182D0/,TEBPNG/381.46D0/,ZFRG/934.5D0/,ZHBSXG/1529.D3/,
. ZRBPXG/0.D0/,ZRBSXG/0.D0/,ZEGIBG/0.D0/,ZEGXBG/0.D0/,ZXBBG/9.D0/,
. ZPDBG/1.3D0/,ZXRBIG/.6405D-2/,ZXRBXG/.794D-2/,ZXBG/12.D0/,
. ARBPG/2.245D0/,EPSBAG/1.D0/,EPSBRG/1.D-3/,ITIMBG/10/,ITOMBG/10/,
. KBLCG/2304/;
. DATA(SUPER)=POWER/400.D0/,PRESS/6.7D6/,XSAM/0.D0/;
. DATA(RXCON)=XBETA/.359788D-2/,VRMAX/.72D-1/,TSAM/0.1D0/,
. HRR/8.D0/,PSAFE/426.D0/;
. DATA(REACT0)=REACDC/0.D0/;
. DATA(DUMMY)=TAUFP/50.D6/,TAUFS/50.D6/;

L
C
C ZERO LEVEL LIBRARY
C
*ANALY0
      SUBROUTINE ANALY0
C----------------------------------------------------------------
                              170
```

```fortran
C Subroutine that determines reactivity analytically.
C-------------------------------------------------------------
.       TICIL;
.       COMIN RXCON5;
        CHARACTER*8 SNAME
.       TASNA('ANALY0');
        DKRR=RKRRI0(HRR)
        DKT=REACT0(TPC)
        DELK=DKRR+DKT-DELKRF
        KSUBST=KSUBST-1
        RETURN
        END


*ESTKN0
        SUBROUTINE ESTKN0
C-------------------------------------------------------------
C Subroutine that estimates certain kinetics parameters.
C-------------------------------------------------------------
.       TICIL;
.       COMIN RXCON5;
        CHARACTER*8 SNAME
.       TASNA('ESTKN0');
        SUREST=26.06*(2.0*(RN-PSAV)/TSAM)/(RN+PSAV)
        AS=DABS(SUREST)
        IF(AS .GE. 0.00260) GO TO 401
        GO TO 402
 401    CONTINUE
        TAUEST=26.06/SUREST
        GO TO 403
 402    CONTINUE
        TAUEST=10000.
        IF(SUREST .LT. 0.0)  TAUEST=-10000.
 403    CONTINUE
C----------------------------------------
C Estimate the one group decay parameter.
C----------------------------------------
        DKS=DKS*XBETA*10.
        DC=0.078742*EXP(0.019867*DKS)
        KSUBST=KSUBST-1
        RETURN
        END


*LOWER0
        SUBROUTINE LOWER0
C-------------------------------------------------------------
C A Subroutine that determines when reactivity should be changed
C in order to lower temperature.
C-------------------------------------------------------------
.       TICIL;
.       COMIN RXCON5,SUPER5;
        CHARACTER*8 SNAME
.       TASNA('LOWER0');
```

171

```fortran
C-------------------------------------------------
C Safety section.  Checks allowed power, period,
C and feasibility of control.
C-------------------------------------------------
      CALL ANALY0
      DKS=DELK
      CALL ESTKN0
      SIG1=-1.0
      X1=RKRRD0(HRR)
      X1=X1*VRMAX
      VAL1=(DELK+X1/DC)/X1
      VAL2=TAUEST*DLOG(RN/POWR)
      IF(TPC .LT. TPROG) VAL2=0.0
      IF(RN .LT. POWR) VAL2=0.0
      IF(VAL1 .LT. VAL2) GO TO 455
      DTPCDT=(TPC-TSAV)/TSAM
      VAL3A=1.D6
      IF((TPC .LE. TPROG) .AND. (DTPCDT .GT. 0.0)) VAL3A=(TPROG-TPC)/
     &DTPCDT
      VAL3B=1.D6
      IF((TPC .LE. TPROG) .AND. (RN .GT. QREM)) VAL3B=((TPROG-TPC)/(R
     &N-QREM))*ZMC
      VAL3=DMIN1(VAL3A,VAL3B)
      IF (VAL1 .LT. VAL3) GO TO 455
      GO TO 458
 455  CONTINUE
      SIG1=1.0
      IF(SIGSAV .EQ. -1.0) SIG1=0.0
 458  CONTINUE
C-----------------------------------------------------
C User defined control law for coolant temperature.
C-----------------------------------------------------
      TPERR=TPROG-TPC
      IF(TPERR .GT. 1.0D-2) THEN
        SIGNAL = 1.0
      ELSE IF(TPERR .LE. 1.0D-2) THEN
        SIGNAL = -1.0
      ELSE
        SIGNAL = 0.0
      END IF
C----------------------------
C End of control law section.
C----------------------------
      IF(SIGNAL .LT. SIG1) SIGNAL=SIG1
      VROD=VRMAX
C-----------------------------------------------------------------
C Sequence to ensure the motor stops before reversing directions.
C-----------------------------------------------------------------
      IF(SIGSAV .EQ. -1.0 .AND. SIGNAL .EQ. 1.0) SIGNAL=0.0
      IF(SIGSAV .EQ. 1.0 .AND. SIGNAL .EQ. -1.0) SIGNAL=0.0
      IF(HRR .LT. 3.0 .AND. SIGNAL .EQ. -1.0) SIGNAL=0.0
      IF(HRR .GT. 17.0 .AND. SIGNAL .EQ. 1.0) SIGNAL=0.0
```
172

```
      SIGSAV=SIGNAL
      TSAV=TPC
      PSAV=RN
      KSUBST=KSUBST-1
      RETURN
      END

RAISE0
      SUBROUTINE RAISE0
C---------------------------------------------------------------
C A subroutine that determines when reactivity should be changed in
C order to raise or to maintain temperature.
C---------------------------------------------------------------
.     TICIL;
.     COMIN RXCON5,SUPER5;
      CHARACTER*8 SNAME
.     TASNA('RAISE0');
C---------------------------------------------------------------
C Safety section.  Checks allowed temperature, transient and steady
C period, and feasibility of control.
C---------------------------------------------------------------
      CALL ANALY0
      DKS=DELK
      CALL ESTKN0
      SIG1=1.0
      X1=RKRRD0(HRR)
      X1=X1*VRMAX
      VAL1=(DELK-X1/DC)/X1
C-------------------------------
C Power level constraint section.
C-------------------------------
      VAL2=TAUEST*DLOG(PSAFE/RN)
      IF(RN .GT. PSAFE) VAL2=0.0
      IF(VAL2 .LT. 0.0) GO TO 408
      IF(VAL1 .GE. VAL2) GO TO 405
      DTPCDT=(TPC-TSAV)/TSAM
      VAL3A=1.D6
      IF((TPC .LE. TPROG) .AND. (DTPCDT .GT. 0.0)) VAL3A=(TPROG-TPC)/
     &DTPCDT
      VAL3B=1.D6
      IF((TPC .LE. TPROG) .AND. (RN .GT. QREM)) VAL3B=((TPROG-TPC)/(R
     &N-QREM))*ZMC
      VAL3=DMIN1(VAL3A,VAL3B)
      IF(TPC .GT. TPROG) VAL3=0.0
      IF(VAL1 .GE. VAL3) GO TO 405
      GO TO 408
 405  CONTINUE
      SIG1=-1.0
      IF(SIGSAV .EQ. 1.0) SIG1=0.0
 408  CONTINUE
C---------------------------------------------------
C User defined control law for coolant temperature.
```
173

```
C----------------------------------------------------
      TPERR=TPROG-TPC
      IF(TPERR .GT. 1.0D-2) THEN
        SIGNAL = 1.0
      ELSE IF(TPERR .LE. 1.0D-2) THEN
        SIGNAL = -1.0
      ELSE
        SIGNAL = 0.0
      END IF
      VROD=VRMAX
C---------------------------
C End of control law section.
C---------------------------
      IF(SIGNAL .GT. SIG1) SIGNAL=SIG1
      GO TO 450
 445    CONTINUE
      SIGNAL=-1.0
 450    CONTINUE
      VROD=VRMAX
C---------------------------------------------------------------
C Sequence to ensure the motor stops before changing direction.
C---------------------------------------------------------------
      IF(SIGSAV .EQ. -1.0 .AND. SIGNAL .EQ. 1.0) SIGNAL=0.0
      IF(SIGSAV .EQ.  1.0 .AND. SIGNAL .EQ.-1.0) SIGNAL=0.0
      IF(HRR .LT. 1.0 .AND. SIGNAL .EQ. -1.0) SIGNAL=0.0
      IF(HRR .GT. 17.0 .AND. SIGNAL .EQ. 1.0) SIGNAL=0.0
      SIGSAV=SIGNAL
      TSAV=TPC
      PSAV=RN
      KSUBST=KSUBST-1
      RETURN
      END

*REACT0
      FUNCTION REACT0(T)
C-----------------------------------------------------------------------
C A function which returns the reactivity associated with temperature in
C millibeta, given the temperature of primary coolant in degrees Celsius.
C This function is a linear approximation for Doppler reactivity, which
C is actually caused by the temperature of the fuel.
C-----------------------------------------------------------------------
.     TICIL;
.     COMON /REACT5/ REACDC;
.     COMIN RXCON5,REACT5;
      REACT0=REACDC*(T-TPCREF)
      REACT0=(REACT0/XBETA)*1000.0
      RETURN
      END
```

174

*RKRRD0
```
      FUNCTION RKRRD0 (H)
C------------------------------------------------------------------
C Returns differential regulating rod worth in millibeta per inch given
C rod height in inches.  Values based upon typical worth of MITR-II
C regulating.  The MITR rod worth is multiplied by a factor of 3X.
C------------------------------------------------------------------
      IMPLICIT REAL*8(A-H,O-Z)
      IF(H .LE. 1.5) GO TO 370
      IF(H .LE. 2.5) GO TO 375
      IF(H .LE. 4.0) GO TO 380
      IF(H .LE. 7.5) GO TO 385
      GO TO 390
370   RKRRD0=30.5
      GO TO 395
375   RKRRD0=30.5 - 0.5*(H-1.5)
      GO TO 395
380   RKRRD0=30.0 - 2.0*(H-2.5)
      GO TO 395
385   RKRRD0=27.0 - 3.920*(H-4.0)
      GO TO 395
390   RKRRD0=39.78 - 13.153*DLOG(H)
395   CONTINUE
      RKRRD0=RKRRD0*3.0
      RETURN
      END


*RKRRI0
      FUNCTION RKRRI0(H)
C------------------------------------------------------------------
C Regulating rod integral worth given in millibeta as a function of height
C in inches.  Based upon typical rod worth of MITR-II regulating rod.
C The MITR rod worth is multiplied by a factor of 3X.
C------------------------------------------------------------------
      IMPLICIT REAL*8(A-H,O-Z)
      IF(H .LE. 4.) GO TO 350
      IF(H .LE. 10.) GO TO 355
      IF(H .LE. 14.) GO TO 360
      GO TO 365
350   RKRRI0=29.435*H
      GO TO 369
355   RKRRI0=88.033*DLOG(H)-4.3
      GO TO 369
360   RKRRI0=3.899*(H-10.)+198.404
      GO TO 369
365   RKRRI0=1.5*(H-14.)+214.0
369   CONTINUE
      RKRRI0=RKRRI0*3.0
      RETURN
      END
```

```
*RXCON0
      SUBROUTINE RXCON0
C-------------------------------------------------------------------
C This subroutine ensures that the proper supervisory check is
C performed before the reactor temperature controller is allowed to
C take action. The same subroutine, either RAISE or LOWER, is called
C for the duration of the transient, until the setpoint SETSTO is
C changed to a new value.
C-------------------------------------------------------------------
.     TICIL;
      CHARACTER*8 SNAME
.                            COMON/RXCON5/DELKRF,POWR,VRMAX,TSAM,XBE-
TA,TPC,TPCREF,RN,HRR,
.      HRRREF,HRRSAV,SETSTO,RNREF,TSAV,PSAV,SIGSAV,SIGNAL,DKRR,DKT,
.        DELK,TAUEST,DKS,DC,TPROG,ZMC,DTPCDT,PSAFE,VAL1,VAL2,VAL3,
.        QREM,VROD;
.   COMIN NEUTR5,TPOWR5,FDBEK5,CORTP5,CNTRL5,TIMER5,UPLEN5,LPLEN5;
.      COMIN IHXMA5,BOILG5,RXCON5,SUPER5;
.      TASNA('RXCON0');
C----------------------
C Initialize variables.
C----------------------
      TPC=(TECX+TEAPX)/2.0
      RN=PWJ/1.E+06
      POWR=POWER
      QREM=POWR
      TPROG=(TPHZ+TPCZ)/2.0
      IF(JTIM .GT. 0) GO TO 109
 106  CONTINUE
      SETSTO=TPROG
      RNREF=RN
      TSAV=TPC
      PSAV=RN
      SIGSAV=0.0
      SIGNAL=0.0
      HRRSAV=HRR
      HRRREF=HRR
      TPCREF=TECA
      DKRR=RKRRI0(HRRREF)
      DKT=REACT0(TPCREF)
      DELKRF=DKRR+DKT
      CALL SODCP1(TECA,CC,XXXP)
      ZMC=(QMF*CF+QML*CL+(VC/ROCA)*CC)/1.E+06
C----------------------------
C Determine type of transient.
C----------------------------
      IF(POWR .GE. RNREF) GO TO 107
      GO TO 108
 107  CONTINUE
      CALL RAISE0
      IFLAG=1
      GO TO 110
```
176

```fortran
108   CONTINUE
      CALL LOWER0
      IFLAG=-1
      GO TO 110
C--------------------
C Commence transient.
C--------------------
109   CONTINUE
      HRR=HRRSAV+(SIGNAL*VROD*TSAM)
      IF(TPROG .NE. SETSTO) GO TO 106
      IF(IFLAG .EQ. 1) CALL RAISE0
      IF(IFLAG .NE. 1) CALL LOWER0
110   CONTINUE
      DKRR=RKRRI0(HRR)-RKRRI0(HRRREF)
      RKCN=DKRR*XBETA/1000.0
      HRRSAV=HRR
115   CONTINUE
      KSUBST=KSUBST-1
      RETURN
      END


*SUPER0
      SUBROUTINE SUPER0
C-----------------------------------------------------------------------
C The module supervisory controller to determine the programmed values
C of flows and temperatures in the PRISM module, given steam demand and
C pressure as input.
C-----------------------------------------------------------------------
.     TICIL;
      CHARACTER*8 SNAME
.     COMON/SUPER5/POWER,PRESS,TPHZ,TPCZ,XSAM,FPZ,FSZ;
.     COMIN SUPER5,RXCON5;
.     TASNA('SUPER0');
C----------------------------------------------------
C Calculate the programmed primary temperatrures.
C This program is for P=6.7 MPa, hfeed=890 kJ/kg
C----------------------------------------------------
      TPHZ=303.9+0.46192*POWER-1.7911E-4*(POWER)**2.0+8.7722E-9*(
     &POWER)**3.0
      TPCZ=221.12+0.26217*POWER+2.2784E-4*(POWER)**2.0-2.5439E-7*
     &(POWER)**3.0
C----------------------------------------------
C Calculate the programmed loop flow rates.
C----------------------------------------------
      FPZ=2913.0+(2913.0/425.0)*(POWER-425.0)
      FSZ=FPZ
      CALL RXCON0
      XSAM=XSAM+1.0
      KSUBST=KSUBST-1
      RETURN
      END
```

177

References

1. J.A. Bernard, D.D. Lanning, "Fault Tolerant Systems Approach Toward Closed-Loop Digital Control of Nuclear Power Reactors," MITNRL -026, (January 1988).

2. E.L.L. Cabral, "Real-Time Three Dimensional Thermal-Hydraulic Model and Non-Linear Controller for Large PWR Cores," Ph.D. Thesis, Dept. of Nucl. Eng., M.I.T., (November 1988).

3. L.M. Lidsky, "Safe Nuclear Power and the Coalition Against It," The New Republic, (December 28, 1987).

4. G.B. Kruger, C.E. Boardman, E.E. Olich, et al.,"PRISM: An Innovative Liquid Metal Fast Breeder Reactor," in Proceedings of the Joint ASME/IEEE Power Generation Conference, Portland, OR, (1986).

5. M.J. Schor, "Control of Multi-Module Nuclear Reactor Stations," M.S. Thesis, M.I.T. Department of Nuclear Engineering, (Oct. 1985).

6. "Small LMR cuts costs and boosts safety," in Nuclear Engineering International, Vol. 32, No. 400 (Nov. 1987).

7. A.E. Waltar, A.B. Reynolds, Fast Breeder Reactors, Pergamon Press, New York, 1981.

8. Y.I. Chang, M.J. Lineberry, et al., "Integral Fast Reactor Shows Its Mettle," in Nuclear Engineering International, Vol. 32, No. 400, (Nov. 1987).

9. G.B. Kruger, C.E. Boardman, et al., "PRISM: An Innovative Liquid Metal Fast Breeder Reactor," from "Proceedings of the Jt. ASME/IEEE Power Generation Conference (1986)," Portland, Ore., (1986).

10. J.T. Madell, "Theory and User Manual for the DSNP Simulation Language, Version PC/A for Microcomputers," System Simulation & Analyses, Inc., (1988).

11. A.F. Henry, "Nuclear-Reactor Analysis," p. 302, The M.I.T. Press, Cambridge, (1975).

12. H.B. Smets, "Problems in nuclear power reactor stability," p. 27, Presses Universitaires de Bruxelles a.s.b.l., Bruxelles, (1962).

13. Y.S. Tang, R.D. Coffield, R.A. Markley, Thermal Analysis of Liquid Metal Fast Breeder Reactors, American Nuclear Society, (1978).

14. C. Scott, "Plant Instrumentation and Control," in Fast Reactor Technology: Plant Design, pp. 579-652, J.G. Yevick, Ed., M.I.T. Press, Cambridge, (1966).

15. A.G. Parlos, "Non-Linear Multivariable Control of Power Plants Based on the Unknown-But-Bounded Modeling Methodology," Sc.D. Thesis, M.I.T. Department of Nuclear Engineering, (June 1986).

16. M.A. Schultz, Control of Nuclear Reactors and Power Plants, pp.128-135, McGraw-Hill Book Company, Inc., New York, (1955).

17. "Analysis and Simulation Study of the Operating Control System for the Enrico Fermi Atomic Power Plant," Holley Carburetor Company, (November 1959).

18. "Enrico Fermi Atomic Power Plant," Atomic Power Development Associates, Inc., APDA-124, (January 1959).

19. "Enrico Fermi Atomic Power Plant," p. 201, Atomic Power Development Associates, Inc., APDA-124, (January 1959).

20. "Enrico Fermi Atomic Power Plant," p. 200, Atomic Power Development Associates, Inc., APDA-124, (January 1959).

21. L.J. Koch, et al., Hazards Summary Report on EBR-II, USAEC Report ANL-5719, Argonne National Laboratory, (May 1957), and Addendum, (1961).

22. C. Scott, "Plant Instrumentation and Control," in Fast Reactor Technology: Plant Design, p.590, J. Yevick, Ed., M.I.T. Press, Cambridge, Ma., (1966).

23. C. Scott, "Plant Instrumentation and Control," in Fast Reactor Technology: Plant Design, p.591, J. Yevick, Ed., M.I.T. Press, Cambridge, Ma., (1966).

24. C. Scott, "Plant Instrumentation and Control," in Fast Reactor Technology: Plant Design, p.591, J. Yevick, Ed., M.I.T. Press, Cambridge, Ma., (1966).

25. R.L. Olson, et al., "The Sodium Graphite Reactor Power Plant for CPPD," in Proceedings of the Second United Nations International Conference on the Peaceful Uses of Atomic Energy, Geneva, 1958, Vol. 9, p. 161, United Nations, New York, (1958).

26. Final Summary Safeguards Report for the Hallam Nuclear Power Facility, Atomics International, USAEC Report NAA-SR-5700, Atomics International, (April 16, 1961).

27. C. Scott, "Plant Instrumentation and Control," in Fast Reactor Technology: Plant Design, p.592, J. Yevick, Ed., M.I.T. Press, Cambridge, Ma., (1966).

28. Clinch River Breeder Reactor Plant Reference Design Report, Vol. 1, pp. 4.1-4.9, Westinghouse Electric Corp., Advanced Reactors Div., (June 1974).

29. "Clinch River Breeder Reactor Plant - Reference Design Report," Vol. 1, p.4-2, Westinghouse Elec. Corp., Advanced Reactors Div., Madison, Pa., (June 1974).

30. "Clinch River Breeder Reactor Plant - Reference Design Report," Vol. 1, p.4-3, Westinghouse Elec. Corp., Advanced Reactors Div., Madison, Pa., (June 1974).

31. J.A. Bernard, A.F. Henry, and D.D. Lanning, "Application of the 'Reactivity Constraint Approach' to Automatic Reactor Control," in "Nuclear Science and Engineering," Vol. 98, pp. 87-95 (1988).

32. J.A. Bernard, A.F. Henry, and D.D. Lanning, "Application of the 'Reactivity Constraint Approach' to Automatic Reactor Control," in "Nuclear Science and Engineering," Vol. 98, pp.89-90 (1988).

33. "Enrico Fermi Atomic Power Plant," p.61, Atomic Power Development Associates, Inc., APDA-124, (January 1959).

34. J.T. Madell, "Theory and User Manual for the DSNP Simulation Language, Version PC/A for Microcomputers," System Simulation & Analyses, Inc., (1988).

35. J.T. Madell, "DSNP - A Simulation Language for the Dynamic Analysis of Nuclear Power Plants," in Simulators V, Simulation Series (Proc. of SCS Simulator Conf. Orlando, 1988) Vol. 19, No. 4., (1988).

36. H.A. Larson, E.M. Dean, et al.,"Dynamic Simulator for Nuclear Power Plants (DSNP): Development, Verification and Expansion of Modules," from "Proceedings of the International Conference on Power Plant Simulation, Cuernavaca, Mexico," pp. 353-358, (November 1984).

37. G.H. Golden and J.V. Tokar, "Thermodynamic Properties of Sodium", ANL 7323, (1967).

38. G.H. Golden and J.V. Tokar, "Thermodynamic Properties of Sodium", ANL 7323, (1967).

39. G.H. Golden and J.V. Tokar, "Thermodynamic Properties of Sodium", ANL 7323, (1967).

40. A.J. Friedland, "Coolant Properties, Heat Transfer, and Fluid Flow", in Fast Reactor Technology: Plant Design, J.G. Yevick, Ed., The M.I.T. Press, Cambridge, Mass., (1966).

41. "Library Level-1 Manual for the DSNP Simulation Language, Version PC/A, Vol. 1", System Simulation & Analyses, Inc., Western Springs, IL, (1988).

42. L.A. Rovere, "A Multimodular Reactor Model for Supervisory Control Studies," ORNL-ACTO Program Report, (Feb. 1989).

43. G.M. Garner, "Fault Detection and Level Validation in Boiling Water Reactors," Ph.D. Thesis, M.I.T. Department of Mechanical Engineering, (Draper Laboratory Report CSDL-T-858), (Sept. 1985).

44. W.H. Strohmayer, "Dynamic Modeling of Vertical U-Tube Steam Generators for Operational Safety Systems," Ph.D. Thesis, M.I.T. Department of Nuclear Engineering, (Draper Laboratory Report CSDL-T-778), (August 1982).